April 2019

Novel Insights into the Multifaceted Roles of BLM in the Maintenance of Genome Stability

Vivek M. Shastri
University of South Florida, shastri.vivek@gmail.com

Novel Insights into the Multifaceted Roles of BLM in the Maintenance of Genome Stability

by

Vivek M. Shastri

A dissertation submitted in partial fulfillment
of the requirements for the degree of
Doctor of Philosophy
with a concentration in Cell and Molecular Biology
Department of Cell Biology, Microbiology and Molecular Biology
College of Arts and Sciences
University of South Florida

Major Professor: Kristina H. Schmidt, Ph.D.
Alvaro Monteiro, Ph.D.
Meera Nanjundan, Ph.D.
Sandy Westerheide, Ph.D.

Date of Approval:
April 5, 2019

Keywords: Bloom syndrome, DNA repair, DNA replication, genome instability

DEDICATION

I offer this work to my Guru, Bhagawan Sri Sathya Sai Baba. I dedicate this dissertation to my Mother, Father, and Brother who made it possible for me to pursue my dream. Their hard work and patience have been a constant source of inspiration to me. I especially thank Jennifer, who has always been by my side and encouraged me to better myself.

ACKNOWLEDGEMENT

First and foremost, I would like to acknowledge Dr. Kristina Schmidt for graciously granting me the opportunity to work in her lab and for being an extremely supportive advisor. I would like to express my gratitude to my committee members for their inputs and patience over the years. Special thanks to past and present members of the lab. I am also thankful for all the help and support from the Department of Cell Biology, Molecular Biology, and Microbiology during my time here.

TABLE OF CONTENTS

LIST OF TABLES

LIST OF FIGURES

LIST OF ACRONYMS

ALT	Alternative Lengthening of Telomeres
AMP	Ampicillin
AR loop	Aromatic rich loop
ATM	Ataxia telangiectasia mutated
ATP	Adenosine triphosphate
ATR	Ataxia telangiectasia and Rad3-related protein
BER	Base excision repair
BGS	Baller-Gerold syndrome
BLAST	Basic Local Alignment Search Tool
BLM	Bloom syndrome helicase
BRCA1	Breast cancer type 1 susceptibility protein
BRCA2	Breast cancer type 2 susceptibility protein
BrdU	Bromodeoxyuridine
BS	Bloom syndrome
BTR	BLM-TopIII-α-RMI1/2 complex
cDNA	Complementary DNA
CHK1	Checkpoint kinase-1
CHK2	Checkpoint kinase-2
CPT	Camptothecin
DBD	DNA binding domain
dbSNP	Short Genetic Variations database
DEAH	DNA-dependent ATPase
dHJ	Double Holliday junction
DNA	Deoxyribonucleic acid
DNA2	DNA synthesis defective protein 2
DNA-PK	DNA-dependent protein kinase
DSB	Double strand break
dsDNA	Double-stranded DNA
DTT	Dithiothreitol
EDTA	Ethylenediaminetetraacetic acid
EXO1	Exonuclease 1
FASP	Filter Aided Sample Preparation
FEN1	Flap endonuclease 1
H2AX	Histone H2AX
H3	Histone 3

HCl	Hydrochloric acid
HR	Homologous recombination
HRDC	Helicase/RNAse D C-terminal
HU	Hydroxyurea
LB	Luria broth
LC-MS/MS	Liquid Chromatography with tandem mass spectrometry
LOH	Loss of heterozygosity
MCM10	Mini chromosome maintenance 10
MCM2	Mini chromosome maintenance 2
MCM2-7	Mini chromosome maintenance complex 2-7
MCM4	Mini chromosome maintenance 4
MCM6	Mini chromosome maintenance 6
MCM7	Mini chromosome maintenance 7
MDC1	Mediator of DNA damage checkpoint protein 1
MLH1	MutL homolog 1
MRC1	Mediator of the replication checkpoint
MRE11	Double-strand break repair protein MRE11
MRN	Mre11-Rad50-Nbs1 protein complex
MSH2	MutS homolog 2
MSH6	MutS homolog 6
NaCl	Sodium chloride
NaOH	Sodium hydroxide
NER	Nucleotide excision repair
NHEJ	Non-homologous end joining
NMR	Nuclear magnetic resonance
OB	Oligonucleotide-binding
ORF	Open reading frame
PCNA	Proliferating cell nuclear antigen
PCR	Polymerase chain reaction
PP2A	Serine/threonine-protein phosphatase
PVDF	Polyvinylidene fluoride
RAD51	DNA repair protein RAD51 homolog 1
RECQL1	Human RecQ-like helicase 1
RECQL4	Human RecQ-like helicase 4, Rothmund-Thomson syndrome protein
RECQL5	Human RecQ-like helicase 5
RNA	Ribonucleic acid
RPA	Replication protein A
RQC	RecQ-C-terminal
RTS	Rothmund-Thomson syndrome

SCE	Sister chromatid exchange
SF	Superfamilies
SF1	Super family 1
SF2	Super family 2
SILAC	Stable Isotope Labeling using Amino acids in Cell Culture
SNPs	Single nucleotide polymorphisms
SSB	Single stranded binding protein
ssDNA	Single stranded DNA
TBST	Tris-buffered saline w/ Tween or Triton
TOP1	Topoisomerase 1
TOP2	Topoisomerase 2
TOPIIIα	Topoisomerase IIIα
UV	Ultraviolet
WB	Western blot
WH	Winged helix subdomain
WRN	Werner syndrome protein
Cdc45	Cell division control protein 45 homolog
Cdt1	DNA replication factor Cdt1
SGS1	Slow growth suppressor 1

x

ABSTRACT

Genomic instability is a hallmark of disorders in which DNA replication and repair genes are dysfunctional. The tumor suppressor RECQ helicase gene *BLM* encodes the 3'-5' DNA Bloom syndrome helicase BLM, which plays important roles during DNA replication, recombination and repair to maintain genome stability. Mutations within *BLM* cause Bloom syndrome, an autosomal recessive disorder characterized by growth defects, immunodeficiency, >10-fold higher sister chromatid exchange compared to normal cells, and an increased predisposition to a wide range of cancers from an early age. Single nucleotide polymorphisms or SNPs in *BLM* have been reported to be associated with susceptibility to a variety of malignancies. However, these are non-coding SNPs with no evidence linking them to SNPs in *BLM* exons. An overwhelming majority of nonsynonymous SNPs in *BLM* for which allelic frequencies are known are rare. Together with their rarity in the human genome and a higher likelihood of being functional, rare SNPs can be an important genetic basis of common human diseases. And since almost all nonsynonymous SNPs in *BLM* are rare, they are prime candidates for functional characterization to determine risk-association. A comprehensive functional evaluation of coding BLM variants using a humanized yeast model identified six variants which totally impair BLM function, with DNA damage sensitivity conferred by these alleles comparable to Bloom syndrome-causing alleles in the human population. An intermediate sensitivity to DNA damage was conferred by three other alleles. Here, functionally evaluated the ability of 8 of these BLM variants to complement cellular defects in the Bloom syndrome patient-derived GM08505 cell line including the elevated sister-chromatid exchanges frequency,

delayed response to DNA damage, and hypersenstivity to DNA damaging agents. We determined that five of these variants are incapable of complementing defects of the GM08505 cell line, which are candidates for adding to the list of thirteen currently known Bloom syndrome causing missense mutations. We identified three other BLM variants that were incapable of complementing the elevated sister-chromatid exchange frequency and delayed DNA-damage response, but were able to suppress hypersensitivity to DNA damaging agents as well as wildtype BLM. These intermediate BLM variants are hypomorphic which, instead of causing Bloom syndrome, may confer increased cancer predisposition or lead to other Bloom-syndrome-associated disorders like type-2 diabetes.

The GM08505 cells used in the functional characterization of BLM variants is aneuploid. Defects in DNA replication, telomere maintenance, chromosomal segregation, cell cycle checkpoint activation, and DNA damage response cause chromosomal instability. Aneuploidy is considered to be an outcome of chromosomal instability. Paradoxically, another school of thought considers aneuploidy as the driver of chromosomal instability. It has been suggested that variable expression of genes on aneuploid chromosomes can potentially dysfunction of their protein product, leading to chromosomal instability phenotypes. It has been proposed that chromosomal instability and aneuploidy are part of a vicious cycle which results is an increasingly diverse karyotype directly impacting gene expression. Using genome engineering, we generated and functionally characterized a diploid *BLM* knockout cell line. This cell line exhibits cellular defects similar to the Bloom syndrome patient derived GM08505 cell line. Being diploid and unaffected by uneven gene dosage, this cell line can provide a good system to investigate dysregulated factors in the absence of BLM.

The prevention of genomic instability depends on multiple pathways ensuring timely progression of replication and appropriate response to DNA damage. BLM functions at the crossroads of response pathways induced by DNA damage during replication. The canonical role of BLM is dissolving double Holliday junction during homologous recombination- mediated DNA double strand repair as part of the BLM/Topoisomerase IIIα /RMI1/RMI2 or BTR complex to yield non-crossover products. Additionally, BLM functions in the key early step of resecting double strand breaks to initiate DNA repair. BLM can also reverse the invasion of the resultant single stranded 3' overhangs in an anti-reombinogenic role and regulate recombinational DNA repair. BLM functions to restart stalled replication forks resulting from DNA damage. Thus far, most studies evaluating the role of BLM in replication have proposed models based on its role in recovery from induced replication stress. However, delayed replication timing, increased replication fork pausing, endogenous DNA damage, and activation of replication checkpoints in unperturbed Bloom-syndrome cells point to a role for BLM in protecting the replisome movement through the genome. A critical aspect of BLM functionality is its substrate specificity to a variety of DNA structures. Notably, it can bind and unwind G-quadruplex structures *in vitro* and has been associated with a functional role in unwinding such regions *in vivo* to aid replisome movement with limited evidence. We immunoprecipitated BLM in mid-S-phase and performed a mass spectrometric screen to identify novel interactors in a bid to identify mechanisms by which BLM maintains genome stability during unperturbed replication. We show that Mcm6, an MCM replicative helicase subunit, is a novel BLM interactor. BLM interacts with Mcm6 via multiple, distinct binding sites in G1 phase, at active replisomes in S-phase, and during response to replication stress induced DNA damage. We show that BLM is a constitutive component of

active replisomes in during unperturbed replication. Finally, we uncover a potential novel role for BLM in G1 requiring interaction with Mcm6.

Our data provides functional and mechanistic insight into polymorphisms in *BLM,* and their implications for the general population. We have also engineered a diploid *BLM* knockout cell line which can serve as a platform for investigating BLM variants in the absence of uneven gene dosage as well as proteomic analysis to identify factors dysregulated in the absence of BLM. We show that BLM is a component of active replisomes in an unperturbed S phase and has a potentially novel function in G1.

CHAPTER ONE:

INTRODUCTION

Genomic stability is dependent on the tight regulation of and coordination between cellular mechanisms involved in DNA metabolism. Factors responsible for faithful DNA replication, DNA damage response, and timely checkpoint activation in the S-phase are key mediators of cell cycle progression in the face of genotoxic stress. Genome instability results when these factors are dysfunctional, manifesting as abnormal development, growth defects, premature aging, and predisposition to cancers and tumorigenesis. At the cellular level, these are characterized by hyperrecombination events, genome rearrangements, and aberrant chromosomal structures [5-7]. Helicases are members of a group of enzymes involved in all aspects of nucleic acid metabolism, including replication, expression, repair and recombination [8, 9]. They function in these pathways by mediating the necessary step of ATP-dependent translocation along DNA, RNA or DNA/RNA structures to unwind them with either a 5'→3' or a 3'→5' polarity. Identification of conserved helicase motifs based on structure and function analysis have led them to be classified into six helicase superfamilies [10, 11]. Helicase superfamily 1 (SF1) and superfamily 2 (SF2) are the two largest of these and are structurally similar. SF1 and SF2 members contain a conserved catalytic region known as the core helicase domain consisting of two domains resembling the recombination protein RecA fold. The conserved helicase motifs are localized to a cleft formed between the two RecA-like domains contains, forming the site of binding and translocation along single strand DNA (ssDNA) [11, 14]. Furthermore, a β-hairpin

1

has been found to localize outside this cleft in various SF1 and SF2 members and functions in strand separation [14, 17]. Phylogenetic analysis of alignments to score sequence-specific features and domain organization of SF1 and SF2 proteins has led to the sub-classification of SF1 into three families and SF2 into nine families [14]. The RecQ helicase family belongs to SF2 and plays important roles in maintaining genome stability [20-23].

THE RECQ HELICASE FAMILY

The family derives its name from the founding member RecQ, a helicase with 3'→5' DNA unwinding activity and a component of the RecF pathway in *Escherichia coli* (*E. coli*) [24]. Since then, other RecQ family members have been identified across various kingdoms of life. While single cell organisms have one or two RecQ genes, higher eukaryotes have multiple genes expressing proteins belonging to the RecQ family [25-27]. Five RecQ helicases have been identified in humans - RECQL1, RECQL4, RECQL5, WRN, and BLM. Structurally, RecQ family members contain three highly conserved domains - the core helicase domain, a RecQ-C-terminal (RQC) domain, and a helicase and RNase-D like C-terminal (HRDC) domain (Figure 1.1) [4, 14].

The core helicase domain

This domain is the most conserved and is a DEAD/H motif region containing seven conserved helicase motifs (I, Ia, II, III, IV, V and VI) critical for ATP hydrolysis and is termed the core helicase or ATPase domain [11, 28-30]. Apart from the seven helicase motifs, the RecQ core helicase contains an additional characteristic sequence located upstream of motif I, referred to as motif 0 [31]. This motif has been shown to be involved in DNA binding and required for helicase activity [32-34]. Crystal structure determination has revealed that the core helicase

2

domain of RecQ family members is bi-lobed with two RecA-like domains N- and C-terminal of a cleft. ATP binding and hydrolysis is mediated by conserved Walker A and Walker B motifs located in the first domain and other elements like an arginine finger located in the second domain [35]. The cleft contains the conserved helicase motifs to function as the putative DNA binding region [2, 36-39]. Mutations within the core helicase domain have been shown to have a deleterious impact, highlighting the functional significance of this domain [15, 32-34, 40, 41].

The RecQ C-terminal domain

RQC is the second conserved domain within all and unique to RecQ family members, although its presence is debated in RecQ4 [42-44]. This domain is divided into two subdomains – the zinc binding (Zn) and winged helix (WH) domain. The Zn domain coordinates a single Zn^{2+} using four cysteine residues and two anti-parallel α-helices. Barring minor differences in the length of α-helices in a few members, the Zn domain has been shown to be structurally similar [36, 39]. Missense mutations in this domain have been implicated in a functional role in maintaining protein stability, DNA binding as well as contributing to helicase activity [33, 41, 45-49]. BLM truncations containing only the ATPase domain and the Zn-binding domain have been shown to perform helicase functions [50]. Although RecQ4 is regarded as lacking the characteristic RQC domain, it has been shown to contain a novel domain featuring a Zn binding region suggesting a different helicase mechanism compared to other human RecQs [44]. These not only indicate the importance of the Zn binding domain, but also signify the functional versatility of RecQ helicases.

While the WH domain is conserved structurally, the sequences have a poor similarity with considerable charge variation within the RecQ family. The structural uniformity is

3

characterized by the presence of a helix-turn-helix fold [36, 39]. Additionally, *E. coli* RecQ, and human RecQ1, WRN and BLM contain a *β*-hairpin loop within the WH domain. Mutation analyses suggest that this loop in *E. coli* RecQ, and human RecQ1, and WRN participates in DNA unwinding, functioning as a strand separation pin [38, 39, 51-53]. There is also evidence for the WH domain's involvement in mediating interaction with DNA. Studies have shown that the WH domain in *E. coli* RecQ, human RecQ1, WRN and BLM can recognize and bind to a variety of DNA structures like double stranded DNA (dsDNA), G-quadruplexes (G4), and double Holliday junctions (dHJs) [53-55]. Resolved crystal structures of *Cronobacter sakazakii* RecQ, RecQ1, and BLM show that the WH domain location varies between different structures, indicating that it is a mobile domain [2, 36, 52, 53].

The helicase and RNase D–like C-terminal domain

The third conserved domain within RecQ helicases is a distal C-terminal region resembling the RNaseD C-terminal region, thus known as the HRDC domain. It is the least conserved structural domain and among human RecQ helicases, present only in BLM and WRN [56]. Crystallographic and biochemical analysis suggests that it plays an important role in structure-specific substrate recognition and functionally differentiating the various RecQ family members [57, 58]. Isolation of various HRDC domains has shown that the core structure is conserved [57-60]. However, the primary sequences as well as surface charges of the HRDC domains are very variable. The HRDC domain of the *Saccharomyces cerevisiae* RecQ family member Sgs1 contains a patch of basic amino acid residues, making the predominantly electropositive surface amenable for DNA binding [60]. The *E. coli* RecQ also has an electropositive surface, but located on a different face of the HRDC domain [57]. While the isolated Sgs1 HRDC domain can interact with single stranded DNA (ssDNA) and partial

dsDNA, *E. coli* RecQ binds preferentially to ssDNA [57, 60]. On the other hand, the WRN HRDC domain does not have an electropositive surface and has been shown to not interact with DNA *in vitro* [58]. Instead, the WRN HRDC domain has been suggested to play a role in protein interactions [55, 58]. Although the BLM HRDC domain has not been isolated yet, studies using solution structures show a weak affinity to ssDNA [61, 62]. While the HRDC domains of *E. coli* RecQ and Sgs1 are dispensable for helicase function, they are required for stable dsDNA binding [31, 63, 64]. A BLM mutant missing the HRDC domain displayed only a minor loss of helicase activity, but had a far greater inability to disrupt dHJs as well as an inability to promote DNA strand annealing [45, 65, 66]. A single amino acid residue change within BLM HRDC also shows that it is required to dissolve dHJs [65, 67].

Taken together, the differing *β*-hairpin loop lengths within the Zn domain, the variable sequence/charge distribution as well as relative mobility of the WH domain, and the role of the HRDC domain in structure-specific DNA recognition indicate the important roles these unique domains plays in conferring substrate specificity to the various RecQ helicases. A comparison of helicase activities and substrate specificities of the human RecQ helicases has been provided in Table 1.1 [3, 34, 68-76].

Non-conserved and unique domains

Unique and non-conserved domains flank the conserved domains described above. Notably, WRN contains a unique N-terminal exonuclease domain which functions in protecting and restarting stalled replication forks resulting from DNA damage [55, 77]. The human RecQs
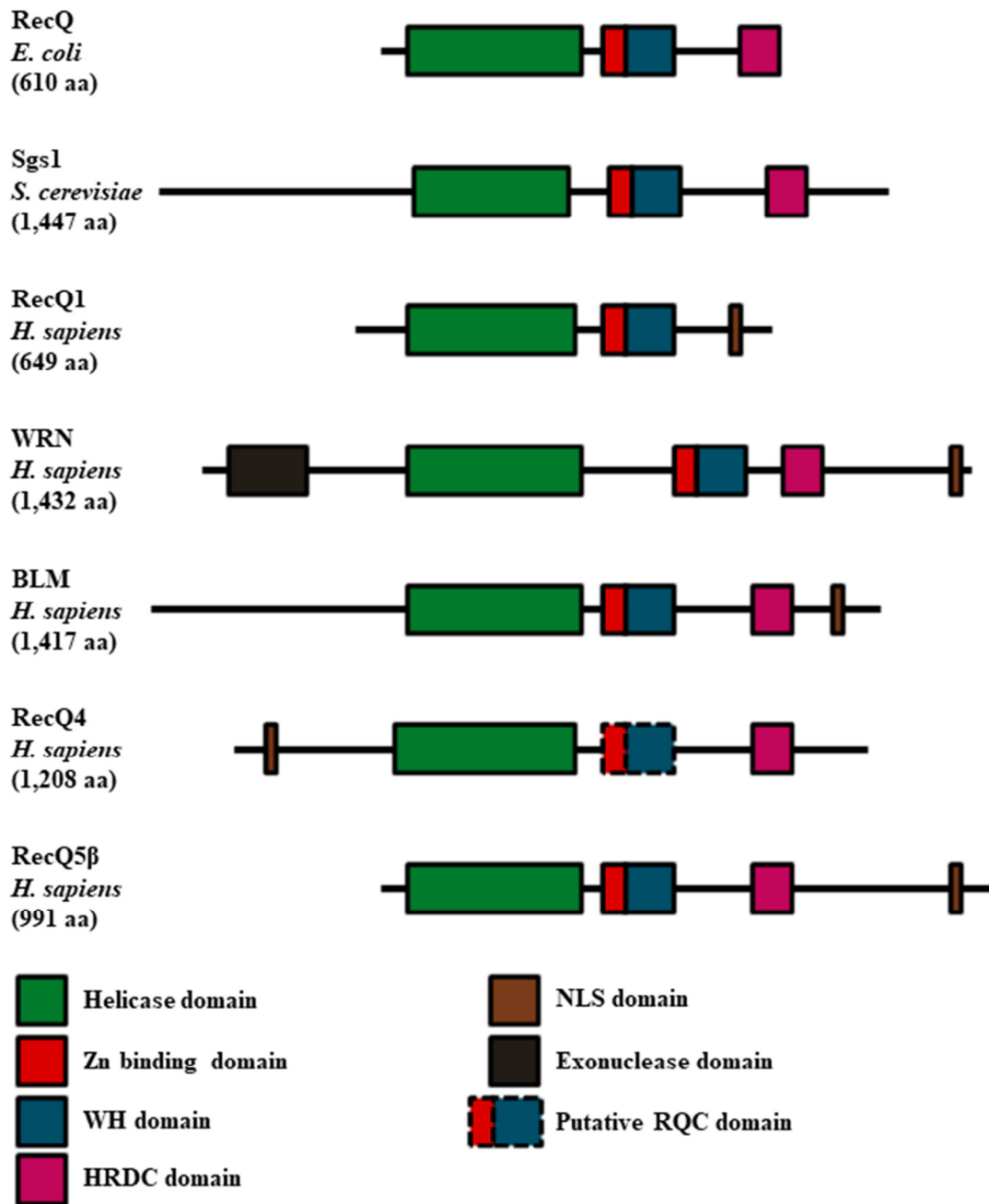
Figure 1.1. Schematic showing domain organization of selected RecQ helicases
Selected RecQ members are aligned according to the helicase domain. The Zn binding and WH domains constitute the RQC domain. In RecQ4, the RQC domain is denoted as putative since its presence has not been shown conclusively. The β isoform of RECQ5, the largest of at least three splice variants known to express, has been used for this alignment. The domain lengths are estimated and not accurately to scale. Adapted and modified from Vindigni & Hickson (2009) and Croteau et al (2014) [3, 4].

contain a nuclear localization signal (NLS) at the extreme end of the C-terminal region with the

exception of RecQ4, which contains the NLS within the N-terminal region [78-81].

Table 1.1. Substrate specificity and helicase activities of human RecQ helicases

Substrate	Relative Helicase Activity [a]				
	RecQ1	BLM	WRN	RecQ4 [b]	RecQ5
Duplex	-	-	-	+/-	ND
Forked duplex	++	+	+	+	+
3'-tailed duplex	++	~/-	~/-	ND	ND
D-loop	+	+	+	-	-
Bubble	~/-	+	+++	-	-
G-quadruplex	-	+++	+++	-	-
Holliday junction	+	+++	+++	-	~
DNA/RNA hybrid	-	+	+	ND	ND

+, weak; ++, moderate; +++, strong; -, no activity; ~/-, partial activity; ND, not determined.
[a] Data in this table is from the following studies: [3, 34, 68-76].
[b] Data for RecQ4 is in the absence of ssDNA.
This table has been adapted from Croteau, et al (2014), Cheok et al (2005), and Sidorova & Monnat Jr (2014) [82, 83].

7

Human diseases resulting from RecQ helicase deficiencies

The human RecQ helicases function in DNA replication, repair, and recombination and are therefore instrumental in maintaining genomic stability [3, 21, 25-27, 84, 85]. While all RecQ helicases play important roles in maintaining a stable genome, defects in RECQL4, WRN, and BLM lead to disease syndromes in humans [3, 9].

Rothmund-Thomson syndrome is caused by mutations in RECQL4

Defective RECQL4 has been linked to three disorders — Rothmund-Thomson syndrome (RTS), RAPADILINO syndrome, and Baller-Gerold syndrome (BGS) [86, 87]. RTS is characterized by sun-sensitive, poikilodermatous rashes from infancy. Other RTS features used in clinical diagnosis include predisposition to osteosarcomas among other malignancies, juvenile cataracts, defects in radial ray, alopecia, and loss of eyebrows and eyelashes [87, 88]. Many individuals with RTS have a short stature along with bone abnormalities [88, 89]. At the cellular level, RTS is characterized by hypersensitivity to ionizing radiation and reduced DNA repair efficiency upon UV exposure [90-92]. The gene mutated in RTS is *RECQL4* [93, 94]. Mutations such as frameshifts, nonsense mutations, splice mutations, and intronic deletions predicted to result in a truncated RECQL4 protein have been found in RTS patients [95]. Multiple short introns within *RECQL4* gene might be a reason for mis-spliced *RECQL4* mRNA [96]. Furthermore, eight missense mutations clustered in the helicase region have been identified in RTS patients [95].

Werner syndrome is caused by defects in WRN

Werner syndrome (WS) is the result of defects in the *WRN* gene. A broad spectrum of mutations within *WRN*, including frameshifts, nonsense mutations, and splice mutations, has

been identified in WS patients. However, no missense mutations in *WRN* have been identified in WS patients [84, 86]. WS patients exhibit progeroid features beginning at puberty, including premature graying and hair loss, cataracts, type II diabetes, hypogonadism, atherosclerosis, osteoporosis, along with increased sarcomas [97]. The cellular phenotype of WS cells includes increased rate of somatic mutations, chromosome loss and deletions [98, 99]. The S-phase is prolonged in WS cells with a reduction in both initiation frequencies and replicative life span [100]. WS cells are mildly sensitive to ionizing radiation, and hypersensitive to DNA interstrand cross-link-inducing agents and topoisomerase inhibitors [97].

BLM deficiency causes Bloom syndrome

BLM deficiency causes Bloom syndrome (BS), which will be described in detail in the following section.

BLOOM SYNDROME

Clinical features of Bloom syndrome

BS is an autosomal recessive disorder first described as a unique human disease syndrome in children with erythema and short stature by a dermatologist, David Bloom [101-103]. Thereafter, James German observed that BS patients exhibited increased chromosomal breakage and an elevated predisposition to cancer from a young age [103, 104]. The early predisposition to a wide range of cancers remains the most common feature of BS, occurring at greater frequency compared to the general population and is the most common cause of the reduced life expectancy of ~27 years [105, 106]. Additionally, ~10-fold higher than normal rates of crossovers between sister chromatids or sister chromatid exchanges (SCEs) were observed in

9

cells from BS patients, and it remains the hallmark and only clinical diagnostic feature of BS [107-110].

Other clinical features used as recognizable patterns in BS patients include growth defects impacting height and weight, long and narrow face, prominent ears/nose, and a smaller head circumference [102, 103, 108]. However, these features are variable and all BS patients may not exhibit these features. Prenatal onset of growth deficiencies has been observed, with the affected fetus being smaller for the gestational age. Children with BS exhibit malnourishment and significant wasting [106, 111]. These deficiencies are life-long and BS patients are smaller than the general population [112]. There have been reports of children with BS undergoing growth hormone therapy. However, this has been proposed to be contra-indicated since hormone therapy carries a potential risk of cancer and BS patients are predisposed to cancers [113].

Apart from growth deficiencies, additional endocrine dysfunctions in BS patients include hypothyroidism, increased insulin resistance, glucose tolerance and susceptibility to early onset type-2 diabetes mellitus (T2DM) [112].

Problems with feeding in infants and children are another clinical description used in BS diagnosis. Slow feeding, disinterest in food, and gastroesophageal reflux (GER) have been reported as typical issues faced by children with BS [106, 111]. This has been compounded by obesity in some BS patients prescribed with a high caloric density formula and growth supplements [112].

BS patients typically have normal skin at birth, which progressively goes on to present dermatological complications. One of the first identified clinical BS presentations, facial rashes form a typical butterfly-like pattern and have been described as poikiloderma in some individuals

[114]. Apart from erythema, unusual skin manifestations in BS patients include fissures, blisters, and sudden loss of eyebrow and eyelash hair [115, 116]. Multiple forms of skin cancer have been reported in ~10% of the 226 malignancies in 145 BS patients diagnosed at a mean age of 31.5 [117].

Infections of the upper respiratory and gastrointestinal tracts with no consistent causative pathogen have suggested an impaired immune function in BS patients [102, 103]. Decreased levels of one or more serum immunoglobulins classes have also been observed in BS patients who have had evaluations of their immune system [112, 118]. Though they usually have normal T- and B-cells with no defects in counts, various abnormalities in their functions and lineage in BS patients have been observed and point to an impaired adaptive immune system [102]. Serious pulmonary complication related deaths have been reported in individuals with BS, with treatment unable to stop acute respiratory failure in one individual [105, 119, 120]. It has been proposed that possible immunodeficiency and recurrent respiratory infections during childhood lead to chronic lung disease, making it a significant cause of early mortality in BS patients [119, 120].

Impaired fertility is another characteristic feature of some BS patients, with males invariably being infertile and some females undergoing delayed puberty as well as entering menopause prematurely [103, 121, 122].

Cellular defects of Bloom syndrome

Apart from the characteristically elevated SCE levels, BS cells exhibit various other chromosomal aberrations such as a significant increase in chromatid breaks and the presence of quadriradial chromosomes, which suggest illegitimate inter-chromosomal recombination events [107, 123-125]. Replication timing of early- as well as late-replicating loci is abnormal in BS

11

cells and is accompanied by a constitutive increase in the appearance of DNA damage sites [126]. The replication fork progression rate is reduced in BS cells along, with fork pausing observed at an increased frequency and endogenous activation of DNA double-strand break (DSB) checkpoint response [127]. Thus, not surprisingly, BS cells are hypersensitive to genotoxic and replication stress inducing agents like hydroxyurea (HU). In response to such stress, replication fork reactivation is compromised and cell division is delayed [128]. Recruitment of DNA damage response (DDR) factors like BRCA1, 53BP1 and the MRN complex to stalled replication forks is delayed in BS cells [129, 130]. Consequently, stalled replication forks accumulate with less than 40% of them being restarted and potentially cause unscheduled origin firing leading to genomic instability [131]. In the absence of appropriate replication restart, DNA DSBs develop and lead to extensive apoptosis of BS cells [129]. DNA/RNA hybrids known as R-loops have been observed to accumulate in BS cells [132]. Additionally, increased oxidative stress and mitochondrial abnormalities have been reported in BS cells [133-136].

MUTATIONS AND POLYMORPHISM IN THE *BLM* GENE

Homozygosity and linkage disequilibrium studies identified chromosome 15, specifically a locus within 15q26.1, as the genetic locus mutated in BS [137-140]. Approximately 20% of BS patients have a small population of venous lymphocytes which display normal levels of SCEs as opposed to the high SCE levels observed otherwise [141]. Somatic hybridization between low SCE lymphocytes and high SCE cells led to the identification of a single gene responsible for high SCEs in BS patient cells, the *BLM* gene [142].

12

Bloom syndrome causing mutations

BS was observed to be more frequent in the Ashkenazi Jewish population compared to any other population examined, estimated to be around 1/48,000 [143]. A homozygous 6-bp deletion and 7-bp insertion was found in *BLM* from four BS patients of Ashkenazi Jewish ancestry and is referred to as the *blm^Ash* mutation [139]. Initial studies found this to be the most common *BLM* mutation, with 26/28 of BS patients with both parents being Ashkenazi Jewish found to be homozygous for the *blm^Ash* mutation. 97% of chromosomes in BS patients with at least one Ashkenazi Jewish parent carried the *blm^Ash* mutation [144]. The carrier frequency for this mutation is estimated to be between 1/110-1/45 within Ashkenazi Jewish populations across various geographic locations [145-148]. The *blm^Ash* mutation was also found in 5/91 unrelated, non-Ashkenazi Jewish BS patients, who were all from Christian families of Spanish ancestry from southwestern United States, Mexico, or El Salvador [144].

Apart from this founder mutation, various recurrent and unique mutations in *BLM* have been identified in other populations as well. In a survey of 134 BS patients, 64 mutations in *BLM* were identified in 125 individuals, with 54 of them causing premature termination of protein and 10 being missense mutations [149]. BS causing mutations within *BLM* encompass missense mutations resulting in single amino-acid substitutions, frameshifts, splice-site mutations and nonsense mutations [1, 149-153].

Heterozygosity in *BLM* and cancer risk

Reports from various studies indicate an uncertain association between heterozygosity for pathogenic *BLM* mutations and cancer risk [145, 154-164]. Crossing mice heterozygous for the *Blm^Cin/+* null mutation with mice carrying a mutated *Apc* tumor suppressor gene resulted in

earlier development as well as double the number of lymphoma compared to wildtype mice [154]. This suggests that heterozygosity for genome stability maintenance genes could have a potential association with increased cancer risk [154]. This was tested in a study comparing the frequency of the founder mutation *blmAsh* in Ashkenazic populations to the frequency in controls and it was found that 1/54 Ashkenazi Jewish individuals with colorectal cancer carried *blm^{Ash}* as opposed to 1/118 in the control group [145]. However, other studies report no significant increase in the prevalence of colorectal cancer among *blm^{Ash}* carriers compared to controls [155-158]. A founder nonsense *BLM* mutation in Slavic populations (Gln548*) was found to occur more frequently in those with a family history of breast cancer, apart from also being associated with an increased risk of breast cancer development [159, 160]. Conversely, the same mutation was found to have no positive association with either prostate or ovarian cancers [161, 162]. A study using whole exome sequencing to screen breast cancer families identified mutations in *BLM* in 2/438 breast cancer families compared to none in either healthy controls or the 1000Genomes Project data [165, 166]. A recent study using molecular inversion probes for targeted sequencing screened colorectal cancer patients and identified deleterious mutations in *BLM* in 1.6 % of the patients compared to 0.2% in the control group [167].

One challenge with faced by these studies investigating cancer risk of *BLM* heterozygosity was their low power. Additionally, it is unclear if mutations in *BLM* are solely responsible for any associated risk or if other mutations contribute as well. These need to be addressed in order to establish meaningful cancer association with heterozygosity in *BLM* in otherwise unaffected populations.

Polymorphism in *BLM* and disease risk

Single nucleotide polymorphisms (SNPs) in *BLM* have been reported to be associated with susceptibility to breast cancer, bladder cancer, malignant melanoma, acute myeloid lymphoma, and myelodysplastic syndromes [168, 169]. These are non-coding SNPs and there is no evidence of linking them to SNPs in *BLM* exons. Among nonsynonymous SNPs in BLM for which allelic frequencies are known, only three alleles (V1190I, P868L/R, and V1321I) are not rare with a minor allele frequency >0.05 [170, 171]. An analysis of the association between rare SNPs and risk of common disease found that rare SNPs have a higher likelihood of being functional with a stronger effect size compared to common SNPs. Combined with the rarity of SNPs in the human genome, it is proposed that rare SNPs are a critical genetic basis of common human diseases [172]. And since almost all nonsynonymous SNPs in *BLM* are rare (with an allele frequency <0.05), they are prime candidates for functional characterization as the first step in determining risk-association.

Functional relevance of coding SNPs in *BLM*

So far, 74 SNPs in *BLM* resulting in coding variants of uncertain clinical significance have been identified [171, 173, 174]. A comprehensive functional evaluation of coding *BLM* variants was undertaken in an earlier study using a humanized yeast model [40]. *S. cerevisiae* cells expressing a chimera consisting of the disordered N-terminal half of Sgs1 and C-terminal half of BLM were used to perform complementation assays to identify functional significance of various coding *BLM* variants. 41 missense and 2 rare variants contained in the BLM C-terminal region in the chimera were ranked for their probability to impair BLM function. Eventually, 27 variants ranging from the highest to lowest probability to impair BLM function were chosen for

functional evaluation. This analysis identified nine new BLM variants not currently associated with BS which are candidates for adding to the list of thirteen currently known BS causing missense mutations. Furthermore, these deleterious mutations in *BLM* not yet associated with BS were characterized in human cells expressing full length BLM variants and led to the identification of 5 candidates for new BS causing mutations and 3 hypomorphic alleles, which may have a cancer predisposition role or confer BS-like symptoms [15]. Five of these BLM variants exhibit functional defects similar to known BS causing missense mutants, which suggests that they have the potential to cause BS in a homozygous state or in a compound heterozygous state with any known BS causing mutation. Three other BLM variants appeared to be only partially defective, with P868L being the most common and occurring at a frequency of 0.051 in the general population [170, 171, 173]. Based on its allele frequency, approximately 1 in 10 individuals are carriers and 1 in 380 individuals are predicted to be homozygous for P868L. This number far exceeds the number BS cases, indicating that P868L is not associated with BS. However, the functional analysis of P868L revealed at least a partial loss of function, which suggests that a considerable number of individuals lack a fully functional *BLM* allele and might an increased cancer predisposition [15, 40]. The association of P868L with increased colorectal cancer and its partially impaired function support this possibility [15, 175].

These findings have significant implications for the role of mutations and polymorphism in the *BLM* gene beyond BS. Conventionally, biallelic mutations in caretaker genes have been regarded as being relevant to cancers [176]. These studies provide evidence that biallelic alterations in *BLM* not leading to BS might still be associated with a higher risk for cancer development compared to the general population. Furthermore, hypomorphic *BLM* alleles could

be impaired in response to genomic stress in otherwise asymptomatic individuals and potentiate genome instability.

STRUCTURE OF THE BLM HELICASE

The BLM C-terminal region contains the helicase core

The product of the *BLM* gene is the BLM helicase, which unwinds DNA with a 3'→5'polarity [41, 177]. BLM is a 1,417 amino acid polypeptide. The helicase core stretching from residues 640-1290 is its best characterized structure and contains structural domains characteristic of the RecQ helicase family (Figure 1.5) [45]. The two RecA-like ATPase domains are located within residues 640-857 and 858-993 respectively, and contain the conserved helicase motifs (0, I, Ia, II, III, IV, V and VI) [2]. This domain is critical for ATP hydrolysis [1, 2, 32, 50].

Downstream from the core helicase is the RQC domain containing the Zn binding (residues 994-1068) and WH (residues 1069-1192) sub-domains [2, 37]. Structural and functional characterization of the Zn binding domain have revealed that it plays important roles in the ATPase and helicase catalytic activities of BLM, apart from being implicated in maintaining protein stability. Mutating the cysteines involved in coordinating the Zn^{2+} ion further determined that while it is not important for ATP binding, duplex DNA binding was reduced and G4 DNA binding was completely abrogated [178]. Moreover, missense mutations affecting residues C1036 and C1055 in the Zn binding domain being found in BS patients underscores its importance in BLM function [41]. A co-crystal structure of BLM 640-1291 in complex with a 3'-overhang duplex DNA has shown that BLM RQC binds to dsDNA using a binding mode similar to other RecQ proteins WRN and RECQ1 [179]. However, the BLM RQC

domain can be structurally differentiated from the RQC of WRN and RECQ1 [37, 180]. Two β-strands form a prominent β-hairpin structure in the BLM WH domain, which is thought to function as the DNA strand separation pin found in other RecQ helicases [37-39, 42, 51]. Notably, the aromatic residue at the tip of this β-hairpin in the BLM WH is missing and instead features acidic residues forming an extensive polar interface with dsDNA [2]. This suggests that the BLM WH plays a structural role in DNA strand separation despite the dissimilar sequence and is involved in substrate specificity. Unique to BLM among human RecQ helicases, an insertion between the α1- and α2-helices of the WH domain forms a loop perpendicular to the β-hairpin and plays a role in binding dHJs [180]. Another loop structure extends from the C-terminal region of WH domain and is proposed to be involved in positioning the HRDC domain [180]. A co-crystal structure has also revealed that upon WH binding dsDNA, a lysine rich loop ([868]PKKPKK[873]) outside WH becomes available as another interaction site by connecting the first β-strand of the WH domain to the α-1 of the C-terminal lobe of the ATPase domain [2]. Overall, the WH has an important role in DNA binding.

The HRDC domain is unique to BLM and WRN among human RecQ helicases [2, 4, 56]. The least conserved among the three characteristic RecQ helicase domains, the BLM HRDC is predominantly electronegative [62]. This domain has been shown to confer substrate specificity and, while dispensable for dsDNA binding, is critical for dHJ binding and dissolution [65]. The HRDC domain (residues 1193–1290) is C-terminal of the WH domain, separated by an extended linker rich in lysine (residues 1199–1208) which creates a gap in the surface by pushing it away from the rest of protein [2]. Significantly, a co-crystal structure indicates that the HRDC domain is in a position to form an intramolecular association with the C-terminal ATPase domain and exhibits a weak binding affinity in solution studies in the presence of ATP. Enzymatic

18

characterization of BLM mutants that interrupted this HRDC-ATPase domain interaction indicated a slightly reduced ATPase activity and dHJ dissolution efficiency [2]. Furthermore, BLM mutants lacking the entire HRDC domain showed reduced helicase activity and less efficient coupling of ATP hydrolysis to DNA unwinding [179]. Put together, these data point to the involvement of the HRDC domain in BLM catalytic function.

Similar to other human RecQ proteins, BLM has a nuclear localization signal sequence (NLS) C-terminal of the conserved RecQ helicase domains located between residues 1134-1357 [78, 79, 181-183].

The BLM N-terminal region is predicted to be intrinsically disordered and forms a major site for protein interactions

In contrast to the highly conserved and structured C-terminal region, the BLM N-terminal tail spanning residues 1-639 is poorly conserved at the amino acid level and predicted to be intrinsically disordered (Figure 1.2). Therefore, the crystallographic and mutational analyses which delineated functional domains in the C-terminal region could not be applied to identify the functions of the BLM N-terminal tail. Sgs1, the *S. cerevisiae* ortholog of BLM, has served as a model to understand the BLM N-terminus and predictions show that the property of disorder is conserved between BLM and Sgs1 [184]. Moreover, the N-terminal regions of various RecQ helicases have been shown to be involved in protein interactions and are therefore biologically relevant [4, 26]. Similarly, BLM N-terminus forms a platform for various protein interactions and regulates BLM activity [185-192].
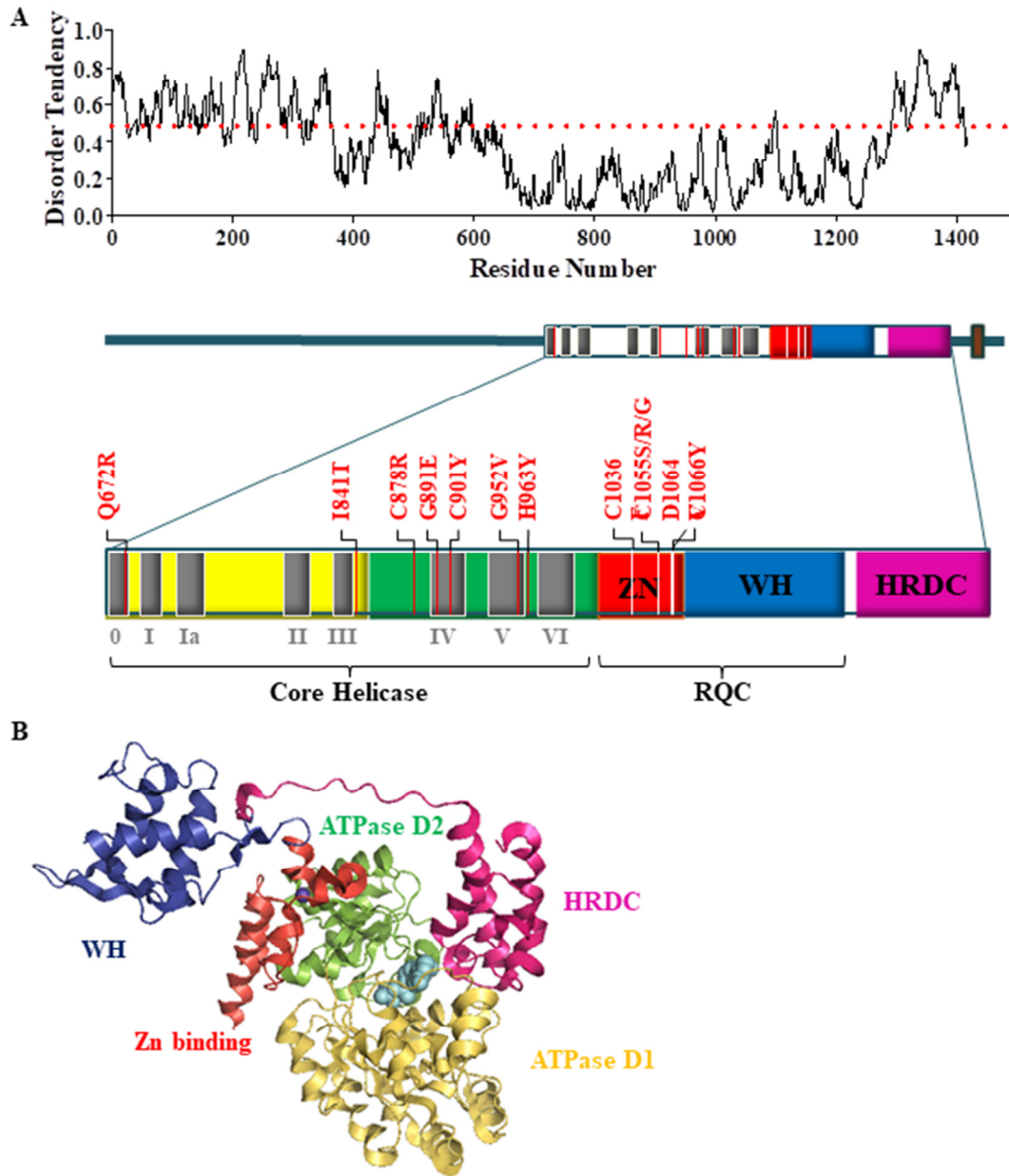
Figure 1.2. Structure of the BLM helicase
A) IUPRED prediction of disordered BLM N-terminal region and map of the conserved C-terminal domains. BLM catalytic core has been magnified to show the location of BS causing missense mutations. **B)** Structure of BLM with bound Zn ion and ADP depicted as spheres. Adapted from [1, 2]. BLM structure graphic created using PyMol [12].

INTERACTIONS AND FUNCTIONS OF BLM

BLM functionally interacts with numerous proteins via both the N- and C-terminal regions to participate in DNA repair, recombination and replication pathways to preserve genomic stability. Known interactions and functions of BLM are summarized in Figure 1.5 and Table 1.2.

Canonical role of BLM in recombinational DNA repair

The best understood function of BLM is in dissolving dHJs during homologous recombination (HR) mediated DNA double strand break repair (DSBR) (Figure 1.3) [67, 193]. When a homologous template is available, the 5'-end of DNA DSBs can be resected to generate a 3'-overhang in a key early step determining repair pathway choice [194]. End resection is initiated by the MRE11 as part of the MRE11-RAD50-NBS1 (MRN) complex along with its cofactor CtIP [195]. End resection is further accelerated by recruitment of BLM to DSB ends by MRN. BLM plays a role in long range resection catalyzed either by DNA2 or the 5′ to 3′ exonuclease EXO1 [196, 197]. BLM physically interacts with DNA2 to promote DNA end resection in an ATP-dependent manner, where BLM unwinds DNA to enable the nuclease functions of DNA2 [198]. The single strand DNA (ssDNA) binding protein RPA interacts with BLM and enhances end resection at DSBs by stimulating BLM helicase activity and stabilizing the nascent 3'-overhang [188, 189, 199]. The MRN cofactor CtIP also physically interacts with BLM, enhancing long range resection by possibly stimulating BLM/DNA2 activity after MRN induced nick [200]. Alternatively, it is proposed that EXO1 promotes further resection upon stimulation of its nuclease activity by BLM, MRN, and RPA [197, 201]. Unlike DNA2, stimulation of EXO1 mediated end resection does not require BLM helicase activity and instead

depends on a physical interaction between the two to increase EXO1 affinity to DSB ends [197, 201]. Thus, BLM is an important part of two DSB end resection machineries —

BLM/DNA2/RPA/MRN and EXO1/BLM/RPA/MRN [197].

The resultant processed ends form substrates for the HR-mediated DSBR pathway. Rad51 displaces RPA from the nascent 3'-overhangs to form nucleoprotein filaments which invade homologous duplex, form the intermediate D-loop structure and initiate the search for sequence homology [202]. This is a defining step committing to the HR pathway. The intact homologous sequence is used as a template by the invading strand for DNA synthesis and the D-loop forms dHJs when the second processed end is captured. The dHJs form the substrate for the structure specific BTR complex comprising BLM, TopoIIIα and RMI1/RMI2 [203-206]. Using a mechanism distinct from Holliday junction resolution, the BTR complex resolves dHJ structures without resulting in exchange of sequences flanking the intermediate structure. This mechanism is termed dissolution and the complex is known as the BTR dissolvasome [67, 206]. The dHJs are dissolved by branch migration of the two Holliday junctions towards each other until a hemicatenated intermediate is formed, which is then decatenated. Within the complex, BLM is the catalytic component driving branch migration. Once the dHJs fuse to form the hemicatenated intermediate, TopoIIIα drives the decatenation to topologically separate the two duplexes resulting in dHJ dissolution. Furthermore, BLM ATPase activity is required for the decatenation step [67, 207, 208]. While RMI1 and RMI2 interact with BLM and TopoIIIα to stimulate the dissolution reaction, it is also speculated that they help with DNA binding via putative OB fold domains [205, 209, 210]. The products of dHJ dissolution are always non-crossover. Conversely, resolution of dHJs by resolvases can yield either crossover or non-crossover products.

22
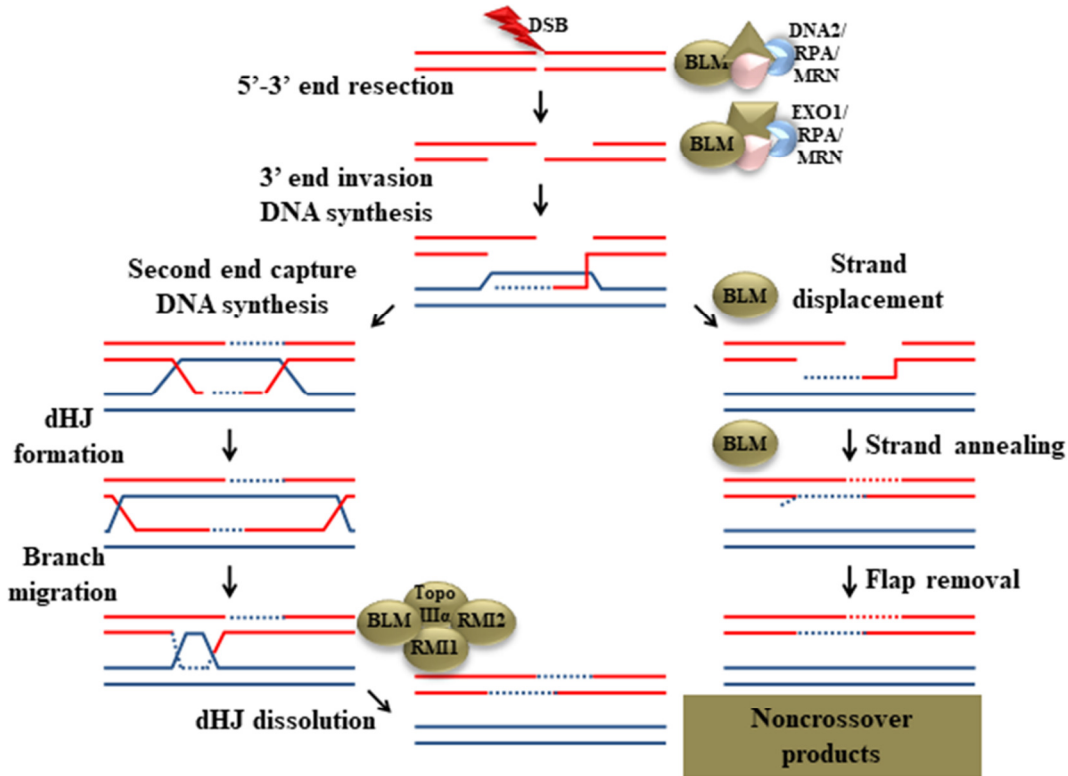
Figure 1.3. BLM functions in HR-mediated DNA double-strand break repair
Diagrammatic models showing BLM functions at key steps of DSBR repair pathway. BLM participates in the initial end resection as part of either BLM/DNA2/RPA/MRN or EXO1/BLM/RPA/MRN machineries. Post second-end capture, BLM mediates dissolution of dHJs as part of the BTR dissolvasome. Conversely, BLM can mediate strand displacement to initiate the SDSA pathway of DSBR. All BLM functions in DSBR always result in the formation of non-crossover products. Adapted from Maloisel et al (2008) [16].

BLM physically interacts with Rad51 and plays a regulatory role within the HR-mediated DSBR pathway [211-213]. BLM can play an anti-recombinogenic role by displacing Rad51 to prevent nucleoprotein filament formation, inhibiting strand invasion, and further disrupting nascent D-loops [214-216]. DSBR proceeds via the synthesis-dependent strand annealing (SDSA) HR pathway after the invading strand displacement and D-loop disruption by BLM, resulting in non-crossover products. It has been shown that BLM promotes Rad51 mediated strand invasion by ATP-bound RAD51 filaments, but inhibits inactive ADP-bound Rad51 filament invasion [217]. By playing a pro- and anti-recombinogenic role during this step in HR,

23

BLM potentially suppresses illegitimate recombination events. Moreover, it is evident that HR mediated DSBR in the presence of BLM predominantly results in non-crossover products. With evidence suggesting that HR-mediated DSBR is major pathway involved in repairing chromosomal DNA DSBs, the function of BLM in this pathway to predominantly yield non-crossover products is very significant [218]. Illegitimate mitotic recombination product formation when collapsed replication forks undergo DSBR might be an explanation for the high SCE levels in BS cells.

BLM functions in response to DNA replication stress

Defective replication stress response in BS cells led to investigations into the possible functions of BLM in rescuing replication forks. Indeed, studies have shown that BLM localizes to stalled replication forks which develop into DSBs [129]. BLM is necessary for timely recruitment and functions of DDR factors like BRCA1, NBS1, and 53BP1 to DSBs, providing further evidence of BLM being associated with facilitating replication fork protection [129, 130]. Furthermore, BLM is required for efficient replication restart in response to replication stress [131, 219, 220]. BLM can promote replication fork restart through its function in HR-mediated DSBR pathway [221]. Given its structural affinity to replication and recombination intermediates, it has been proposed that BLM can mediate the formation of favorable DNA structures to restart forks stalled by lesions on the leading strand. *In vitro* analyses have shown that BLM can promote regression of model replication forks by creating a "chicken foot" structure in which the newly synthesized leading and lagging strands are annealed [222, 223]. BLM-mediated replication fork regression allows the leading strand to bypass the lesion by template switching. Following lesion bypass, replication can restart either by reversal of the

regressed fork regression by BLM-mediated branch migration or an HR-mediated pathway dependent on dHJ dissolution by BTR (Figure 1.4) [223].
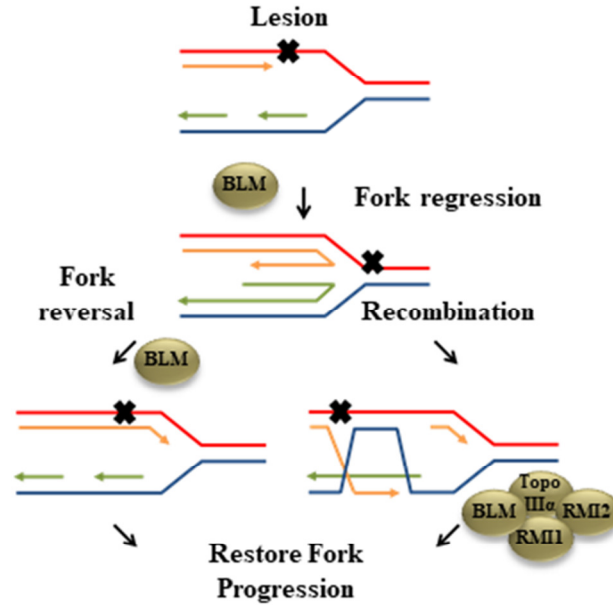
Figure 1.4. BLM-mediated replication fork restart
Replication forks can stall due to lesions on the leading strand during DNA replication. BLM mediates regression of the stalled fork via template switching to bypass the lesion. BLM may reverse the regressed fork to facilitate replication restart. Conversely, the regressed arm can invade the parental chromosome, generating a dHJ which can be dissolved by BLM as part of the BTR dissolvasome.

BLM also associates with Fanconi anemia (FA) proteins to play important roles in replication restart [224-226]. FANCM is thought to bind to RMI1/RMI2 and recruit the BTR complex to sites of damage [224, 227]. Notably, BLM physically interacts with the 5' to 3' helicase FANCJ and thought to cooperate during replication restart [228, 229]. FANCD2 is also thought to mediate phosphorylation of the BTR complex in response to DNA damage, promote replication fork restart, and suppress unscheduled firing of new replication origins [230, 231].

BLM physically interacts with and recruits p53 to Rad51 sites at stalled replication forks [232]. The BLM-p53 interaction at Rad51 sites is proposed to regulate the HR pathway and

suppress excessive recombination by either inhibiting Rad51 activity or inhibiting BLM-mediated inhibition of Rad51 activity.

In response to replication stress, BLM also interacts with the DDR protein 53BP1 [233-235]. Phosphorylation of both 53BP1 and BLM (on residue T99) enhances their binding and co-localization with Rad51 at DSB sites. Interactions between these three proteins have been shown to have an antirecombinogenic role during HR-mediated DSBR after replication stress induction [234].

BLM interacts with TopBP1, an important hub for protein interactions during DNA replication stress response, and evidence suggests that this interaction is necessary to suppress SCEs and unscheduled origin firing [186, 236]. The regulation of BLM protein levels by TopBP1 is a debated role [89, 186].

BLM was identified as a member of the BRCA1-associated genome surveillance complex (BASC) along with BRCA1, MSH2, MSH6, MLH1, ATM and the MRN complex [237]. BRCA1, BLM, and the MRN complex have been shown to colocalize to putative DNA DSB sites after replication stress. All members of this complex can recognize and bind non-canonical DNA structures, leading to suggestions that BASC is DNA damage sensor. The interaction between BLM and MLH1 is not required for DNA mismatch repair, further indicating a role in replication stress induced damage response [238].

BLM unwinds stable DNA structures that impede DNA replication

G4s are stable secondary DNA structures which cannot be easily unwound by the replicative helicase and impede replication fork progression [239, 240]. G4 motifs are prevalent and distributed throughout the genome, including a vast majority of replication origins and

26

coding sequences [241]. BLM can recognize, bind, and unwind G4 structures *in vitro* and has also been associated with a functional role in facilitating timely replisome movement by unwinding G4 rich regions *in vivo* [68, 242, 243]. Further evidence of a role for BLM in recognizing G4 structure is provided by the observation of SCEs being enriched at coding regions, specifically sites containing G4 motifs, in the absence of BLM [244]. It is proposed that BLM suppresses recombination at G4 structures in transcribed regions and protects genomic integrity. Recently, BLM interaction with WRN and RPA facilitated by HERC2 has been shown to be important for suppressing G4 structures [192].

BLM can unfold 3′-ssDNA tails containing G4 motifs using a mechanism involving three discrete steps to mediate unidirectional translocation [245]. It can repeatedly unfold G4 structures containing connected dsDNA and ssDNA by remaining anchored to the ss/dsDNA junction. Lastly, BLM can also unfold G4 structures by spooling in ssDNA. This suggests that BLM can potentially use a different mechanism to unfold G4 structures in different molecular environments [245].

R-loops are DNA:RNA hybrids which cause replication fork stalling. Underscoring its specificity to a variety of non-canonical DNA substrates, BLM can also unwind model R-loops *in vitro* [246]. Observations of R-loop accumulation causing DNA damage in BS cells and BLM/R-loop proximity *in vivo* seem to imply BLM involvement in maintaining replisome stability at sites of collision with R-loops [132].

BLM functions in telomere replication and maintenance

G4 structures are the primary barriers the replisome encounters while replicating telomeres [247]. There is evidence of increased telomeric G4 structures and slow moving

27

replication forks originating within telomeres in BS cells, indicating a role for BLM in telomere synthesis [248]. The shelterin component TRF1 physically interacts with BLM to facilitate lagging strand synthesis during telomeric replication, where the template is the TTAGGG repeat [249]. The BLM-TRF1 interaction potentially plays a role in unwinding the secondary structures formed within these sequences. The predominant role of BLM in telomere maintenance appears to be in the HR pathways in alternative lengthening of telomeres (ALT) cells during ALT-mediated telomere replication [250-252]. The BTR dissolvasome functions in ALT-mediated telomere synthesis possibly by processing recombination intermediates formed during strand invasion, leading to POLD3-dependent telomere synthesis and subsequent dissolution to prevent exchange of telomeric DNA [251]. BLM, BRCA1 and FANCM are recruited to ALT telomeres in response to replication stress in an interdependent manner [250]. In ALT cells lacking FANCM, BLM and BRCA1 interact to initiate DNA end resection leading to HR-mediated DSBR to counter replication stress [250]. BLM and BRCA1 interact during S- and G2-phases and co-localize with RAD50 at telomeres in ALT cells [253]. *In vitro* assays using DNA substrates resembling forked structure containing telomeric repeats suggests that BRCA1 enhances BLM unwinding activity [253]. Additionally, exposure to replication stress induces the formation of late-replicating intermediates known as ultra-fine bridges (UFBs). BLM contributes to telomere maintenance by dissolving these late-replicating intermediate structures [252].

BLM and ultrafine anaphase bridges

Distinct DNA structures linking two sister chromatids, termed anaphase bridges, can be stained during mitosis. Subsequently, a subclass of anaphase bridges was classified as ultrafine anaphase bridges (UFBs) [254, 255]. The BTR dissolvasome and the PLK1-interacting checkpoint helicase (PICH) localize to these UFBs [255]. PICH specifically interacts with and

recruits BLM while the localization of the rest of the BTR dissolvasome to UFBs depends on BLM [255]. Most UFBs arise at centromeres, where the BTR dissolvasome and PICH potentially associate with Topo IIα and promote centromere disjunction [256, 257]. Indeed, *in vitro* and *in vivo* interactions between BLM and Topo IIα support this notion [258, 259]. FS-UFBs are a different class found only at common fragile sites (CFS) and proposed to be the result of incomplete DNA replication [259, 260]. In the face of replication fork stalling, additional initiation occurs to complete DNA replication. But these initiations do not occur at CFS and DNA replication is incomplete when mitosis begins, resulting in FS-UFBs [261]. It is proposed that recruitment of FANCD2/FANCI to CFS in late S- and early G2-phase specifies FS-UFBs, which are then coated by BLM and PICH. BLM also mediates FANCM localization to FS-UFBs. FANCM is observed on FS-UFBs even after BLM dissociation, suggesting that BLM either recruits FANCM to FS-UFBs or makes the FS-UFBs more accessible to FANCM [254]. UFBs generated by HR constitute a third class of UFBs, termed HR-UFBs [262, 263]. HR-UFBs in anaphase can be stained with PICH and BLM, and subsequently visualized as RPA-coated, ssDNA bridges [263]. Lastly, BLM is also a part of a fourth class of telomeric UFBs or T-UFBs induced by overexpressed TRF2 interfering with telomere the replication leading to chromosomal end-on-end fusion [252, 263, 264]. Topo IIα inhibition has also been shown to induce T-UFBs, suggesting that they consist of catenanes or replication intermediates [265].

Lack of UFB resolution could lead to DNA damage that can be repaired by the error-prone non-homologous end joining (NHEJ) pathway during the subsequent cell cycle. However, this can potentially result in chromosomal aberrations. The cytogenetic features of BS and the presence of BLM on UFBs further highlight the significance of BLM in maintaining genomic stability.

Table 1.2. Known BLM interacting partners and their functional significance

BLM Interactor	Metabolic Pathway
WRN, HERC2	G-quadruplex unwinding
EXO1, RAD51, RMI1, RMI2 RPA, Topo IIIα, DNA2, MRE11	Recombinational DNA repair
BRCA1, FANCJ, FANCD2, FANCM H2AFX, MLH1, MSH2, MSH6, RAD50 TopBP1, p53, 53BP1, XRCC2, Mus81	Response to replication stress
TERF1, TERF2, BRCA1, FANCM	Telomere replication and maintenance
FANCD2, FANCI, FANCM, Topo IIα	UFB resolution

REGULATION OF BLM FUNCTION

Multiple studies have uncovered different modes of BLM regulation, particularly mediated via posttranslational modifications (PTMs). These regulate BLM stability, cell cycle specific expression, localization, and interactions.

Phosphorylation of BLM during the replication stress response

Apart from its functions in recombinational DNA repair, BLM also functions in intra S-phase checkpoint signaling in response to replication stress. This serves to pause the cell cycle, inhibits replication origin firing, and mediates recruitment of DDR proteins to sites of DNA damage [266]. BLM is phosphorylated by the checkpoint kinases ATM in response to ionizing radiations and ATR in response to replication stress induced damage at residues T99 and T122 [131, 267, 268]. Replication restart is delayed without impacting BLM localization in the

30
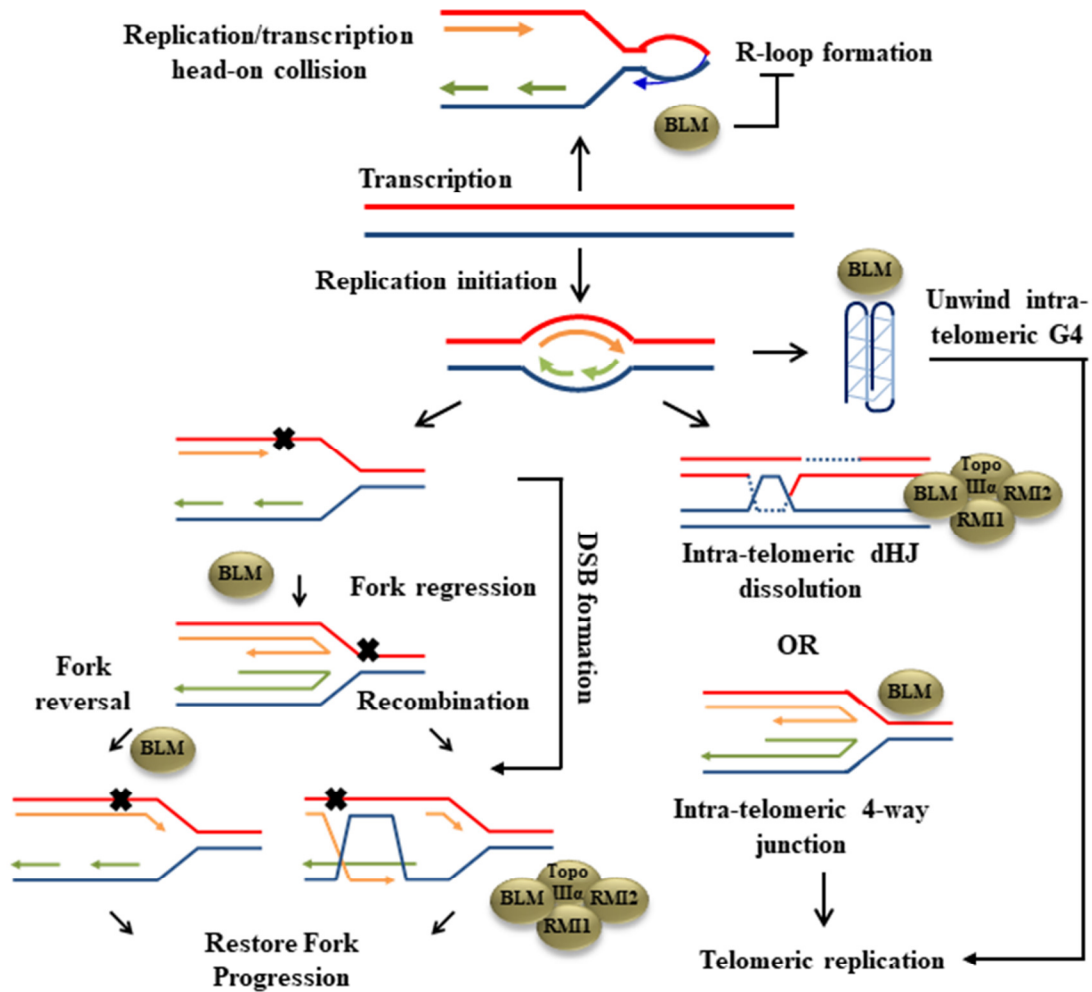
Figure 1.5. Known and putative functions of the BLM helicase
A summary of known and putative functions of BLM in DNA repair, recombination and replication to maintain genomic stability.

absence of this phosphorylation, while phosphorylation at T99 enhances its localization with the

DSB markers γ-H2AX and 53BP1 [131, 234, 269]. BLM is also a substrate for constitutive

phosphorylation by Chk1 and Chk2 kinases at residue S646, which decreases upon DNA damage

and is thought to aid BLM localization to damage sites [233, 270].

Regulation of sub-cellular localization of BLM

BLM localizes to discrete sub-nuclear structures known as PML bodies (PML-NBs) in

the absence of DNA damage [271]. PML-NBs are associated with a role in damage sensing and

also harbor other DDR factors like the MRN complex, Rad51/52, p53, TopBP1 and Topo IIIα [272]. Significantly, all these factors are known BLM interactors. With its ability to associate with the small ubiquitin-like modifier SUMO, it is thought that PML-NB interacting proteins contain SUMO interacting motifs (SIM) and localize to SUMOylated PML-NBs [272]. Consistent with this, BLM contains two SIMs at residues 217-220 and 235-238 which have been shown to be critical for its localization to PML-NBs [273]. Furthermore, BLM function in DNA damage response is negatively regulated by SUMOylation at K317 and K337 [274]. Mono-ubiquitinated BLM also localizes to PML-NBs in an anti-recombinogenic mechanism which suppresses excessive HR [275]. BLM is phosphorylated in the absence of DNA damage on S714 and T766 by Cdc2, which is thought to exclude it from chromatin binding without impacting its ability to form the BTR complex [276, 277]. MPS1 phosphorylates BLM at S144, playing a role in spindle assembly checkpoint (SAC) to ensure faithful segregation of chromosome [278]. Appropriate SAC function is critical in preventing chromosome loss and aneuploidy, and this lack of this role of BLM might explain the chromosomal instability observed in BS cells.

PTMs regulate the pro- and anti-recombinogenic activities of BLM

It is speculated that phosphorylation by Chk1, Chk2 [233, 270] and MPS1 [276, 277] which impact the recruitment of BLM to chromatin could be involved in regulating its role in the end resection step of HR mediated DSBR. The phosphorylation of BLM at T99 is involved in association with 53BP1 and RIF1 to suppress the CtIP/MRE11- initiated error-prone alternative end-joining (A-EJ) repair pathway after the end resection step [279]. SUMOylation of BLM has been shown to enhance interaction with Rad51, and might regulate the pro- and anti-recombinogenic functions of BLM during the strand invasion step of the HR mediated DSBR pathway [280]. The recruitment of BLM to stalled replication forks to perform an anti-

32

recombinogenic role in association with 53BP1 is regulated by poly-ubiquitination at K105, K225, and K259 [232, 235].

Regulation of BLM by TopBP1 and MIB1

BLM expression levels are low in G1, peak during S phase and persist in G2 phase, consistent with its known functions in the HR pathways [89, 276, 281]. It is suggested that the E3 ubiquitin ligase MIB1 ubiquitinates BLM at residues K38 and K39/40 and targets for proteasome mediated degradation in G1 [89]. On the other hand, phosphorylation of BLM at S338 enhances its interaction with TopBP1 and stabilizes it [89]. BLM stabilization by TopBP1 binding appears to be debatable, with another study showing that phosphorylation of BLM at S304 is necessary for TopBP1 interaction, while the interaction itself is not required for BLM stability in S phase [186].

HYPOTHESES AND AIMS

Defects in BLM cause Bloom syndrome (BS) is an autosomal recessive disorder characterized by subfertility, short stature and highly elevated predisposition to cancer. Functional characterizations have identified deleterious as well as hypomorphic *BLM* alleles in a humanized yeast model. Furthermore, SNPs in *BLM* have been found in human tumor samples. We rank and functionally characterize nonsynonymous SNPs in the *BLM* coding region to investigate their functional significance. We hypothesize that *BLM* contains additional risk-associated rare variations which might increase susceptibility to the disease, apart from an increased cancer risk. BLM is an important replication stress response factor, functioning to facilitate replication fork restart and suppress illegitimate recombination events to maintain genomic stability. Most studies evaluating the role of BLM in replication have focused on its role

33

in response to replication stress. And despite BS cells exhibiting a host of replication defects in the absence of any exogenous stress, the current understanding of a role for BLM in an unperturbed S phase is limited. BLM expression peaking in S phase and its affinity to a variety of non-canonical DNA substrates suggest a role beyond replication stress response as well. Identifying novel interactors of BLM in S phase is warranted to investigate its role in pathways during unperturbed replication. Cell lines established from BS patients are aneuploid, with some uncertainty regarding the nature of chromosomal instability and gene product dosage in such cells. We generate and functionally characterize a diploid *BLM* knockout cell line and in conjunction with its isogenic parental cell line perform a proteomic-based screen to identify novel BLM interactors. Members of the RecQ helicase family have been shown to interact with various components involved in replication associated pathways. We hypothesize that BLM associates with similar components in an undisturbed S phase and assist in maintaining replication fork progression. The following specific aims have been designed to test these hypotheses:

AIM 1 (Chapter two): Assess the ability of uncharacterized BLM variants of uncertain significance to complement cellular defects in BLM deficient human cells.

AIM 2 (Chapter three): Generate a diploid *BLM* knockout cell line using CRISPR/Cas9-mediated genome engineering and characterize the cellular defects in DNA repair and the DNA damage response.

AIM 3 (Chapter four): Determine the composition of the BLM complex in unperturbed S phase and determine the functional significance of novel BLM interactions.

REFERENCES

1. Guo, R.-B., et al., *Structural and functional analyses of disease-causing missense mutations in Bloom syndrome protein.* Nucleic acids research, 2007. **35**(18): p. 6297-6310.

2. Newman, J.A., et al., *Crystal structure of the Bloom's syndrome helicase indicates a role for the HRDC domain in conformational changes.* Nucleic Acids Res, 2015. **43**(10): p. 5221-35.

3. Croteau, D.L., et al., *Human RecQ Helicases in DNA Repair, Recombination, and Replication.* Annual Review of Biochemistry, 2014. **83**(1): p. 519-552.

4. Vindigni, A. and I.D. Hickson, *RecQ helicases: Multiple structures for multiple functions?* HFSP Journal, 2009. **3**(3): p. 153-164.

5. Aguilera, A. and T. García-Muse, *Causes of Genome Instability.* Annual Review of Genetics, 2013. **47**(1): p. 1-32.

6. Aguilera, A. and B. Gómez-González, *Genome instability: a mechanistic view of its causes and consequences.* Nature Reviews Genetics, 2008. **9**: p. 204.

7. Vijg, J. and Y. Suh, *Genome Instability and Aging.* Annual Review of Physiology, 2013. **75**(1): p. 645-668.

8. Soultanas, P. and D.B. Wigley, *Unwinding the 'Gordian knot' of helicase action.* Trends Biochem Sci, 2001. **26**(1): p. 47-54.

9. van Brabant, A.J., R. Stan, and N.A. Ellis, *DNA helicases, genomic instability, and human genetic disease.* Annu Rev Genomics Hum Genet, 2000. **1**: p. 409-59.

10. Gorbalenya, A.E. and E.V. Koonin, *Helicases: amino acid sequence comparisons and structure-function relationships.* Current Opinion in Structural Biology, 1993. **3**(3): p. 419-429.

11. Singleton, M.R., M.S. Dillingham, and D.B. Wigley, *Structure and Mechanism of Helicases and Nucleic Acid Translocases.* Annual Review of Biochemistry, 2007. **76**(1): p. 23-50.

12. Prlić, A., et al., *NGL viewer: web-based molecular graphics for large complexes.* Bioinformatics, 2018. **34**(21): p. 3755-3758.

13. Muftuoglu, M., et al., *The clinical characteristics of Werner syndrome: molecular and biochemical diagnosis.* Human genetics, 2008. **124**(4): p. 369-377.

14. Fairman-Williams, M.E., U.-P. Guenther, and E. Jankowsky, *SF1 and SF2 helicases: family matters.* Current Opinion in Structural Biology, 2010. **20**(3): p. 313-324.

15. Shastri, V.M. and K.H. Schmidt, *Cellular defects caused by hypomorphic variants of the Bloom syndrome helicase gene BLM.* Molecular Genetics & Genomic Medicine, 2016. **4**(1): p. 106-119.

16. Maloisel, L., F. Fabre, and S. Gangloff, *DNA polymerase delta is preferentially recruited during homologous recombination to promote heteroduplex DNA extension.* Molecular and cellular biology, 2008. **28**(4): p. 1373-1382.

17. Büttner, K., S. Nehring, and K.-P. Hopfner, *Structural basis for DNA duplex separation by a superfamily-2 helicase.* Nature Structural &Amp; Molecular Biology, 2007. **14**: p. 647.

18. Bartyik, K., et al., *Rothmund-thomson syndrome and cutan T-cell lymphoma in childhood.* Open Journal of Pediatrics, 2013. **3**: p. 270-273.

19. Wang, L.L., et al., *Clinical manifestations in a cohort of 41 Rothmund-Thomson syndrome patients.* American Journal of Medical Genetics, 2001. **102**(1): p. 11-17.

20. Hickson, I.D., *RecQ helicases: caretakers of the genome.* Nature Reviews Cancer, 2003. **3**: p. 169.

21. Nakayama, H., *RecQ family helicases: roles as tumor suppressor proteins.* Oncogene, 2002. **21**: p. 9008.

22. Brosh, R.M., Jr., *DNA helicases involved in DNA repair and their roles in cancer.* Nature reviews. Cancer, 2013. **13**(8): p. 542-558.

23. Suhasini, A.N. and R.M. Brosh, Jr., *DNA helicases associated with genetic instability, cancer, and aging.* Advances in experimental medicine and biology, 2013. **767**: p. 123-144.

24. Nakayama, H., et al., *Isolation and genetic characterization of a thymineless death-resistant mutant of Escherichia coli K12: Identification of a new mutation (recQ1) that blocks the RecF recombination pathway.* Molecular and General Genetics MGG, 1984. **195**(3): p. 474-480.

25. Bachrati, C.Z. and I.D. Hickson, *RecQ helicases: suppressors of tumorigenesis and premature aging.* Biochemical Journal, 2003. **374**(3): p. 577.

26. Bachrati, C.Z. and I.D. Hickson, *RecQ helicases: guardian angels of the DNA replication fork.* Chromosoma, 2008. **117**(3): p. 219-33.

27. Bohr, V.A., *Rising from the RecQ-age: the role of human RecQ helicases in genome maintenance.* Trends in biochemical sciences, 2008. **33**(12): p. 609-620.

28. Lohman, T.M., E.J. Tomko, and C.G. Wu, *Non-hexameric DNA helicases and translocases: mechanisms and regulation.* Nat Rev Mol Cell Biol, 2008. **9**(5): p. 391-401.

29.   von Hippel, P.H., *Helicases become mechanistically simpler and functionally more complex.* Nat Struct Mol Biol, 2004. **11**(6): p. 494-6.

30.   Bernstein, K.A., S. Gangloff, and R. Rothstein, *The RecQ DNA helicases in DNA repair.* Annual review of genetics, 2010. **44**: p. 393-417.

31.   Bernstein, D.A. and J.L. Keck, *Domain mapping of Escherichia coli RecQ defines the roles of conserved N- and C-terminal regions in the RecQ family.* Nucleic Acids Research, 2003. **31**(11): p. 2778-2785.

32.   Bahr, A., et al., *Point mutations causing Bloom's syndrome abolish ATPase and DNA helicase activities of the BLM protein.* Oncogene, 1998. **17**: p. 2565.

33.   Onoda, F., et al., *Elevation of sister chromatid exchange in Saccharomyces cerevisiae sgs1 disruptants and the relevance of the disruptants as a system to evaluate mutations in Bloom's syndrome gene.* Mutation Research/DNA Repair, 2000. **459**(3): p. 203-209.

34.   Garcia, P.L., et al., *Human RECQ5β, a protein with DNA helicase and strand-annealing activities in a single polypeptide.* The EMBO Journal, 2004. **23**(14): p. 2882-2891.

35.   Enemark, E.J. and L. Joshua-Tor, *On helicases and other motor proteins.* Current opinion in structural biology, 2008. **18**(2): p. 243-257.

36.   Bernstein, D.A., M.C. Zittel, and J.L. Keck, *High-resolution structure of the E.coli RecQ helicase catalytic core.* Embo j, 2003. **22**(19): p. 4910-21.

37.   Kitano, K., *Structural mechanisms of human RecQ helicases WRN and BLM.* Front Genet, 2014. **5**: p. 366.

38.   Lucic, B., et al., *A prominent β-hairpin structure in the winged-helix domain of RECQ1 is required for DNA unwinding and oligomer formation.* Nucleic acids research, 2011. **39**(5): p. 1703-1717.

39.   Pike, A.C., et al., *Structure of the human RECQ1 helicase reveals a putative strand-separation pin.* Proc Natl Acad Sci U S A, 2009. **106**(4): p. 1039-44.

40.   Mirzaei, H. and K.H. Schmidt, *Non-Bloom syndrome-associated partial and total loss-of-function variants of BLM helicase.* Proceedings of the National Academy of Sciences, 2012. **109**(47): p. 19357.

41.   Ellis, N.A., et al., *The Bloom's syndrome gene product is homologous to RecQ helicases.* Cell, 1995. **83**(4): p. 655-66.

42.   Mojumdar, A., et al., *The Human RecQ4 Helicase Contains a Functional RecQ C-terminal Region (RQC) That Is Essential for Activity.* Journal of Biological Chemistry, 2017. **292**(10): p. 4176-4184.

43.   Vindigni, A., F. Marino, and O. Gileadi, *Probing the structural basis of RecQ helicase function.* Biophysical Chemistry, 2010. **149**(3): p. 67-77.

44.   Kaiser, S., F. Sauer, and C. Kisker, *The structural and functional characterization of human RecQ4 reveals insights into its helicase mechanism.* Nature Communications, 2017. **8**: p. 15907.

45.   Janscak, P., et al., *Characterization and mutational analysis of the RecQ core of the bloom syndrome protein.* J Mol Biol, 2003. **330**(1): p. 29-42.

46.   Ren, H., et al., *The zinc-binding motif of human RECQ5β suppresses the intrinsic strand-annealing activity of its DExH helicase domain and is essential for the helicase activity of the enzyme.* Biochemical Journal, 2008. **412**(3): p. 425-433.

47.   Sami, F., et al., *Site-directed mutants of human RECQ1 reveal functional importance of the zinc binding domain.* Mutation Research/Fundamental and Molecular Mechanisms of Mutagenesis, 2016. **790**: p. 8-18.

48.   Zargarian, L., et al., *Structural and functional characterizations reveal the importance of a zinc binding domain in Bloom's syndrome helicase.* Nucleic Acids Research, 2005. **33**(10): p. 3109-3124.

49.   Liu, J.L., et al., *The zinc finger motif of Escherichia coli RecQ is implicated in both DNA binding and protein folding.* J Biol Chem, 2004. **279**(41): p. 42794-802.

50.   Gyimesi, M., et al., *Complex activities of the human Bloom's syndrome helicase are encoded in a core region comprising the RecA and Zn-binding domains.* Nucleic Acids Res, 2012. **40**(9): p. 3952-63.

51.   Kitano, K., S.Y. Kim, and T. Hakoshima, *Structural basis for DNA strand separation by the unconventional winged-helix domain of RecQ helicase WRN.* Structure, 2010. **18**(2): p. 177-87.

52.   Manthei, K.A., et al., *Structural mechanisms of DNA binding and unwinding in bacterial RecQ helicases.* Proc Natl Acad Sci U S A, 2015. **112**(14): p. 4292-7.

53.   Pike, A.C., et al., *Human RECQ1 helicase-driven DNA unwinding, annealing, and branch migration: insights from DNA complex structures.* Proc Natl Acad Sci U S A, 2015. **112**(14): p. 4286-91.

54.   Huber, M.D., et al., *A conserved G4 DNA binding domain in RecQ family helicases.* J Mol Biol, 2006. **358**(4): p. 1071-80.

55.   von Kobbe, C., et al., *Werner syndrome protein contains three structure-specific DNA binding domains.* J Biol Chem, 2003. **278**(52): p. 52997-3006.

56.   Morozov, V., et al., *A putative nucleic acid-binding domain in Bloom's and Werner's syndrome helicases.* Trends Biochem Sci, 1997. **22**(11): p. 417-8.

57.   Bernstein, D.A. and J.L. Keck, *Conferring substrate specificity to DNA helicases: role of the RecQ HRDC domain.* Structure, 2005. **13**(8): p. 1173-82.

58.   Kitano, K., N. Yoshihara, and T. Hakoshima, *Crystal structure of the HRDC domain of human Werner syndrome protein, WRN.* J Biol Chem, 2007. **282**(4): p. 2717-28.

59.   Killoran, M.P. and J.L. Keck, *Structure and function of the regulatory C-terminal HRDC domain from Deinococcus radiodurans RecQ.* Nucleic Acids Res, 2008. **36**(9): p. 3139-49.

60.   Liu, Z., et al., *The three-dimensional structure of the HRDC domain and implications for the Werner and Bloom syndrome proteins.* Structure, 1999. **7**(12): p. 1557-66.

61.   Kim, Y.M. and B.S. Choi, *Structure and function of the regulatory HRDC domain from human Bloom syndrome protein.* Nucleic Acids Res, 2010. **38**(21): p. 7764-77.

62.   Sato, A., et al., *Solution structure of the HRDC domain of human Bloom syndrome protein BLM.* J Biochem, 2010. **148**(4): p. 517-25.

63.   Bennett, R.J., J.A. Sharp, and J.C. Wang, *Purification and characterization of the Sgs1 DNA helicase activity of Saccharomyces cerevisiae.* J Biol Chem, 1998. **273**(16): p. 9644-50.

64.   Lu, J., et al., *Human homologues of yeast helicase.* Nature, 1996. **383**(6602): p. 678-9.

65.   Wu, L., et al., *The HRDC domain of BLM is required for the dissolution of double Holliday junctions.* Embo j, 2005. **24**(14): p. 2679-87.

66.   Cheok, C.F., et al., *The Bloom's syndrome helicase promotes the annealing of complementary single-stranded DNA.* Nucleic Acids Res, 2005. **33**(12): p. 3932-41.

67.   Wu, L. and I.D. Hickson, *The Bloom's syndrome helicase suppresses crossing over during homologous recombination.* Nature, 2003. **426**(6968): p. 870-4.

68.   Popuri, V., et al., *The human RecQ helicases, BLM and RECQ1, display distinct DNA substrate specificities.* Journal of Biological Chemistry, 2008. **283**(26): p. 17766-17776.

69.   Cui, S., et al., *Characterization of the DNA-unwinding activity of human RECQ1, a helicase specifically stimulated by human replication protein A.* Journal of Biological Chemistry, 2003. **278**(3): p. 1424-1432.

70.   Rossi, M.L., et al., *Conserved helicase domain of human RecQ4 is required for strand annealing-independent DNA unwinding.* DNA Repair, 2010. **9**(7): p. 796-804.

71.   Ferrarelli, L.K., et al., *The RECQL4 protein, deficient in Rothmund-Thomson syndrome is active on telomeric D-loops containing DNA metabolism blocking lesions.* DNA Repair, 2013. **12**(7): p. 518-528.

72.   Sharma, S., et al., *Biochemical analysis of the DNA unwinding and strand annealing activities catalyzed by human RECQ1.* Journal of Biological Chemistry, 2005. **280**(30): p. 28072-28084.

73.   Ghosh, A., et al., *Telomeric D-loops Containing 8-Oxo-2 '-deoxyguanosine Are Preferred Substrates for Werner and Bloom Syndrome Helicases and Are Bound by POT1.* Journal of Biological Chemistry, 2009. **284**(45): p. 31074-31084.

74.   Xu, X.H. and Y.L. Liu, *Dual DNA unwinding activities of the Rothmund-Thomson syndrome protein, RECQ4.* Embo Journal, 2009. **28**(5): p. 568-577.

75.   Cejka, P., et al., *Decatenation of DNA by the S. cerevisiae Sgs1-Top3-Rmi1 and RPA Complex: A Mechanism for Disentangling Chromosomes.* Molecular Cell, 2012. **47**(6): p. 886-896.

76.   Han, H.Y., R.J. Bennett, and L.H. Hurley, *Inhibition of unwinding of G-quadruplex structures by Sgs1 helicase in the presence of N,N '-bis[2-(1-piperidino)ethyl]-3,4,9,10-perylenetetracarboxylic diimide, a G-quadruplex-interactive ligand.* Biochemistry, 2000. **39**(31): p. 9311-9316.

77.   Iannascoli, C., et al., *The WRN exonuclease domain protects nascent strands from pathological MRE11/EXO1-dependent degradation.* Nucleic Acids Res, 2015. **43**(20): p. 9788-803.

78.   Burks, L.M., J. Yin, and S.E. Plon, *Nuclear import and retention domains in the amino terminus of RECQL4.* Gene, 2007. **391**(1-2): p. 26-38.

79.   Kaneko, H., et al., *BLM (the causative gene of Bloom syndrome) protein translocation into the nucleus by a nuclear localization signal.* Biochem Biophys Res Commun, 1997. **240**(2): p. 348-53.

80.   Sakurai, H., et al., *RecQ5 Protein Translocation into the Nucleus by a Nuclear Localization Signal.* Biological and Pharmaceutical Bulletin, 2013. **36**(7): p. 1159-1166.

81.   Shimamoto, A., et al., *Human RecQ5beta, a large isomer of RecQ5 DNA helicase, localizes in the nucleoplasm and interacts with topoisomerases 3alpha and 3beta.* Nucleic Acids Res, 2000. **28**(7): p. 1647-55.

82.   Cheok, C.F., et al., *Roles of the Bloom's syndrome helicase in the maintenance of genome stability.* Biochem Soc Trans, 2005. **33**(Pt 6): p. 1456-9.

83.   Sidorova, J.M. and R.J. Monnat Jr, *Human RECQ helicases: roles in cancer, aging, and inherited disease.* Advances in Genomics and Genetics, 2014. **5**: p. 19-33.

84.   Hickson, I.D., *RecQ helicases: caretakers of the genome.* Nat Rev Cancer, 2003. **3**(3): p. 169-78.

85. Urban, V., J. Dobrovolna, and P. Janscak, *Distinct functions of human RecQ helicases during DNA replication.* Biophysical Chemistry, 2017. **225**: p. 20-26.

86. Harrigan, J.A. and V.A. Bohr, *Human diseases deficient in RecQ helicases.* Biochimie, 2003. **85**(11): p. 1185-1193.

87. Wang, L.L., et al., *Clinical manifestations in a cohort of 41 Rothmund-Thomson syndrome patients.* Am J Med Genet, 2001. **102**(1): p. 11-7.

88. Lindor, N.M., et al., *Rothmund-Thomson syndrome due to RECQ4 helicase mutations: report and clinical and molecular comparisons with Bloom syndrome and Werner syndrome.* Am J Med Genet, 2000. **90**(3): p. 223-8.

89. Wang, J., J. Chen, and Z. Gong, *TopBP1 Controls BLM Protein Level to Maintain Genome Stability.* Molecular Cell, 2013. **52**(5): p. 667-678.

90. Smith, P.J. and M.C. Paterson, *Enhanced radiosensitivity and defective DNA repair in cultured fibroblasts derived from Rothmund Thomson syndrome patients.* Mutat Res, 1982. **94**(1): p. 213-28.

91. Prache-de-Carrere, B., et al., *[Rothmund-Thomson syndrome with reduced DNA repair capacity].* Ann Dermatol Venereol, 1996. **123**(6-7): p. 395-7.

92. Shinya, A., et al., *A case of Rothmund-Thomson syndrome with reduced DNA repair capacity.* Arch Dermatol, 1993. **129**(3): p. 332-6.

93. Kitao, S., et al., *Cloning of two new human helicase genes of the RecQ family: biological significance of multiple species in higher eukaryotes.* Genomics, 1998. **54**(3): p. 443-52.

94. Kitao, S., et al., *Mutations in RECQL4 cause a subset of cases of Rothmund-Thomson syndrome.* Nat Genet, 1999. **22**(1): p. 82-4.

95. Wang, L.L., et al., *Association between osteosarcoma and deleterious mutations in the RECQL4 gene in Rothmund-Thomson syndrome.* J Natl Cancer Inst, 2003. **95**(9): p. 669-74.

96. Wang, L.L., et al., *Intron-Size Constraint as a Mutational Mechanism in Rothmund-Thomson Syndrome.* The American Journal of Human Genetics, 2002. **71**(1): p. 165-167.

97. Epstein, C.J., et al., *Werner's syndrome a review of its symptomatology, natural history, pathologic features, genetics and relationship to the natural aging process.* Medicine (Baltimore), 1966. **45**(3): p. 177-221.

98. Fukuchi, K., G.M. Martin, and R.J. Monnat, Jr., *Mutator phenotype of Werner syndrome is characterized by extensive deletions.* Proc Natl Acad Sci U S A, 1989. **86**(15): p. 5893-7.

99.   Salk, D., et al., *Cytogenetics of Werner's syndrome cultured skin fibroblasts: variegated translocation mosaicism.* Cytogenet Cell Genet, 1981. **30**(2): p. 92-107.

100.   Brosh, R.M., Jr. and V.A. Bohr, *Roles of the Werner syndrome protein in pathways required for maintenance of genome stability.* Exp Gerontol, 2002. **37**(4): p. 491-506.

101.   Bloom, D., *Congenital telangiectatic erythema resembling lupus erythematosus in dwarfs; probably a syndrome entity.* AMA Am J Dis Child, 1954. **88**(6): p. 754-8.

102.   Cunniff, C., J.A. Bassetti, and N.A. Ellis, *Bloom's Syndrome: Clinical Spectrum, Molecular Pathogenesis, and Cancer Predisposition.* Molecular syndromology, 2017. **8**(1): p. 4-23.

103.   German, J., *Bloom's syndrome. I. Genetical and clinical observations in the first twenty-seven patients.* Am J Hum Genet, 1969. **21**(2): p. 196-227.

104.   German, J., R. Archibald, and D. Bloom, *CHROMOSOMAL BREAKAGE IN A RARE AND PROBABLY GENETICALLY DETERMINED SYNDROME OF MAN.* Science, 1965. **148**(3669): p. 506-7.

105.   German, J., *Bloom's syndrome. XX. The first 100 cancers.* Cancer Genet Cytogenet, 1997. **93**(1): p. 100-6.

106.   Sanz, M.M., J. German, and C. Cunniff, *Bloom's Syndrome.* Gene Reviews., ed. R.A. Pagon, M.P. Adam, and H.H. Ardinger. 1993-2019. Initial Posting: March 22, 2006; Last Update: February 14, 2019, Seattle.: University of Washington.

107.   Chaganti, R.S., S. Schonberg, and J. German, *A manyfold increase in sister chromatid exchanges in Bloom's syndrome lymphocytes.* Proc Natl Acad Sci U S A, 1974. **71**(11): p. 4508-12.

108.   German, J., and Ellis, N. A., *Bloom syndrome.* The genetic basis of human cancer, ed. K.W.K. B. Vogelstein. 1998, New York: McGraw-Hill, Health Professions Division.

109.   German, J.a.P., E., *Bloom's syndrome. XII. Report from the Registry for 1987.* Clin Genet, 1989. **35**(1): p. 57-69.

110.   McDaniel, L.D. and R.A. Schultz, *Elevated sister chromatid exchange phenotype of Bloom syndrome cells is complemented by human chromosome 15.* Proceedings of the National Academy of Sciences of the United States of America, 1992. **89**(17): p. 7968-7972.

111.   Keller, C., et al., *Growth deficiency and malnutrition in Bloom syndrome.* J Pediatr, 1999. **134**(4): p. 472-9.

112.   Diaz, A., et al., *Evaluation of short stature, carbohydrate metabolism and other endocrinopathies in Bloom's syndrome.* Horm Res, 2006. **66**(3): p. 111-7.

113. Renes, J.S., et al., *Bloom syndrome in short children born small for gestational age: a challenging diagnosis.* J Clin Endocrinol Metab, 2013. **98**(10): p. 3932-8.

114. Arora, H., et al., *Bloom syndrome.* Int J Dermatol, 2014. **53**(7): p. 798-802.

115. Jian-Bing, W., et al., *A case of Bloom syndrome with uncommon clinical manifestations confirmed on genetic testing.* Cutis, 2016. **97**(2): p. E10-3.

116. McGowan, J., J. Maize, and J. Cook, *Lupus-like histopathology in bloom syndrome: reexamining the clinical and histologic implications of photosensitivity.* Am J Dermatopathol, 2009. **31**(8): p. 786-91.

117. Cunniff, C., et al., *Health supervision for people with Bloom syndrome.* Am J Med Genet A, 2018. **176**(9): p. 1872-1881.

118. Kaneko, H. and N. Kondo, *Clinical features of Bloom syndrome and function of the causative gene, BLM helicase.* Expert Rev Mol Diagn, 2004. **4**(3): p. 393-401.

119. Nair, G., et al., *Bloom syndrome with lung involvement.* Lung India, 2009. **26**(3): p. 92-4.

120. Relhan, V., et al., *Bloom syndrome with extensive pulmonary involvement in a child.* Indian J Dermatol, 2015. **60**(2): p. 217.

121. Kauli, R., et al., *Gonadal function in Bloom's syndrome.* Clin Endocrinol (Oxf), 1977. **6**(4): p. 285-9.

122. Masmoudi, A., et al., *Clinical and laboratory findings in 8 patients with Bloom's syndrome.* J Dermatol Case Rep, 2012. **6**(1): p. 29-33.

123. Groden, J. and J. German, *Bloom's syndrome. XVIII. Hypermutability at a tandem-repeat locus.* Hum Genet, 1992. **90**(4): p. 360-7.

124. Groden, J., Y. Nakamura, and J. German, *Molecular evidence that homologous recombination occurs in proliferating human somatic cells.* Proc Natl Acad Sci U S A, 1990. **87**(11): p. 4315-9.

125. Lonn, U., et al., *An abnormal profile of DNA replication intermediates in Bloom's syndrome.* Cancer Res, 1990. **50**(11): p. 3141-5.

126. Rassool, F.V., et al., *Constitutive DNA damage is linked to DNA replication abnormalities in Bloom's syndrome cells.* Oncogene, 2003. **22**: p. 8749.

127. Rao, V.A., et al., *Endogenous γ-H2AX-ATM-Chk2 Checkpoint Activation in Bloom's Syndrome Helicase–Deficient Cells Is Related to DNA Replication Arrested Forks.* Molecular Cancer Research, 2007. **5**(7): p. 713-724.

128. Sidorova, J.M., et al., *Distinct functions of human RECQ helicases WRN and BLM in replication fork recovery and progression after hydroxyurea-induced stalling.* DNA repair, 2013. **12**(2): p. 128-139.

129. Davalos, A.R. and J. Campisi, *Bloom syndrome cells undergo p53-dependent apoptosis and delayed assembly of BRCA1 and NBS1 repair complexes at stalled replication forks.* J Cell Biol, 2003. **162**(7): p. 1197-209.

130. Franchitto, A. and P. Pichierri, *Bloom's syndrome protein is required for correct relocalization of RAD50/MRE11/NBS1 complex after replication fork arrest.* J Cell Biol, 2002. **157**(1): p. 19-30.

131. Davies, S.L., P.S. North, and I.D. Hickson, *Role for BLM in replication-fork restart and suppression of origin firing after replicative stress.* Nature Structural &Amp; Molecular Biology, 2007. **14**: p. 677.

132. Chang, E.Y.-C., et al., *RECQ-like helicases Sgs1 and BLM regulate R-loop-associated genome instability.* The Journal of cell biology, 2017. **216**(12): p. 3991-4005.

133. Poot, M., et al., *Cell kinetic evidence suggests elevated oxidative stress in cultured cells of Bloom's syndrome.* Free Radic Res Commun, 1989. **7**(3-6): p. 179-87.

134. Nicotera, T.M., *Molecular and biochemical aspects of Bloom's syndrome.* Cancer Genet Cytogenet, 1991. **53**(1): p. 1-13.

135. Zatterale, A., et al., *Oxidative stress biomarkers in four Bloom syndrome (BS) patients and in their parents suggest in vivo redox abnormalities in BS phenotype.* Clin Biochem, 2007. **40**(15): p. 1100-3.

136. Maciejczyk, M., et al., *Oxidative stress, mitochondrial abnormalities and antioxidant defense in Ataxia-telangiectasia, Bloom syndrome and Nijmegen breakage syndrome.* Redox biology, 2016. **11**: p. 375-383.

137. McDaniel, L.D. and R.A. Schultz, *Elevated sister chromatid exchange phenotype of Bloom syndrome cells is complemented by human chromosome 15.* Proc Natl Acad Sci U S A, 1992. **89**(17): p. 7968-72.

138. German, J., et al., *Bloom syndrome: an analysis of consanguineous families assigns the locus mutated to chromosome band 15q26.1.* Proc Natl Acad Sci U S A, 1994. **91**(14): p. 6669-73.

139. Ellis, N.A., et al., *Linkage disequilibrium between the FES, D15S127, and BLM loci in Ashkenazi Jews with Bloom syndrome.* Am J Hum Genet, 1994. **55**(3): p. 453-60.

140. Ellis, N.A., et al., *Somatic intragenic recombination within the mutated locus BLM can correct the high sister-chromatid exchange phenotype of Bloom syndrome cells.* American journal of human genetics, 1995. **57**(5): p. 1019-1027.

141. German, J., et al., *Bloom's syndrome. IV. Sister-chromatid exchanges in lymphocytes.* Am J Hum Genet, 1977. **29**(3): p. 248-55.

142. Weksberg, R., et al., *Bloom syndrome: a single complementation group defines patients of diverse ethnic origin.* Am J Hum Genet, 1988. **42**(6): p. 816-24.

143. German, J., et al., *Bloom's syndrome. VI. The disorder in Israel and an estimation of the gene frequency in the Ashkenazim.* Am J Hum Genet, 1977. **29**(6): p. 553-62.

144. Ellis, N.A., et al., *The Ashkenazic Jewish Bloom syndrome mutation blmAsh is present in non-Jewish Americans of Spanish ancestry.* American journal of human genetics, 1998. **63**(6): p. 1685-1693.

145. Gruber, S.B., et al., *BLM heterozygosity and the risk of colorectal cancer.* Science, 2002. **297**(5589): p. 2013.

146. Li, L., et al., *Carrier frequency of the Bloom syndrome blmAsh mutation in the Ashkenazi Jewish population.* Mol Genet Metab, 1998. **64**(4): p. 286-90.

147. Risch, N., et al., *Geographic distribution of disease mutations in the Ashkenazi Jewish population supports genetic drift over selection.* Am J Hum Genet, 2003. **72**(4): p. 812-22.

148. Roa, B.B., C.V. Savino, and C.S. Richards, *Ashkenazi Jewish population frequency of the Bloom syndrome gene 2281 delta 6ins7 mutation.* Genet Test, 1999. **3**(2): p. 219-21.

149. German, J., et al., *Syndrome-causing mutations of the BLM gene in persons in the Bloom's Syndrome Registry.* Hum Mutat, 2007. **28**(8): p. 743-53.

150. Foucault, F., et al., *Characterization of a new BLM mutation associated with a topoisomerase II alpha defect in a patient with Bloom's syndrome.* Hum Mol Genet, 1997. **6**(9): p. 1427-34.

151. Barakat, A., et al., *Identification of a novel BLM missense mutation (2706T>C) in a Moroccan patient with Bloom's syndrome.* Hum Mutat, 2000. **15**(6): p. 584-5.

152. Rong, S.B., J. Valiaho, and M. Vihinen, *Structural basis of Bloom syndrome (BS) causing mutations in the BLM helicase domain.* Mol Med, 2000. **6**(3): p. 155-64.

153. Amor-Gueret, M., et al., *Three new BLM gene mutations associated with Bloom syndrome.* Genet Test, 2008. **12**(2): p. 257-61.

154. Goss, K.H., et al., *Enhanced tumor formation in mice heterozygous for Blm mutation.* Science, 2002. **297**(5589): p. 2051-3.

155. Cleary, S.P., et al., *Heterozygosity for the BLM(Ash) mutation and cancer risk.* Cancer Res, 2003. **63**(8): p. 1769-71.

156.   Zauber, N.P., et al., *Clinical and genetic findings in an Ashkenazi Jewish population with colorectal neoplasms.* Cancer, 2005. **104**(4): p. 719-29.

157.   Baris, H.N., et al., *Prevalence of breast and colorectal cancer in Ashkenazi Jewish carriers of Fanconi anemia and Bloom syndrome.* Isr Med Assoc J, 2007. **9**(12): p. 847-50.

158.   Laitman, Y., et al., *The risk for developing cancer in Israeli ATM, BLM, and FANCC heterozygous mutation carriers.* Cancer Genet, 2016. **209**(3): p. 70-4.

159.   Prokofyeva, D., et al., *Nonsense mutation p.Q548X in BLM, the gene mutated in Bloom's syndrome, is associated with breast cancer in Slavic populations.* Breast Cancer Res Treat, 2013. **137**(2): p. 533-9.

160.   Sokolenko, A.P., et al., *High prevalence and breast cancer predisposing role of the BLM c.1642 C>T (Q548X) mutation in Russia.* Int J Cancer, 2012. **130**(12): p. 2867-73.

161.   Antczak, A., et al., *A common nonsense mutation of the BLM gene and prostate cancer risk and survival.* Gene, 2013. **532**(2): p. 173-6.

162.   Bogdanova, N., et al., *Prevalence of the BLM nonsense mutation, p.Q548X, in ovarian cancer patients from Central and Eastern Europe.* Fam Cancer, 2015. **14**(1): p. 145-9.

163.   Wang, Q., et al., *Genome-wide haplotype association study identifies BLM as a risk gene for prostate cancer in Chinese population.* Tumour Biol, 2015. **36**(4): p. 2703-7.

164.   Ledet, E., et al., *Germline heterozygous BLM mutations and prostate cancer risk.* Journal of Clinical Oncology, 2019. **37**(7_suppl): p. 321-321.

165.   Thompson, E.R., et al., *Exome sequencing identifies rare deleterious mutations in DNA repair genes FANCC and BLM as potential breast cancer susceptibility alleles.* PLoS Genet, 2012. **8**(9): p. e1002894.

166.   Abecasis, G.R., et al., *A map of human genome variation from population-scale sequencing.* Nature, 2010. **467**(7319): p. 1061-73.

167.   de Voer, R.M., et al., *Deleterious Germline BLM Mutations and the Risk for Early-onset Colorectal Cancer.* Sci Rep, 2015. **5**: p. 14060.

168.   Ding, S.L., et al., *Genetic variants of BLM interact with RAD51 to increase breast cancer susceptibility.* Carcinogenesis, 2009. **30**(1): p. 43-9.

169.   Broberg, K., et al., *Association between polymorphisms in RMI1, TOP3A, and BLM and risk of cancer, a case-control study.* BMC Cancer, 2009. **9**(1): p. 140.

170.   Genomes Project, C., et al., *An integrated map of genetic variation from 1,092 human genomes.* Nature, 2012. **491**(7422): p. 56-65.

171.   Frankish, A., et al., *Ensembl 2018.* Nucleic Acids Research, 2017. **46**(D1): p. D754-D761.

172.   Gorlov, I.P., et al., *Evolutionary evidence of the effect of rare variants on disease etiology.* Clin Genet, 2011. **79**(3): p. 199-206.

173.   Sherry, S.T., et al., *dbSNP: the NCBI database of genetic variation.* Nucleic Acids Res, 2001 Jan 1. **29**(1): p. 308-11.

174.   Stenson, P.D., et al., *The Human Gene Mutation Database: towards a comprehensive repository of inherited mutation data for medical research, genetic diagnosis and next-generation sequencing studies.* Hum Genet, 2017. **136**(6): p. 665-677.

175.   Frank, B., et al., *Colorectal cancer and polymorphisms in DNA repair genes WRN, RMI1 and BLM.* Carcinogenesis, 2010. **31**(3): p. 442-5.

176.   Knudson, A.G., Jr., *Mutation and cancer: statistical study of retinoblastoma.* Proc Natl Acad Sci U S A, 1971. **68**(4): p. 820-3.

177.   Karow, J.K., R.K. Chakraverty, and I.D. Hickson, *The Bloom's Syndrome Gene Product Is a 3'-5' DNA Helicase.* Journal of Biological Chemistry, 1997. **272**(49): p. 30611-30614.

178.   Guo, R.B., et al., *Structural and functional characterizations reveal the importance of a zinc binding domain in Bloom's syndrome helicase.* Nucleic Acids Res, 2005. **33**(10): p. 3109-24.

179.   Swan, M.K., et al., *Structure of human Bloom's syndrome helicase in complex with ADP and duplex DNA.* Acta Crystallogr D Biol Crystallogr, 2014. **70**(Pt 5): p. 1465-75.

180.   Kim, S.Y., T. Hakoshima, and K. Kitano, *Structure of the RecQ C-terminal domain of human Bloom syndrome protein.* Sci Rep, 2013. **3**: p. 3294.

181.   Puranam, K.L. and P.J. Blackshear, *Cloning and characterization of RECQL, a potential human homologue of the Escherichia coli DNA helicase RecQ.* J Biol Chem, 1994. **269**(47): p. 29838-45.

182.   Suzuki, T., et al., *Diverged nuclear localization of Werner helicase in human and mouse cells.* Oncogene, 2001. **20**(20): p. 2551-8.

183.   Duan, Z., et al., *Characterization of the nuclear import pathway for BLM protein.* Arch Biochem Biophys, 2017. **634**: p. 57-68.

184.   Mirzaei, H., et al., *Sgs1 truncations induce genome rearrangements but suppress detrimental effects of BLM overexpression in Saccharomyces cerevisiae.* J Mol Biol, 2011. **405**(4): p. 877-91.

185. Wu, L., et al., *The Bloom's syndrome gene product interacts with topoisomerase III.* J Biol Chem, 2000. **275**(13): p. 9636-44.

186. Blackford, A.N., et al., *TopBP1 interacts with BLM to maintain genome stability but is dispensable for preventing BLM degradation.* Mol Cell, 2015. **57**(6): p. 1133-1141.

187. Braybrooke, J.P., et al., *Functional interaction between the Bloom's syndrome helicase and the RAD51 paralog, RAD51L3 (RAD51D).* J Biol Chem, 2003. **278**(48): p. 48357-66.

188. Brosh, R.M., et al., *Replication Protein A Physically Interacts with the Bloom's Syndrome Protein and Stimulates Its Helicase Activity.* Journal of Biological Chemistry, 2000. **275**(31): p. 23500-23508.

189. Kang, D., et al., *Interaction of replication protein A with two acidic peptides from human Bloom syndrome protein.* FEBS Lett, 2018. **592**(4): p. 547-558.

190. Selak, N., et al., *The Bloom's syndrome helicase (BLM) interacts physically and functionally with p12, the smallest subunit of human DNA polymerase δ.* Nucleic Acids Research, 2008. **36**(16): p. 5166-5179.

191. Wang, X.W., et al., *Functional interaction of p53 and BLM DNA helicase in apoptosis.* J Biol Chem, 2001. **276**(35): p. 32948-55.

192. Wu, W., et al., *HERC2 Facilitates BLM and WRN Helicase Complex Interaction with RPA to Suppress G-Quadruplex DNA.* Cancer Res, 2018. **78**(22): p. 6371-6385.

193. Karow, J.K., et al., *The Bloom's syndrome gene product promotes branch migration of holliday junctions.* Proc Natl Acad Sci U S A, 2000. **97**(12): p. 6504-8.

194. Jasin, M. and R. Rothstein, *Repair of strand breaks by homologous recombination.* Cold Spring Harbor perspectives in biology. **5**(11): p. a012740-a012740.

195. Sartori, A.A., et al., *Human CtIP promotes DNA end resection.* Nature, 2007. **450**(7169): p. 509-14.

196. Gravel, S., et al., *DNA helicases Sgs1 and BLM promote DNA double-strand break resection.* Genes Dev, 2008. **22**(20): p. 2767-72.

197. Nimonkar, A.V., et al., *BLM-DNA2-RPA-MRN and EXO1-BLM-RPA-MRN constitute two DNA end resection machineries for human DNA break repair.* Genes & development, 2011. **25**(4): p. 350-362.

198. Daley, J.M., et al., *Multifaceted role of the Topo IIIα-RMI1-RMI2 complex and DNA2 in the BLM-dependent pathway of DNA break end resection.* Nucleic acids research, 2014. **42**(17): p. 11083-11091.

199. Chen, H., M. Lisby, and L.S. Symington, *RPA coordinates DNA end resection and prevents formation of DNA hairpins.* Mol Cell, 2013. **50**(4): p. 589-600.

200. Daley, J.M., et al., *Enhancement of BLM-DNA2-Mediated Long-Range DNA End Resection by CtIP.* Cell reports, 2017. **21**(2): p. 324-332.

201. Nimonkar, A.V., et al., *Human exonuclease 1 and BLM helicase interact to resect DNA and initiate DNA repair.* Proc Natl Acad Sci U S A, 2008. **105**(44): p. 16906-11.

202. San Filippo, J., P. Sung, and H. Klein, *Mechanism of eukaryotic homologous recombination.* Annu Rev Biochem, 2008. **77**: p. 229-57.

203. Bussen, W., et al., *Holliday Junction Processing Activity of the BLM-Topo IIIα-BLAP75 Complex.* Journal of Biological Chemistry, 2007. **282**(43): p. 31484-31492.

204. Hu, P., et al., *Evidence for BLM and Topoisomerase IIIalpha interaction in genomic stability.* Hum Mol Genet, 2001. **10**(12): p. 1287-98.

205. Singh, T.R., et al., *BLAP18/RMI2, a novel OB-fold-containing protein, is an essential component of the Bloom helicase–double Holliday junction dissolvasome.* Genes & Development, 2008. **22**(20): p. 2856-2868.

206. Mankouri, H.W. and I.D. Hickson, *The RecQ helicase-topoisomerase III-Rmi1 complex: a DNA structure-specific 'dissolvasome'?* Trends Biochem Sci, 2007. **32**(12): p. 538-46.

207. Bachrati, C.Z. and I.D. Hickson, *Dissolution of double Holliday junctions by the concerted action of BLM and topoisomerase IIIalpha.* Methods Mol Biol, 2009. **582**: p. 91-102.

208. Bizard, A.H. and I.D. Hickson, *The dissolution of double Holliday junctions.* Cold Spring Harbor perspectives in biology. **6**(7): p. a016477-a016477.

209. Raynard, S., W. Bussen, and P. Sung, *A double Holliday junction dissolvasome comprising BLM, topoisomerase IIIalpha, and BLAP75.* J Biol Chem, 2006. **281**(20): p. 13861-4.

210. Raynard, S., et al., *Functional role of BLAP75 in BLM-topoisomerase IIIalpha-dependent holliday junction processing.* J Biol Chem, 2008. **283**(23): p. 15701-8.

211. Wu, L., et al., *Potential role for the BLM helicase in recombinational repair via a conserved interaction with RAD51.* J Biol Chem, 2001. **276**(22): p. 19375-81.

212. Bergeron, K.L., et al., *Critical interaction domains between bloom syndrome protein and RAD51.* The protein journal, 2011. **30**(1): p. 1-8.

213. Wang, Y., et al., *BASC, a super complex of BRCA1-associated proteins involved in the recognition and repair of aberrant DNA structures.* Genes Dev, 2000. **14**(8): p. 927-39.

214. Bugreev, D.V., et al., *Novel pro- and anti-recombination activities of the Bloom's syndrome helicase.* Genes Dev, 2007. **21**(23): p. 3085-94.

215. Patel, D.S., et al., *BLM helicase regulates DNA repair by counteracting RAD51 loading at DNA double-strand break sites.* The Journal of Cell Biology, 2017. **216**(11): p. 3521-3534.

216. Bachrati, C.Z., R.H. Borts, and I.D. Hickson, *Mobile D-loops are a preferred substrate for the Bloom's syndrome helicase.* Nucleic Acids Res, 2006. **34**(8): p. 2269-79.

217. Bugreev, D.V., O.M. Mazina, and A.V. Mazin, *Bloom syndrome helicase stimulates RAD51 DNA strand exchange activity through a novel mechanism.* J Biol Chem, 2009. **284**(39): p. 26349-59.

218. Liang, F., et al., *Homology-directed repair is a major double-strand break repair pathway in mammalian cells.* Proc Natl Acad Sci U S A, 1998. **95**(9): p. 5172-7.

219. Petermann, E. and T. Helleday, *Pathways of mammalian replication fork restart.* Nat Rev Mol Cell Biol, 2010. **11**(10): p. 683-7.

220. Wu, L., *Role of the BLM helicase in replication fork management.* DNA Repair, 2007. **6**(7): p. 936-944.

221. Jones, R.M. and E. Petermann, *Replication fork dynamics and the DNA damage response.* Biochem J, 2012. **443**(1): p. 13-26.

222. Machwe, A., et al., *The Werner and Bloom syndrome proteins catalyze regression of a model replication fork.* Biochemistry, 2006. **45**(47): p. 13939-46.

223. Ralf, C., I.D. Hickson, and L. Wu, *The Bloom's Syndrome Helicase Can Promote the Regression of a Model Replication Fork.* Journal of Biological Chemistry, 2006. **281**(32): p. 22839-22846.

224. Deans, A.J. and S.C. West, *FANCM connects the genome instability disorders Bloom's Syndrome and Fanconi Anemia.* Mol Cell, 2009. **36**(6): p. 943-53.

225. Meetei, A.R., et al., *A multiprotein nuclear complex connects Fanconi anemia and Bloom syndrome.* Mol Cell Biol, 2003. **23**(10): p. 3417-26.

226. Pichierri, P., A. Franchitto, and F. Rosselli, *BLM and the FANC proteins collaborate in a common pathway in response to stalled replication forks.* Embo j, 2004. **23**(15): p. 3154-63.

227. Hoadley, K.A., et al., *Defining the molecular interface that connects the Fanconi anemia protein FANCM to the Bloom syndrome dissolvasome.* Proc Natl Acad Sci U S A, 2012. **109**(12): p. 4437-42.

228. Suhasini, A.N., et al., *Interaction between the helicases genetically linked to Fanconi anemia group J and Bloom's syndrome.* Embo j, 2011. **30**(4): p. 692-705.

229. Dhar, S. and R.M. Brosh, *BLM's balancing act and the involvement of FANCJ in DNA repair.* Cell Cycle, 2018. **17**(18): p. 2207-2220.

230. Chaudhury, I., et al., *FANCD2 regulates BLM complex functions independently of FANCI to promote replication fork recovery.* Nucleic Acids Res, 2013. **41**(13): p. 6444-59.

231. Raghunandan, M., et al., *FANCD2, FANCJ and BRCA2 cooperate to promote replication fork recovery independently of the Fanconi Anemia core complex.* Cell Cycle, 2015. **14**(3): p. 342-353.

232. Sengupta, S., et al., *BLM helicase-dependent transport of p53 to sites of stalled DNA replication forks modulates homologous recombination.* EMBO J, 2003. **22**(5): p. 1210-22.

233. Sengupta, S., et al., *Functional interaction between BLM helicase and 53BP1 in a Chk1-mediated pathway during S-phase arrest.* J Cell Biol, 2004. **166**(6): p. 801-13.

234. Tripathi, V., S. Kaur, and S. Sengupta, *Phosphorylation-dependent interactions of BLM and 53BP1 are required for their anti-recombinogenic roles during homologous recombination.* Carcinogenesis, 2008. **29**(1): p. 52-61.

235. Tripathi, V., T. Nagarjuna, and S. Sengupta, *BLM helicase-dependent and -independent roles of 53BP1 during replication stress-mediated homologous recombination.* J Cell Biol, 2007. **178**(1): p. 9-14.

236. Sun, L., et al., *Structural Insight into BLM Recognition by TopBP1.* Structure, 2017. **25**(10): p. 1582-1588.e3.

237. Wang, Y., et al., *BASC, a super complex of BRCA1-associated proteins involved in the recognition and repair of aberrant DNA structures.* Genes & development, 2000. **14**(8): p. 927-939.

238. Langland, G., et al., *The Bloom's syndrome protein (BLM) interacts with MLH1 but is not required for DNA mismatch repair.* J Biol Chem, 2001. **276**(32): p. 30031-5.

239. Bochman, M.L., K. Paeschke, and V.A. Zakian, *DNA secondary structures: stability and function of G-quadruplex structures.* Nat Rev Genet, 2012. **13**(11): p. 770-80.

240. Lopes, J., et al., *G-quadruplex-induced instability during leading-strand replication.* Embo j, 2011. **30**(19): p. 4033-46.

241. Besnard, E., et al., *Unraveling cell type-specific and reprogrammable human replication origin signatures associated with G-quadruplex consensus motifs.* Nat Struct Mol Biol, 2012. **19**(8): p. 837-44.

242. Sun, H., et al., *The Bloom's syndrome helicase unwinds G4 DNA.* J Biol Chem, 1998. **273**(42): p. 27587-92.

51

243.   Wu, W.Q., et al., *BLM unfolds G-quadruplexes in different structural environments through different mechanisms.* Nucleic Acids Res, 2015. **43**(9): p. 4614-26.

244.   van Wietmarschen, N., et al., *BLM helicase suppresses recombination at G-quadruplex motifs in transcribed genes.* Nature Communications, 2018. **9**(1): p. 271.

245.   Wu, W.-Q., et al., *BLM unfolds G-quadruplexes in different structural environments through different mechanisms.* Nucleic Acids Research, 2015. **43**(9): p. 4614-4626.

246.   Grierson, P.M., et al., *BLM helicase facilitates RNA polymerase I-mediated ribosomal RNA transcription.* Human molecular genetics, 2012. **21**(5): p. 1172-1183.

247.   Lam, E.Y., et al., *G-quadruplex structures are stable and detectable in human genomic DNA.* Nat Commun, 2013. **4**: p. 1796.

248.   Drosopoulos, W.C., S.T. Kosiyatrakul, and C.L. Schildkraut, *BLM helicase facilitates telomere replication during leading strand synthesis of telomeres.* The Journal of Cell Biology, 2015. **210**(2): p. 191-208.

249.   Zimmermann, M., et al., *TRF1 negotiates TTAGGG repeat-associated replication problems by recruiting the BLM helicase and the TPP1/POT1 repressor of ATR signaling.* Genes & development, 2014. **28**(22): p. 2477-2491.

250.   Pan, X., et al., *FANCM, BRCA1, and BLM cooperatively resolve the replication stress at the ALT telomeres.* Proc Natl Acad Sci U S A, 2017. **114**(29): p. E5940-9.

251.   Sobinoff, A.P., et al., *BLM and SLX4 play opposing roles in recombination-dependent replication at human telomeres.* The EMBO Journal, 2017. **36**(19): p. 2907-2919.

252.   Barefield, C. and J. Karlseder, *The BLM helicase contributes to telomere maintenance through processing of late-replicating intermediate structures.* Nucleic Acids Res, 2012. **40**(15): p. 7358-67.

253.   Acharya, S., et al., *Association of BLM and BRCA1 during Telomere Maintenance in ALT Cells.* PLOS ONE, 2014. **9**(8): p. e103819.

254.   Chan, K.L. and I.D. Hickson, *New insights into the formation and resolution of ultra-fine anaphase bridges.* Semin Cell Dev Biol, 2011. **22**(8): p. 906-12.

255.   Chan, K.L., P.S. North, and I.D. Hickson, *BLM is required for faithful chromosome segregation and its localization defines a class of ultrafine anaphase bridges.* Embo j, 2007. **26**(14): p. 3397-409.

256.   Ke, Y., et al., *PICH and BLM limit histone association with anaphase centromeric DNA threads and promote their resolution.* Embo j, 2011. **30**(16): p. 3309-21.

257.   Rouzeau, S., et al., *Bloom's syndrome and PICH helicases cooperate with topoisomerase IIalpha in centromere disjunction before anaphase.* PLoS One, 2012. **7**(4): p. e33905.

258. Bhattacharyya, S., et al., *Telomerase-associated protein 1, HSP90, and topoisomerase IIalpha associate directly with the BLM helicase in immortalized cells using ALT and modulate its helicase activity using telomeric DNA substrates.* J Biol Chem, 2009. **284**(22): p. 14966-77.

259. Russell, B., et al., *Chromosome breakage is regulated by the interaction of the BLM helicase and topoisomerase IIalpha.* Cancer Res, 2011. **71**(2): p. 561-71.

260. Naim, V. and F. Rosselli, *The FANC pathway and BLM collaborate during mitosis to prevent micro-nucleation and chromosome abnormalities.* Nat Cell Biol, 2009. **11**(6): p. 761-8.

261. Ozeri-Galai, E., et al., *Failure of origin activation in response to fork stalling leads to chromosomal instability at fragile sites.* Mol Cell, 2011. **43**(1): p. 122-31.

262. Heyer, W.D., K.T. Ehmsen, and J. Liu, *Regulation of homologous recombination in eukaryotes.* Annu Rev Genet, 2010. **44**: p. 113-39.

263. Chan, Y.W. and S.C. West, *A new class of ultrafine anaphase bridges generated by homologous recombination.* Cell Cycle, 2018. **17**(17): p. 2101-2109.

264. Nera, B., et al., *Elevated levels of TRF2 induce telomeric ultrafine anaphase bridges and rapid telomere deletions.* Nat Commun, 2015. **6**: p. 10132.

265. Stagno d´Alcontres, M., et al., *TopoIIα prevents telomere fragility and formation of ultra thin DNA bridges during mitosis through TRF1-dependent binding to telomeres.* Cell Cycle, 2014. **13**(9): p. 1463-1481.

266. Branzei, D. and M. Foiani, *Maintaining genome stability at the replication fork.* Nat Rev Mol Cell Biol, 2010. **11**(3): p. 208-19.

267. Beamish, H., et al., *Functional link between BLM defective in Bloom's syndrome and the ataxia-telangiectasia-mutated protein, ATM.* J Biol Chem, 2002. **277**(34): p. 30515-23.

268. Ababou, M., et al., *ATM-dependent phosphorylation and accumulation of endogenous BLM protein in response to ionizing radiation.* Oncogene, 2000. **19**(52): p. 5955-63.

269. Rao, V.A., et al., *Phosphorylation of BLM, dissociation from topoisomerase IIIalpha, and colocalization with gamma-H2AX after topoisomerase I-induced replication damage.* Mol Cell Biol, 2005. **25**(20): p. 8925-37.

270. Kaur, S., et al., *Chk1-dependent constitutive phosphorylation of BLM helicase at serine 646 decreases after DNA damage.* Mol Cancer Res, 2010. **8**(9): p. 1234-47.

271. Zhong, S., et al., *A role for PML and the nuclear body in genomic stability.* Oncogene, 1999. **18**(56): p. 7941-7.

272. de The, H., M. Le Bras, and V. Lallemand-Breitenbach, *The cell biology of disease: Acute promyelocytic leukemia, arsenic, and PML bodies.* J Cell Biol, 2012. **198**(1): p. 11-21.

273. Zhu, J., et al., *Small ubiquitin-related modifier (SUMO) binding determines substrate recognition and paralog-selective SUMO modification.* J Biol Chem, 2008. **283**(43): p. 29405-15.

274. Eladad, S., et al., *Intra-nuclear trafficking of the BLM helicase to DNA damage-induced foci is regulated by SUMO modification.* Hum Mol Genet, 2005. **14**(10): p. 1351-65.

275. Tikoo, S., et al., *Ubiquitin-dependent recruitment of the Bloom syndrome helicase upon replication stress is required to suppress homologous recombination.* EMBO J, 2013. **32**(12): p. 1778-92.

276. Dutertre, S., et al., *Cell cycle regulation of the endogenous wild type Bloom's syndrome DNA helicase.* Oncogene, 2000. **19**(23): p. 2731-8.

277. Dutertre, S., et al., *Dephosphorylation and subcellular compartment change of the mitotic Bloom's syndrome DNA helicase in response to ionizing radiation.* J Biol Chem, 2002. **277**(8): p. 6280-6.

278. Leng, M., et al., *MPS1-dependent mitotic BLM phosphorylation is important for chromosome stability.* Proc Natl Acad Sci U S A, 2006. **103**(31): p. 11485-90.

279. Grabarz, A., et al., *A role for BLM in double-strand break repair pathway choice: prevention of CtIP/Mre11-mediated alternative nonhomologous end-joining.* Cell Rep, 2013. **5**(1): p. 21-8.

280. Ouyang, K.J., et al., *SUMO modification regulates BLM and RAD51 interaction at damaged replication forks.* PLoS Biol, 2009. **7**(12): p. e1000252.

281. Gharibyan, V. and H. Youssoufian, *Localization of the Bloom syndrome helicase to punctate nuclear structures and the nuclear matrix and regulation during the cell cycle: comparison with the Werner's syndrome helicase.* Mol Carcinog, 1999. **26**(4): p. 261-73.

CHAPTER TWO:

CELLULAR DEFECTS CAUSED BY HYPOMORPHIC VARIANTS OF THE BLOOM

SYNDROME HELICASE GENE *BLM*

 Corresponding author: Kristina Schmidt, Department of Cell Biology, Microbiology and Molecular Biology, University of South Florida, 4202 E. Fowler Avenue, ISA2015, Tampa, FL 33620. Phone: (813) 974-1592. Fax: (813) 974-1614.; E-mail: kschmidt@usf.edu

ABSTRACT

Background

Bloom syndrome is an autosomal recessive disorder characterized by extraordinary cancer incidence early in life and an average life expectancy of ~27 years. Premature stop codons in *BLM*, which encodes a DNA helicase that functions in DNA double-strand-break repair, make up the vast majority of Bloom syndrome mutations, with only 13 single amino acid changes identified in the syndrome. Sequencing projects have identified nearly one hundred single nucleotide variants in *BLM* that cause amino acid changes of uncertain significance.

Methods and results

Here, in addition to identifying five BLM variants incapable of complementing certain defects of Bloom syndrome cells, making them candidates for new Bloom syndrome causing mutations, we characterize a new class of BLM variants that cause some, but not all, cellular defects of Bloom syndrome. We find elevated sister-chromatid exchanges, a delayed DNA damage response and inefficient DNA repair. Conversely, hydroxyurea sensitivity and quadriradial chromosome accumulation, both characteristic of Bloom syndrome cells, are absent. These intermediate variants affect sites in BLM that function in ATP hydrolysis and in contacting double-stranded DNA.

Conclusion

Allele frequency and cellular defects suggest candidates for new Bloom syndrome causing mutations, and intermediate BLM variants that are hypomorphic which, instead of causing Bloom syndrome, may increase a person's risk for cancer or possibly other Bloom-syndrome-associated disorders, such as type-2 diabetes.

INTRODUCTION

Bloom syndrome (MIM 210900 for *BLM*) is a rare chromosome breakage disorder characterized by short stature and an extraordinary predisposition to a broad range of cancers, often multiple, early in life (German and Passarge 1989; German and Ellis 1998). Other symptoms that can be present in persons with Bloom syndrome include sun-sensitive skin with telangiectatic and hyper- and hypo-pigmented areas, immunodeficiency, subfertility in females and infertility in males, and type 2 diabetes mellitus (Bloom 1954; German and Passarge 1989; German and Ellis 1998; Ellis et al. 2008).

The gene defective in persons with Bloom syndrome – the tumor suppressor gene *BLM* – encodes a 3′ to 5′ DNA helicase that belongs to the evolutionarily conserved RecQ helicase family (Ellis et al. 1995; Bennett and Keck 2004). The helicase core of BLM spans amino acid residues 658 to 1197 and consists of the DNA-dependent ATPase (DEAH) domain with seven conserved helicase motifs, and the RecQ-C-terminal (RQC) domain with Zn-binding (Zn) and winged-helix (WH) subdomains (Hickson 2003; Bennett and Keck 2004). C-terminal of the RQC domain is the conserved Helicase and RNase D C-terminal (HRDC) domain, which plays a role in DNA binding and is thought to regulate helicase activity (Huber et al. 2006; Kim and Choi 2010). The best understood roles for BLM are in the repair of DNA double strand breaks (DSBs) by homologous recombination (HR) where – in a complex with topoisomerase Topo IIIα and Rmi1/Rmi2 – BLM dissolves double Holliday junctions (dHJ) into noncrossover products (Hickson 2003). BLM/Topo IIIα/Rmi1/Rmi2 has also been implicated in the processing of the ends of DSBs into single-strand 3′ overhangs for the strand invasion step of HR and in the control of HR levels by reversing strand invasion events (Bachrati et al. 2006; Daley et al. 2014; Sturzenegger et al. 2014). As a result, cells that lack functional BLM exhibit elevated levels of mitotic recombination, chromatid breaks, increased crossover formation between sister chromatids (~10-fold higher in cells from persons with Bloom syndrome), and signs of illegitimate interchromosomal recombination events suggested by the presence of quadriradial chromosomes (Chaganti et al. 1974; Groden et al. 1990; Lonn et al. 1990; Groden and German 1992). Consistent with the role of BLM in maintaining genome integrity, Bloom syndrome cells are sensitive to genotoxic agents, including hydroxyurea (HU), which causes replication stress by depleting the nucleotide pool, and camptothecin (CPT), a natural product that interferes with replication and transcription by trapping topoisomerase I on nicked DNA.

57

The elevated level of mitotic recombination between homologous chromosomes is thought be a major contributor to the extraordinary cancer predisposition in Bloom syndrome as it can lead to the loss of heterozygosity (LOH) at loci carrying tumor-suppressor genes (Chester et al. 1998; Traverso et al. 2003).

BLM is transcribed as a 97.93 kb pre-messenger RNA, with 21 exons coding for a 1417 amino acid protein. In the majority of persons with Bloom syndrome the *BLM* gene is inactivated by small insertion/deletion mutations or nonsense mutations that lead to a premature stop codon upstream or within exons 7–18, which code for the helicase core of BLM. The most common Bloom syndrome mutation is a 6 bp deletion/7 bp insertion in exon 9 (6-BP DEL/7-BP INS, rs113993962:ATCTGA>TAGATTC) (Ellis et al. 1994, 1998; Li et al. 1998; Straughen et al. 1998; German et al. 2007). This frameshift indel mutation changes the amino acids encoded by codons 736–739 before causing a premature stop in codon 740 (p.Tyr736fsX4). This mutation, also referred to as blm^{Ash}, occurs with a frequency of ~0.01 in the Ashkenazi Jewish population (Li et al. 1998). In addition to mutations causing premature chain termination, 13 missense mutations in the ATPase and RQC domains of the BLM helicase core have been identified in persons with Bloom syndrome (Ellis et al. 1995; Foucault et al. 1997; Barakat et al. 2000; German et al. 2007). Seven of the missense mutations alter amino acid residues in the ATPase domain (Q672R, I841T, C878R, G891E, C901Y, G952V, H963Y) whereas the six missense mutations in the RQC domain mostly affect the highly conserved cysteine residues involved in Zn coordination (C1036F, C1055S, C1055R, C1055G, D1064V, C1066Y) (Fig. 1A). The lack of differences in the expression of Bloom syndrome between individuals with these missense mutations, either in the homozygous or compound heterozygous state, and individuals with early chain-terminating mutations suggests that they all inactivate BLM (Ellis et al. 1995).

58

There is some evidence that heterozygosity for *BLM* mutations leads to increased colorectal cancer risk in humans and mice (Goss et al. 2002; Gruber et al. 2002), and causes increased sensitivity to DNA-damaging agents in a diploid yeast model (Mirzaei and Schmidt 2012). However, it is unclear if besides fully inactivating mutations that cause Bloom syndrome other naturally occurring *BLM* mutations cause more subtle functional defects that might be new cancer risk factors in otherwise healthy individuals. To address this question we used a yeast model to screen coding single nucleotide polymorphisms (SNPs) in the human *BLM* gene for those that impair BLM function as estimated by the hypersensitivity of cells to HU (Mirzaei and Schmidt 2012). This yeast model expressed a chimera of the N-terminal 648 residues of Sgs1 (the BLM-related RecQ helicase in *Saccharomyces cerevisiae*) and the C-terminal 800 residues of human BLM to which 41 nonsynonymous SNPs from the Short Genetic Variations database (dbSNP) map. We ranked these 41 coding SNPs and two additional SNPs reported in the literature (German et al. 2007) based on their probability to impair BLM function using PolyPhen (Ramensky et al. 2002) and evaluated the 22 SNPs predicted to be 'probably' or 'possibly' damaging (PolyPhen score >1.5) for their effect on BLM function in vivo (Mirzaei and Schmidt 2012). The screen identified eight SNPs that impaired BLM function, all of which had a PolyPhen score >2 (rs761589072:C>T, P690L; rs28406486:G>C, R717T; rs55880859:C>T, R791C; rs148394770:T>C, W803R; rs145029382:A>G, Y811C; rs2227935:C>T, P868L; rs150475674, G972V:G>T; rs139773499:G>A, G1120R) (Table 1) (Fig. 1A). Interestingly, this screen suggested that in addition to rare null alleles that had not yet been associated with Bloom syndrome more common *BLM* alleles may also be functionally impaired. The higher frequency of these alleles in the human population (e.g. rs2227935:C>T, P868L; 5.13%) suggests that they are insufficient for full-scale Bloom

syndrome, but their lower functional activity may lead to an increased cancer risk later in life or an increased risk for developing other symptoms of Bloom syndrome, such as type 2 diabetes mellitus or fertility problems. Here, we have quantified functional defects of cells expressing these new *BLM* alleles, with an emphasis on the first three hypomorphic *BLM* allele candidates (rs2227935, rs55880859, rs139773499) by assessing chromosomal abnormalities, their ability to respond to genotoxic agents and their ability to repair DSBs.

MATERIALS AND METHODS

Cell lines, plasmids, and transfection

GM08505 is an SV40-transformed skin fibroblast cell line established from a patient with Bloom syndrome (Ellis et al. 1995) and was obtained from Coriell Cell Repository. GM00637 is an SV40-transformed skin fibroblast cells line from an unaffected individual (Coriell Cell Repository). Cells were grown in minimal essential medium (Corning, Tewksbury, MA) supplemented with 10% FBS and 2 mmol/L glutamine at 37°C in the presence of 5% CO_2. GM08505 cells were plated 24 h before transfections at approximately 2×10^4 per cm^2. BLM cDNA cloned into pcDNA3 vector and mutated at stated sites using site-directed mutagenesis was transfected using Polyfect (Qiagen, Valencia, CA). Stable clones were selected in the presence of G418 (750 μg/mL). Clones were maintained in the presence of G418 (350 μg/mL). BLM cDNA in pcDNA3 was a kind gift from Dr. Ian Hickson, University of Copenhagen. Cell lines expressing the BLM variants evaluated in this study are listed in Table 2.

Subcellular fractionation and western blotting

Nuclear extracts were prepared from exponentially growing cells to detect BLM expression. Cells were lysed in 20 mmol/L Tris pH 7.4, 10 mmol/L KCl, 1 μmol/L EDTA, 0.2%

NP40, 50% glycerol, 0.6 mmol/L β-mercaptoethanol, 1 mmol/L PMSF, and protease inhibitor cocktail (Pierce, Rockford, IL), followed by nuclear extraction in 20 mmol/L Tris pH 7.4, 10 mmol/L KCl, 0.4 mol/L NaCl, 1 mmol/L EDTA, 50% glycerol, 0.6 mmol/L BME, 1 mmol/L PMSF, and protease inhibitor cocktail (Pierce). Mouse monoclonal antibody BLM-F5 (SCBT, Dallas, TX) was used to detect BLM and a monoclonal tubulin antibody (Abcam, Cambridge, MA) was used as a loading control.

Differential sister-chromatid staining

Sister chromatid exchanges (SCEs) were quantified using protocols described previously (Perry and Wolff 1974; Bayani and Squire 2001; Campos et al. 2009). Briefly, cells were cultured for two cell cycles in growth medium supplemented with BrdU Labeling Reagent (Life Technologies, Carlsbad, CA) and metaphase arrest was induced by the addition of 0.1 μg/mL colcemid for 1 h. Chromosome spreads were prepared after hypotonic treatment with 75 mmol/L KCl and fixation with 3:1 (vol/vol) methanol-acetic acid. Metaphase spreads were differentially stained using Hoechst 33258 (75 μg/mL; Life Technologies) and Giemsa (3.5%; Life Technologies). Images of intact metaphases were acquired on a Zeiss Axiovert 100 deconvolution microscope with a Plan-Apochromat 100x/1.40 Oil DIC M27 objective Zeiss, Thornwood, NY. For each cell line, a minimum of 1500 chromosomes were analyzed. The mean ± SD is reported.

Clonogenic survival assay

Cells were seeded at a density of 500 cells/well for colony formation. On the next day, either fresh medium containing HU (0.1, 0.2, 0.3, 0.4, or 0.5 mmol/L) or drug-free medium was added. The medium was removed after 48 h and cells were washed with PBS before colonies

were allowed to grow in fresh complete growth medium for up to 4 weeks. Colonies were fixed in 3:1 (vol/vol) methanol-acetic acid and stained with 0.01% crystal violet. Colonies with more than 50 cells were scored as survivors.

γH2AX accumulation and elimination

Exponentially growing cells were exposed to 1 μmol/L CPT for 1 h, released into fresh media, and harvested at various time points (10 min, 20 min, 30 min, 45 min, 1 h, 8 h, 24 h, and 48 h). To detect γH2AX, chromatin fractions were prepared from nuclear extracts using 0.5 mol/L HCl, 50% glycerol, 100 mmol/L β-mercaptoethanol and then neutralized using NaOH in 40 mmol/L Tris pH 7.4 with protease inhibitor cocktail (Pierce) (Rios-Doria et al. 2009). Chromatin fractions were separated on 16% Tricine-SDS polyacrylamide (Schagger 2006) and Western blots were probed with PhosphoDetect Anti-H2AX [pSer[139]] (Upstate Cell Signalling, Billerica, MA) and polyclonal histone H3 antibody (Abcam). Changes in γH2AX levels with respect to histone H3 levels were quantified using ImageJ (Rasband 1997). To inhibit PP2A-mediated dephosphorylation of γH2AX, 25 nmol/L okadaic acid was added to cells immediately after CPT treatment.

Comet assay

Neutral comet assays were performed according to protocols described earlier (Olive and Banath 2006; Nowsheen et al. 2012). Briefly, replication-dependent DNA breaks were induced by addition of 1 μmol/L CPT to cell cultures for 1 h. Cells were harvested immediately after treatment and after growth in drug-free media for 1, 24, and 48 h. Single cell suspensions in 1% low melt agarose were plated on slides, lysed using neutral lysis buffer and electrophoresed for 30 min. Slides were fixed in 70% ethanol and stained with SYBR Gold (Life Technologies).

Images were acquired on an UltraVIEW VoX Life Cell Imager (Perkin Elmer, Waltham, MA) equipped with a Zeiss Axiovert 200 and a 20x/0.8 M27 Plan-Apochromat objective using Volocity software. At least 50 comets were imaged for three independent cell lines for a minimum of 150 comets at each time point. The mean of the tail DNA percentage was calculated using OpenComet (Gyori et al. 2014).

RESULTS

Skin fibroblast cell lines established from persons with Bloom syndrome (e.g., GM08505) exhibit a spontaneous, approximately 10-fold increase in the frequency of SCEs compared to cells from unaffected persons; they also present with quadriradial chromosomes in metaphase spreads, are hypersensitive to HU, and show a delay in activating the DNA damage response after exposure to the topoisomerase poison CPT. To determine the ability of eight SNPs that cause single amino acid changes in BLM (Table 1) to complement the cellular defects of Bloom syndrome cells, the SNPs were introduced into *BLM* cDNA in vector pcDNA3 and expressed in cell line GM08505, in which both *BLM* alleles are inactivated by the blm^{Ash} mutation. For each of the eight BLM variants at least three stable cell lines, expressing each BLM variant at levels similar to that of wildtype BLM in a skin fibroblast cell line from an unaffected individual (GM00637), were constructed and analyzed for DNA-damage sensitivity using a clonogenic (survival) assay (Fig. 1). Expression of wildtype BLM improved survival of Bloom syndrome cells GM08505 in the presence of HU to that of GM00637, whereas expression of P690L, R717T, W803R, Y811C, and G972V caused no improvement (Fig. 1C), suggesting that they eliminate BLM function. Survival of GM08505 cells expressing the R791C, P868L and G1120R variants, however, was not significantly different from wildtype BLM (Fig. 1D).

63

The decreased ability of BLM-deficient cells to dissolve intermediates of HR as noncrossovers is thought to be a cause of the increased frequency of exchange of genetic material between sister chromatids, which can be visualized by differential staining with Hoechst/Giemsa after two rounds of cell division in the presence of the thymidine analog BrdU (Perry and Wolff 1974) (Fig. 2B, panel a). We measured a 12-fold increase in the SCE frequency in GM08505 cells compared to GM00637 (Fig. 2A), consistent with previous findings in cell lines derived from persons with Bloom syndrome (Ellis et al. 1999). Since the P690L, R717T, W803R, Y811C, and G972V mutations caused the same HU hypersensitivity in human cells as the known Bloom syndrome causing blm^{Ash} mutation (Fig. 1C), and the same HU hypersensitivity as the helicase-dead *blm-K695A* mutation in yeast (Mirzaei and Schmidt 2012) we focused the evaluation of chromosome abnormalities on the R791C, P868L, and G1120R alleles, and only included two representatives from the group of null alleles, P690L (Walker A motif) and W803R (conserved aromatic-rich loop). As expected, we found that expression of wildtype BLM in GM08505 lowered the SCE frequency to levels seen in normal fibroblasts whereas expression of variants that exhibited a null phenotype in the HU survival assay had no significant effect on SCE frequency, remaining 7-fold (P690L) to 8-fold (W803R) higher than cells expressing wildtype BLM (Fig. 2A). Expression of variants R791C, P868L, and G1120R, which suppressed HU hypersensitivity of GM08505 cells as effectively as wildtype BLM, lowered SCE frequency of Bloom syndrome cells ($P < 0.01$) (Fig. 2A), but levels were still significantly higher (4–5-fold, $P < 0.01$) than in cells expressing wildtype BLM, indicating reduced BLM activity.

In contrast with genetic exchange between sister chromatids, recombination between homologous chromosomes can give rise to LOH; it can thus be considered mutagenic and a

driver of tumorigenicity in Bloom syndrome. Such recombination events between nonsister chromatids of homologous chromosomes and, potentially, nonhomologous chromosomes are captured in metaphase spreads as quadriradial chromosomes (Fig. 2B, panel d). As expected, we did not find quadriradials in normal GM00637 fibroblasts, but observed ~13 for every 10 metaphases in GM08505 cells (Fig. 2C). Quadriradial formation was reduced ~5-fold to fewer than three quadriradials for every 10 metaphases upon expression of wildtype BLM. The same reduction was achieved by expression of R791C, P868L, and G1120R, whereas quadriradials still formed readily in GM08505 cells expressing P690L or W803R (Fig. 2C).

In addition to increased recombination events between sister and nonsister chromatids, cells from Bloom syndrome patients show a delay in the induction of the DNA damage response after exposure to genotoxic agents, such as CPT (Rao et al. 2005), which at low concentrations (≤ 1 μmol/L) induces replication-specific DSBs (Holm et al. 1989; Pommier 2006). Phosphorylation of the histone H2A variant H2AX at serine 139 is one of the first markers of DSB formation in eukaryotic cells (Rogakou et al. 1998). Phosphorylated H2AX, γH2AX, is thought to recruit and retain DNA damage response and repair factors at DSBs and increase their accessibility to the DSB site by facilitating chromatin remodeling (Celeste et al. 2002; Fernandez-Capetillo et al. 2002; Stucki et al. 2005; Tsukuda et al. 2005; Kolas et al. 2007). Results obtained from an H2AX-S139A mutant suggest that H2AX phosphorylation also plays a role in checkpoint activation (Rios-Doria et al. 2009). Upon completion of DSB repair, elimination of γH2AX, either by dephosphorylation or exchange with H2AX, is needed for cell cycle progression (Rogakou et al. 1998; Chowdhury et al. 2005; Keogh et al. 2006). To determine the effect of BLM variants on the induction of the DNA damage response we exposed cells to 1 μmol/L CPT for 1 h, removed the drug, and assessed the accumulation of γH2AX every

10 min for 1 h (Fig. 3). To follow completion of DSB repair and cessation of the DNA damage response we extended this time course to 48 h to evaluate the kinetics of the elimination of cellular γH2AX. γH2AX accumulation in Bloom syndrome cells complemented with wildtype BLM peaked 1 h after CPT removal and then γH2AX levels declined rapidly, being undetectable by Western blot after 24 h (Fig. 3A, Fig. S1). In contrast, in Bloom syndrome cells γH2AX levels did not peak until 32 h after drug removal and declined only slowly, with most of the H2AX still phosphorylated after 48 h (Fig. 3B). Bloom syndrome cells expressing the P690L variant, a representative of the five alleles that were hypersensitive to HU in human cells and in yeast, followed the same kinetics of γH2AX accumulation and elimination as Bloom syndrome cells, further supporting the null phenotype of this BLM variant (Fig. 3C). Interestingly, in Bloom syndrome cells expressing R791C, P868L, or G1120R mutations, γH2AX accumulation reached its peak 1 h after CPT removal as in cells expressing wildtype BLM, but there was distinctly less γH2AX, especially at early time points. Even more noticeable, at the 24-hour time point, when γH2AX was undetectable in complemented Bloom syndrome cells, most of the γH2AX was still present in these mutants, thus resembling the severely delayed elimination of γH2AX in Bloom syndrome cells (Fig. 3D–F, Fig. S1).

We therefore wanted to test if this impaired elimination of γH2AX in cells with the intermediate phenotype (Fig. 3D–F) affected the cells' ability to mount a response to repeated exposure to a genotoxin. We first tested Bloom syndrome cells complemented with wildtype BLM. Cells were exposed to 1 μmol/L CPT for 1 h and then released into media without CPT, with aliquots being removed every 10 min for 1 h and again after 8 h since at this time point γH2AX levels had declined significantly (Fig. 3A). At this 8 h time point cells were again exposed to 1 μmol/L CPT for 1 h, released into fresh media, and aliquots collected at the same

time points as in the first cycle (Fig. 4A). The kinetics of the two cycles of H2AX accumulation/elimination were nearly indistinguishable, suggesting that wildtype cells were capable of mounting proficient responses to repeated insults from CPT. To test blm-P868L, the intermediate BLM variant with the highest allele frequency in the human population (5.13%), we exposed cells to a second dose of CPT after 24 h (instead of 8 h) because only then did we start to see significant elimination of γH2AX (Fig. 3E). As wildtype cells, blm-P868L cells responded equally well to both exposures of CPT; however, with a marked >16 h delay in γH2AX elimination in both cycles (Fig. 4B). Despite lower initial H2AX phosphorylation and severely delayed dephosphorylation compared to wildtype cells, blm-P868L cells responded significantly better to repeated CPT exposure than Bloom syndrome cells (Fig. 3 and 4C).

At low concentrations (<50 nmol/L) okadaic acid selectively inhibits the γH2AX phosphatase PP2A (Honkanen and Golden 2002). Loss of PP2A activity has been shown to cause cell cycle changes, increased sensitivity to DNA damaging agents, and delay in DNA repair, probably enhanced by affecting the activity of other PP2A substrates in addition H2AX, such as ATM, Chk2, and DNA-PK (Douglas et al. 2001; Dozier et al. 2004; Goodarzi et al. 2004; Chowdhury et al. 2005). Bloom syndrome cells complemented with BLM or blm-P868L survived treatment with 25 nmol/L okadaic acid with sustained maximum levels of γH2AX (Fig. S2), whereas Bloom syndrome cells died. To test if the marked delay in γH2AX accumulation and elimination after CPT removal in cells expressing P868L corresponded to unrepaired DSBs, we performed a neutral comet assay (Fig. 5). Cells were exposed to 1 μmol/L CPT for 1 h and released into fresh media, with cells being removed for lysis and electrophoresis at the end of the incubation with CPT (0 h) and then after 1, 24, and 48 h. In wildtype cells, DNA breaks were significantly reduced over the 48 h time course, with 23% and 14% of DNA damage

remaining after 24 and 48 h respectively. In blm-P868L cells twice as much DNA damage (28%, $P < 0.0001$) was still unrepaired after 48 h, indicating a lag of DNA repair of at least 24 h. This presents a significant loss in DNA break repair activity of the P868L variant, but not as great as that of Bloom syndrome cells where the amount of unrepaired DNA breaks after 48 h was three times higher (43%, $P < 0.0001$) than in wildtype cells.

DISCUSSION

In this study, we have identified variable functional defects of novel variants of the tumor-suppressor BLM. Five of the eight variants cause cellular defects that are indistinguishable from those of Bloom syndrome cells, indicating that they encode nonfunctional BLM variants that would cause Bloom syndrome in the homozygous or compound heterozygous state. The amino acid changes in these five BLM variants – P690L, R717T, Y811C, W803R, G972V – cluster along the catalytic cleft between the N-terminal and the C-terminal lobe of the ATPase domain of the helicase core. Residues that make up the seven conserved helicase motifs of BLM are located at the surface of this cleft to bind ATP, Mg^{2+} and single-stranded DNA and, eventually, to hydrolyze ATP. The null phenotype exhibited by the five BLM variants can be explained by the location of the mutated residues in or near these conserved helicase motifs. These new null alleles are the first to inactivate BLM by mutation of residues in or near motifs I (P690L), Ia (R717T), VI (G972V), and the conserved aromatic loop (W803R, Y811C), whereas the known Bloom syndrome-associated amino acid changes map to motifs 0 (Q672R) and IV (G891E, C901Y) or fall outside of the conserved motifs (I841T, C878R) (Guo et al. 2007). The location of the new missense mutations in the (Walker A) motif I for ATP binding or in other conserved helicase motifs suggests that the null phenotype of the new BLM variants is due to loss of ATPase activity. While it is not surprising that ATPase activity would be required for

68

BLM's role in suppressing SCEs by dissolving dHJ as noncrossovers, our findings also implicate ATPase activity in the role of BLM as a transducer of H2AX phosphorylation in response to replication-dependent DSBs (Rao et al. 2005), most likely to mediate early events (e.g., resection, unwinding) at collapsed replication forks. Resembling the known Bloom syndrome causing missense mutations, with each having been identified in only one person (German et al. 2007), the new null variants are very rare in the human population, with allele frequencies of <0.01 (Sherry et al. 2001, Exome Variant Server, 2015).

In addition to new null alleles, we identified the first BLM variant, P868L (rs11852361), that exhibits some, but not all, defects of Bloom syndrome causing mutations and does not, based on its relatively high allele frequency, cause Bloom syndrome. The frequency of P868L in the human population is 5.13%, ranging from 0.6% in the Japanese to 12.3–15.3% (15/122 alleles, 1000 Genomes Project Consortium; 15/98 alleles, CSHL-HAPMAP) in the population of African descent in the South Western United States (ASW) (International HapMap, 2003, Thorisson et al. 2005, 1000 Genomes Project Consortium, 2012). Homozygosity for P868L in the ASW population was 1 in 61 (1/61 genomes, 1000GENOMES) and 1 in 25 (2/49 genomes, CSHL-HAPMAP), with the next highest frequencies in the Finnish (3/93 genomes) and the British (2/89 genomes) (International HapMap Consortium 2003, Thorisson et al. 2005, 1000 Genomes Project Consortium 2012). In our study, cells expressing the P868L variant exhibited a significantly elevated SCE frequency (Fig. 2A), an aberrant (slow) DNA-damage response, and inefficient repair of DNA-damage-induced, replication-dependent DSBs (Fig. 3B). On the other hand, blm-P868L expressing cells showed similar HU sensitivity and frequency of quadriradial chromosomes as cells expressing wildtype BLM. When mapped onto the recently released crystal structure of human BLM (Swan et al. 2014), P868L affects a residue in a loop of

unknown function in the C-terminal lobe of the ATPase domain. This lysine-rich loop is not near the catalytic cleft where the null mutations map, but instead appears to contact double-stranded (ds) DNA bound by the WH domain just before it is unwound (Fig. 6A). Based on this location we propose that replacing the helix breaker proline with hydrophobic leucine disrupts the flexibility and hydrophilicity of the loop, weakening dsDNA binding. Biochemical analysis of the purified BLM variant will be necessary to determine if less efficient dsDNA binding, in and of itself, causes the slower and abnormal DNA break repair exhibited by the P868L variant, or if it is due to less efficient ATP hydrolysis since the ATPase activity of BLM is single-stranded (ss) DNA-dependent.

In addition to P868L we identified two other BLM variants that fall into this new class of intermediate (hypomorphic) mutations. G1120R is the first BLM missense mutation from the human population that maps to the WH domain and impairs BLM function. The WH domain is conserved structurally, but not at the amino acid level. We found that one of the few exceptions is the first glycine (G1120) in the loop between the second and third α-helix of the domain ($\alpha 2$–$\alpha 3$ loop), which is conserved in members of the RecQ helicase family from bacteria, to yeast, to humans. It is still unclear how the WH domain contributes to BLM function since BLM lacking this domain still possesses helicase activity (Gyimesi et al. 2012). Nonetheless, the loop with G1120 has been shown to expand in the related human RecQ helicase WRN upon DNA binding, exposing an arginine for dsDNA binding (Kitano et al. 2010). Similarly, the corresponding loop in the recently released crystal structure of human BLM is near dsDNA (Swan et al. 2014) (Fig. 6 B). We propose that the G1120R mutation, by removing the helix-terminating glycine, extends the $\alpha 2$-helix, eliminating or at least reducing the loop structure for dsDNA binding.

Unlike P868L, G1120R is rare, having been identified once in 2197 genomes (Exome Variant Server 2015).

The third hypomorphic BLM variant that causes elevated SCEs and inefficient DNA break repair, but normal HU sensitivity and wildtype frequency of quadriradial chromosomes, is R791C. The affected residue is in the N-terminal lobe of the ATPase domain in the internal β-sheet that precedes helicase motif II (Walker B) required for Mg^{2+} binding and ATP hydrolysis (Fig. 6C). Hence, the DNA break repair defect of cells expressing the R791C variant is likely due to diminished ATPase activity. The allele has been identified once in 97 genomes from the Han Chinese in Beijing (1000 Genomes Project Consortium 2012) and twice in 6496 genomes from European-American and African-American populations in the United States (Exome Variant Server 2015). Although R791C is so rare it is listed three times in The Cancer Genome Atlas (TCGA); twice in nonsmall cell lung carcinoma and once in a lymphoid neoplasm (Barretina et al. 2012), raising the possibility that it contributes to tumorigenesis.

Taken together, we have identified five new BLM missense mutations that exhibit defects of the Bloom syndrome associated blm^{ASH} null allele and are therefore new candidates for Bloom syndrome causing alleles, and three new BLM missense mutations that exhibit some defects (elevated interchromatid crossover recombination (SCEs), slower accumulation and markedly delayed elimination of γH2AX after genotoxin exposure, and inefficient repair of replication-dependent DSBs), but not others (HU hypersensitivity, accumulation of quadriradial chromosomes) (Table 2). H2AX and its phosphorylation at S139 have been shown to play a role in DSBR by HR between sister chromatids, which is potentially error-free (Kadyk and Hartwell 1992; Johnson and Jasin 2000), while preventing error-prone HR, such as single-strand annealing (SSA) (Xie et al. 2004). Thus, the severe delay in γH2AX accumulation in cells

71

expressing BLM null alleles (e.g. P690L, R717T, W803R, Y811C, and G972V in this study), and the lesser, but significant, delay in cells expressing the P868L, G1120R, or R791C variants may be indicative of dysregulation of DSBR, resulting in increased utilization of SSA or HR between homologs, which are prone to deletions and LOH respectively. In contrast with H2AX phosphorylation and its effects on DSBR, the signaling of γH2AX elimination and the consequences of persistence of γH2AX, as seen in cells expressing fully or partially defective BLM variants in this study, are less well-understood, but involves direct dephosphorylation by PP2A-B56ε (Xie et al. 2004; Chowdhury et al. 2005). Our findings indicate that the requirement of BLM for the accumulation of γH2AX (Rao et al. 2005) extends to its enzymatic activity, suggesting its requirement for DNA processing rather than protein binding or recruitment at DSBs. Our findings further extend the role of BLM's enzymatic activity to the elimination of γH2AX. Our assays cannot distinguish whether BLM is part of the signaling pathway for γH2AX elimination or the effect is solely through BLM's role in DSB processing and rejoining, but the severely delayed (>40 h) elimination of cellular γH2AX is associated with delayed and, possibly, error-prone DNA damage repair as well as delays in restoration of chromatin integrity and the cell cycle.

The functional evaluation of new BLM variants in this study also provides insight into the *in silico* predictability of the impact of SNPs on BLM function (Table 1). Initially we used Polyphen (Ramensky et al. 2002) to rank 43 coding SNPs in BLM, with 22 scoring as either probably or possibly damaging. All eight SNPs that are functionally impaired in yeast and in human cells were predicted to be 'probably damaging' (score > 2). However, Polyphen was unable to distinguish between the null alleles and the intermediate/hypomorphic alleles. Its successor, PolyPhen2 (Adzhubei et al. 2010), had enhanced predictability, classifying P868L as

an intermediate (possibly damaging) allele. In contrast, both SIFT (Kumar et al. 2009) and FIS (Reva et al. 2011) categorized R717T as being 'tolerated' or of 'low' impact respectively. Thus, for our limited set of variants, this comparison suggests that for the evolutionarily conserved and highly structured catalytic core of BLM, Polyphen2 was the most accurate predictor of functional impact.

The biological relevance of the functional defects of the new class of intermediate BLM variants for human health and aging is currently unclear, as is their importance for a person's sensitivity to genotoxins. Although all defects caused by hypomorphic BLM variants were significantly less pronounced than in Bloom syndrome cells, any increased mutation load over a person's lifetime is likely to be associated with increased cancer risk; this risk is known to be extraordinarily high for *BLM* null alleles, leading to Bloom syndrome, and now remains to be defined for the newly identified class of hypomorphic BLM variants, currently represented by R791C, P868L, and G1120R.

FUTURE DIRECTIONS

SNPs have also been reported in the region coding for the BLM N-terminal tail (Sherry et al. 2001). Whereas the C-terminal region of BLM exhibits a high degree of sequence and structure conservation, the N-terminal region is predicted to be highly disordered with very little sequence similarity between its orthologs. The N-terminal region constitutes a long (~639 residues) tail and like the N-terminus of other RecQ helicases is biologically functional as the binding site for protein interactions. However, the mutational approach used to characterize and understand the C-terminal region BLM and other RecQs cannot be used for the intrinsically disordered BLM-terminal region. Given its role in complex with other proteins to preserve

73

genomic stability (Hickson 2003; Bachrati et al. 2006; Daley et al. 2014; Sturzenegger et al. 2014, Croteau et al. 2014), identifying single residue alterations disrupting BLM interactions with specific binding partners while not impacting others would be a good approach to delineate the functions of BLM in different pathways.

Based on PolyPhen2 predictions of impaired function and the predicted presence of α-helical regions indicating protein binding propensity (Adzhubei et al. 2010; Muñoz & Serrano 1994; Dyson &Wright 2002), the following 16 SNPs have been identified as candidates for functional evaluation — A2S, V4A, R15C, L60I, D64V, K17R, E140G, F160S, D239H, S269G, D295Y, K323R, A363T, L401F, L410F, E507K (Table S2.1). Single residue changes within an α-helix have been shown to disrupt Sgs1/Top3 interaction (Kennedy et. 2013). The corresponding Topo IIIα interacting region in BLM contains a helical region, which is predicted to be disrupted by R15C (Figure S2.3). Furthermore, S269G is predicted to disrupt an α-helix in the region involved in BLM/p53 binding (Figure S2.3). K137R and E140G also map to regions with increased helical content, but are not predicted to be as disruptive. However, they are located in the region involved in BLM dimerization as well as interacting with Topo IIIα and Rad51 (Wu et al. 2000; Bergeron et al. 2012).

As a preliminary step towards this approach, we tested the ability of a few BLM N-terminal variants to suppress HU sensitivity and complement defective response to CPT-mediated replication stress in GM08505 cells. Similar to the three hypomorphic variants identified in the BLM C-terminal region, all BLM N-terminal variants tested were able to suppress HU sensitivity as well as wildtype BLM (Figure S2.4). On the other hand, the response to CPT-mediated replication stress was varied. While γH2AX accumulation appeared to be similar to wildtype BLM, every BLM N-terminal variant except D64V exhibited varying degrees

74

of delay in γH2AX elimination. Cells expressing the S269G, F160S and E140G variants showed a more pronounced delay in the γH2AX elimination profile (Figure S2.5). Based on this, we selected S269G to perform a neutral comet assay along with the hypomorphic variant P868L. Based on the role of the BLM/Topo III α /RMI1/2 complex in DSBR, we assayed the R15C variant as well. Remarkably, both R15C and S269G exhibit a loss of DSBR efficiency similar to P868L.

The preliminary data suggests that single residue changes within putative structural elements in the BLM N-terminal tail can be functionally characterized using assays utilized to evaluate C-terminal variants. This opens up the possibility of identifying separation of function alleles. Further, rationally designed mutations disrupting these predicted regions can be of use to understand the underlying mechanism of functional defects of population derived SNPs.
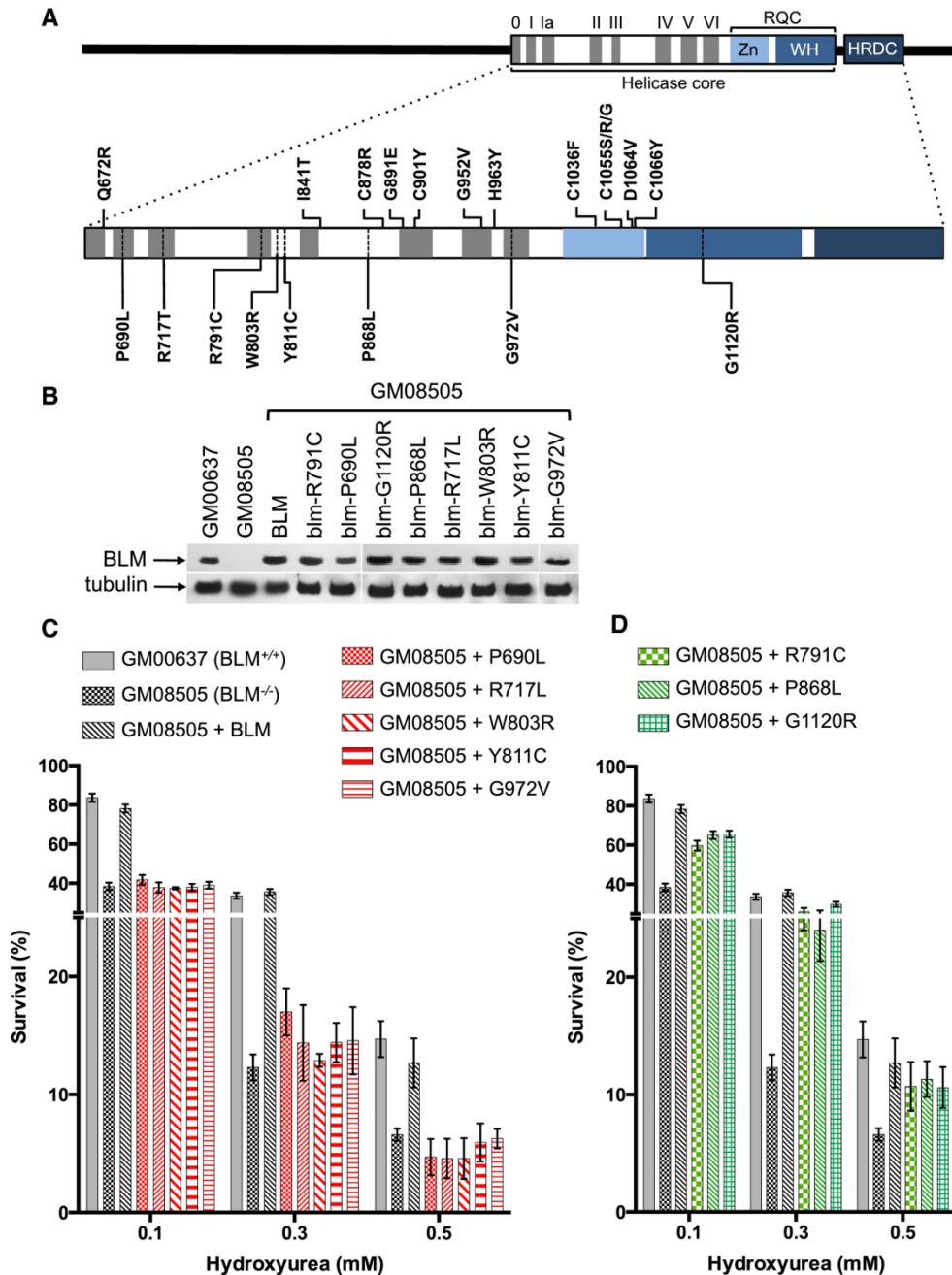
Figure 2.2. Ability of BLM variants to complement the hydroxyurea sensitivity of the BLM-deficient cell line GM08505.
(A) Map of human BLM with conserved helicase motifs I-VI, the RecQ-C-terminal (RQC) domain consisting of Zn-binding and winged helix (WH) subdomains, and the Helicase- and RNaseD-C-terminal (HRDC) domain. Sites of known Bloom syndrome causing missense mutations are indicated above the map and locations of BLM variants analyzed in this study are indicated below the map. (B) GM08505 cells, which are homozygous for the blm^{ASH} mutation and do not express full-length BLM (lane 2), express stably transfected BLM variants (lanes 4–

11) at similar levels as wildtype BLM (lane 3). Endogenous BLM expression in the normal fibroblast cell line GM00637 is shown lane 1. (C–D) Cells were exposed to increasing concentrations of hydroxyurea (0.1–0.5 mmol/L) for 48 h and survivors (colonies with ~50 or more cells) were counted after up to 4 weeks of growth in hydroxyurea-free media. Three independently generated stable cell lines were analyzed for BLM and every BLM variant. Mean ± SD is shown.
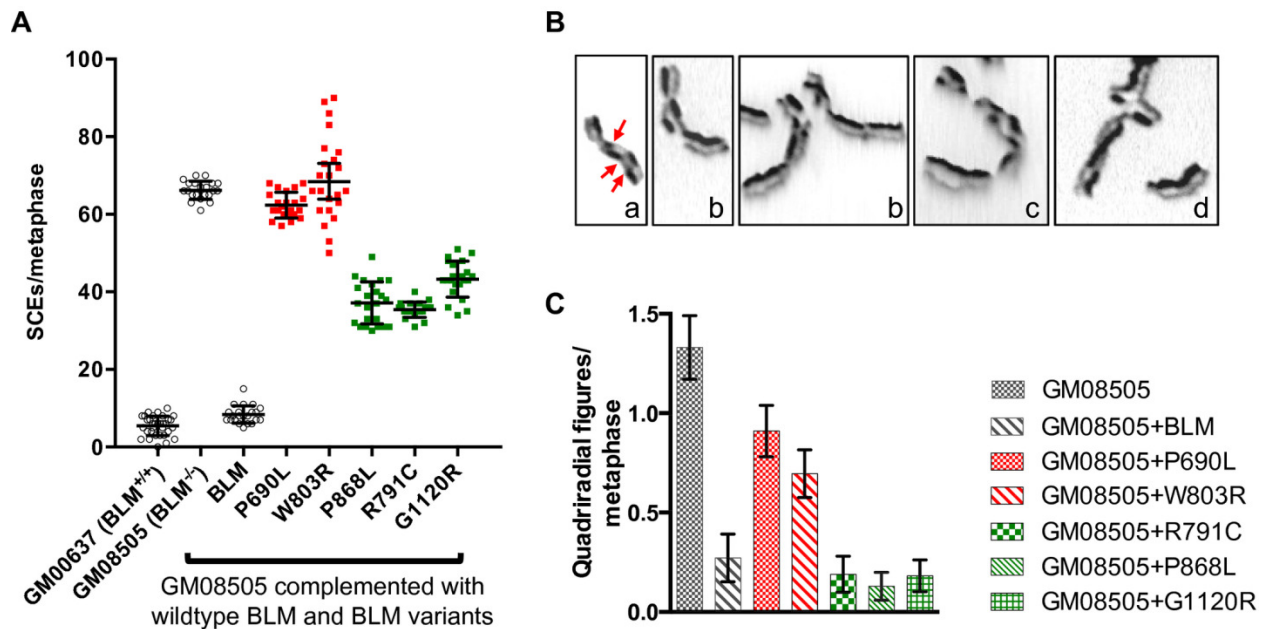
Figure 3.2. Chromosomal aberrations in GM08505 cells expressing BLM variants
(A) Analysis of sister-chromatid exchanges (SCEs) by differential sister-chromatid staining of metaphase chromosomes identifies two groups of BLM variants; variants that cause hypersensitivity to HU (see Fig. C), here represented by P690L and W803R, show SCE levels similar to GM08505, whereas variants that do not cause hypersensitivity to 0.5 mmol/L HU (R791C, P868L, G1120R) (Fig. D) had reduced levels of SCEs compared to Bloom syndrome cells, but levels were still higher than in GM08505 cells expressing wildtype BLM. SCEs per 46 metaphase chromosomes are shown. (B) Types of chromosomal aberrations commonly observed in Bloom syndrome cells include (a) SCEs, (b) chromatid gaps, (c) segmented chromosomes, and (d) quadriradial chromosomes. (C) Appearance of quadriradial chromosomes in metaphase spreads of GM08505 cells expressing BLM variants R791C, P868L, and G1120R is reduced to wildtype levels, whereas expression of P690L or W803R variants caused significantly elevated formation of quadriradial chromosomes.
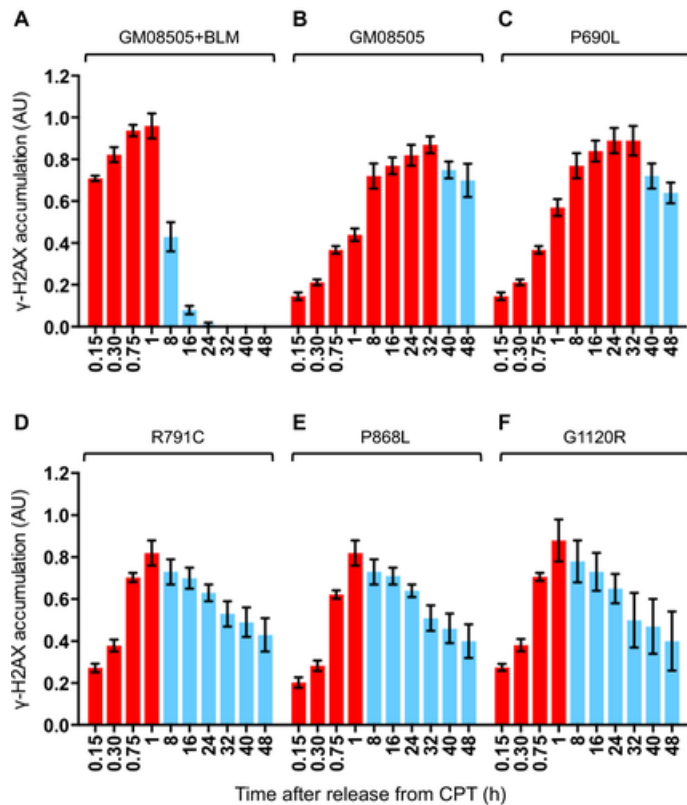
Figure 2.3. Response of Bloom syndrome cells (GM08505) expressing BLM variants to replication-dependent DNA breaks

DNA breaks were induced by exposure to 1 μmol/L CPT for 1 h. Accumulation and elimination γH2AX in comparison to histone H3 was quantified by Western blot of extracts from cells collected over a 48 h time course (Fig. S1). Increasing levels of γH2AX are indicated in red, and declining levels in blue. Three independent, stable cell lines were analyzed for GM08505 cells expressing wildtype BLM (A) or BLM variants (C–F). Mean ± SD is shown.
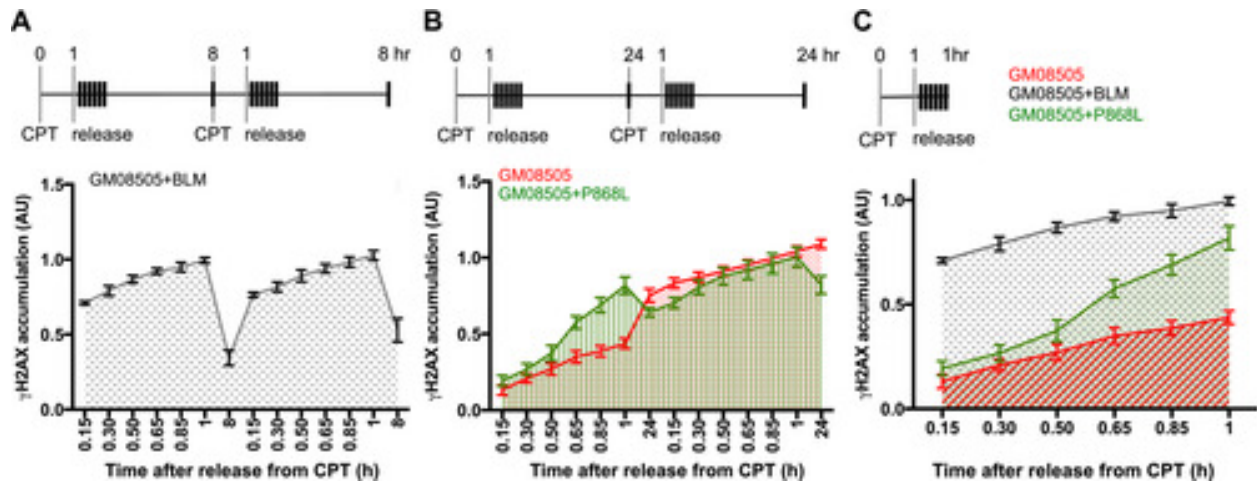
Figure 2.4. DNA-damage response after repeated induction of DNA breaks by camptothecin (CPT)

(A) GM08505 + BLM cells were exposed to 1 µmol/L CPT for 1 h, released into drug-free media, and γH2AX levels analyzed by Western blot every 10 min for 1 h and again after 8 h. At the 8-hour time point cells were exposed to a second round of 1 µmol/L CPT treatment since at this point γH2AX levels in GM08505 + BLM cells had significantly declined (see Fig. A). γH2AX levels were analyzed again every 10 min for 1 h and then after 8 h. (B) Cells expressing variant P868L were exposed twice to CPT as in (A), but the second exposure to CPT occurred after 24 h since this was the first time point at which a significant decline in γH2AX was detected in cells expressing the P868L variant (see Fig. E). (C) Comparison of γH2AX accumulation in the first hour after CPT removal. γH2AX levels were quantified by Western blot for GM08505 cells and three independent stable cell lines expressing wildtype BLM or the P868L variant. Western blots were analyzed using ImageJ (Schneider et al.). Mean ± SD is shown.
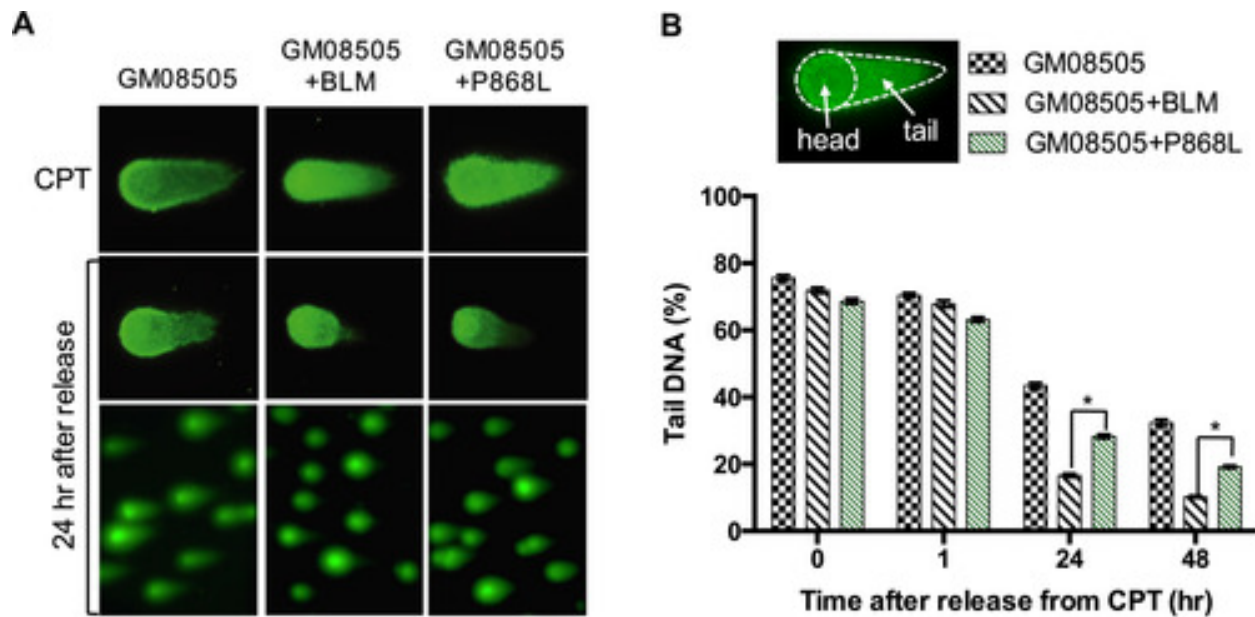
Figure 2.5. Efficiency of repair of replication-dependent DNA double-strand breaks
(A) Neutral comet assay indicates varying levels of double-strand break repair 24 h after CPT treatment of GM08505 cells expressing no BLM, wildtype BLM, or BLM variant P868L. (B) Tail DNA content was quantified with OpenComet in 150 comets from GM08505 cells and three independent stable cell lines expressing BLM or BLM variant P868L. Mean ± SD is shown. The asterisks indicates $P < 0.001$.
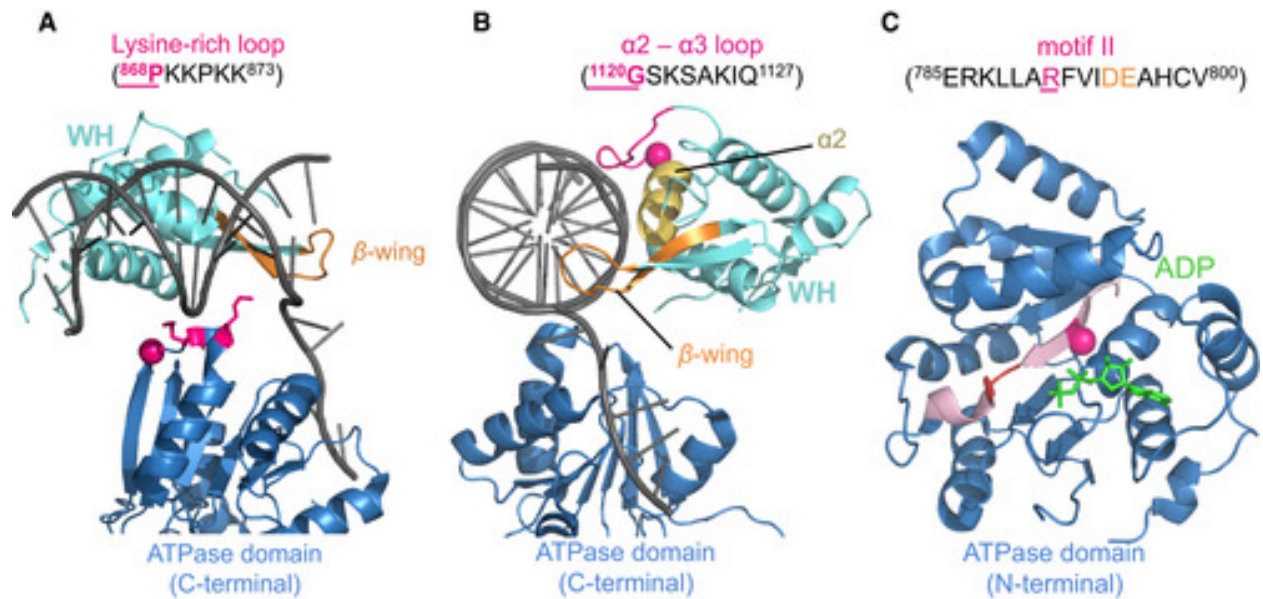
Figure 2.6. Location in the crystal structure of human BLM of amino acid changes with intermediate functional impact

(A) P868L maps to a lysine-rich loop at the periphery of the C-terminal lobe of the ATPase domain. The loop appears to be in contact with dsDNA, which is also contacted by the WH domain. P868L is at the C-terminal end of a β-strand that transverses lobe 2 of the ATPase domain from the catalytic cleft to the periphery where DNA is contacted, possibly connecting DNA-substrate binding to ATP-hydrolysis. The crystal structure of BLM in a complex with ADP and duplex DNA is from PDB (ID: 4O3M). (B) G1120 is located in a loop between the second and third α-helix of the WH-domain that contacts dsDNA. BLM crystal structure is PDB ID 4O3M. (C) R791 maps to an internal β-strand that precedes the loop of the Walker B motif involved in Mg2+-binding and ATP hydrolysis. Since the loop in helicase motif II (Walker B) is not resolved in 4O3M (Swan et al.), the R791C mutation is shown in BLM crystal structure 4CDG (Newman et al.). The amino acid residues changed by the missense mutations are shown as red spheres. Images were generated with PyMOL v1.3.
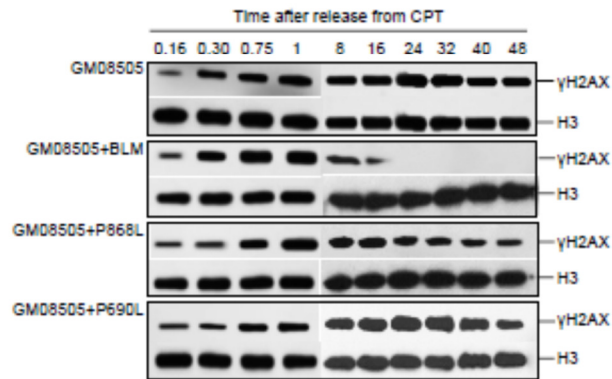
Figure S2.1. Response GM08505 expressing BLM variants to replication-dependent DNA breaks

Representative examples of the response of Bloom syndrome cells (GM08505) expressing wildtype BLM and BLM variants to replication-dependent DNA breaks induced by exposure to 1 μM CPT for 1 hour. Accumulation and elimination of γH2AX was determined by Western blot over a 48-hour time-course.
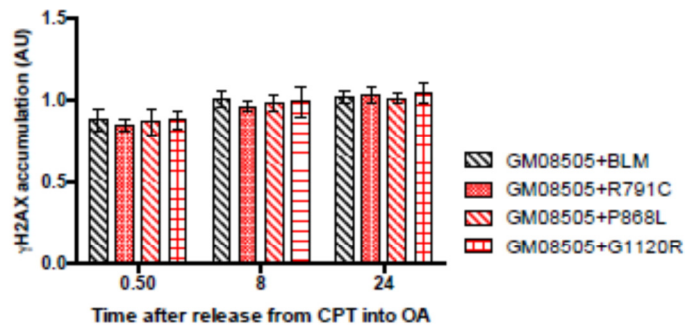
Figure S2.2. Effect of PP2A inhibition on γH2AX accumulation in Bloom syndrome cells expressing wildtype BLM and hypomorphic BLM variants

Cells were exposed to 1 μM CPT for 1 hour and released into media with 25 nM ocadaic acid (OA). H2AX phosphorylation levels were determined after 0.5, 8 and 24 hours. Non-complemented Bloom syndrome cells were not viable at the 24 hour time point.
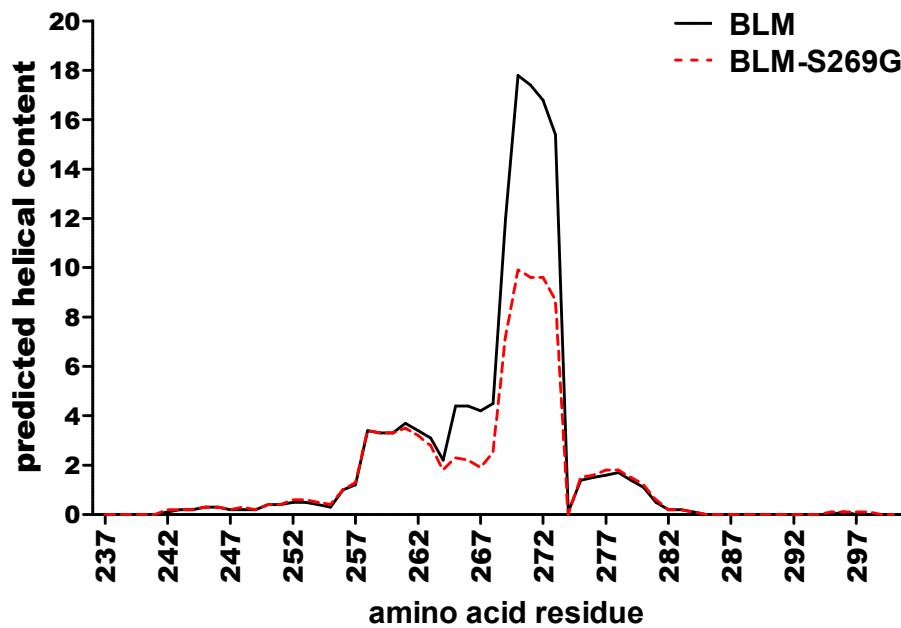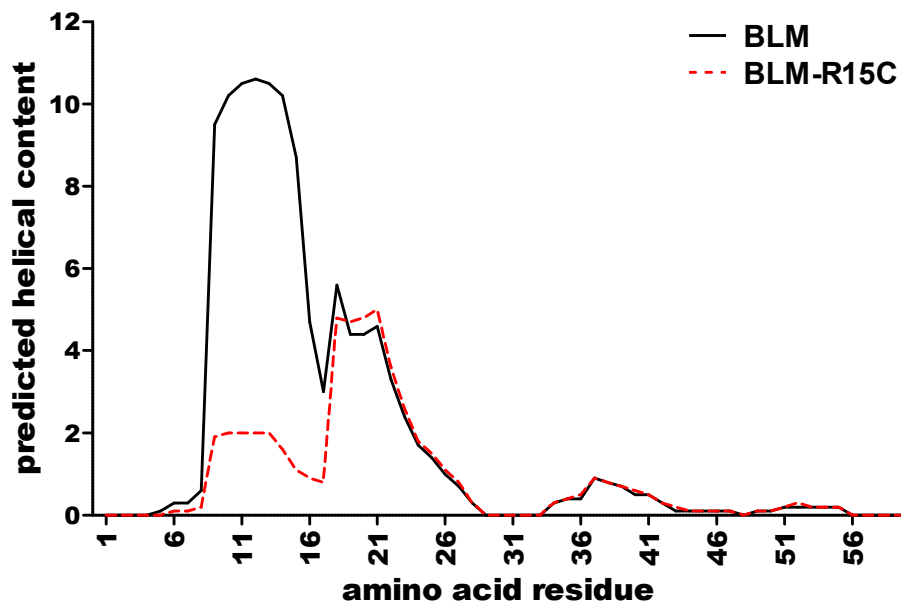
Figure S.2.3. Disruption of predicted helical content in BLM N-terminal region
R15C and S269G disrupt predicted α-helical content in the Topo III α and p53 binding regions respectively.
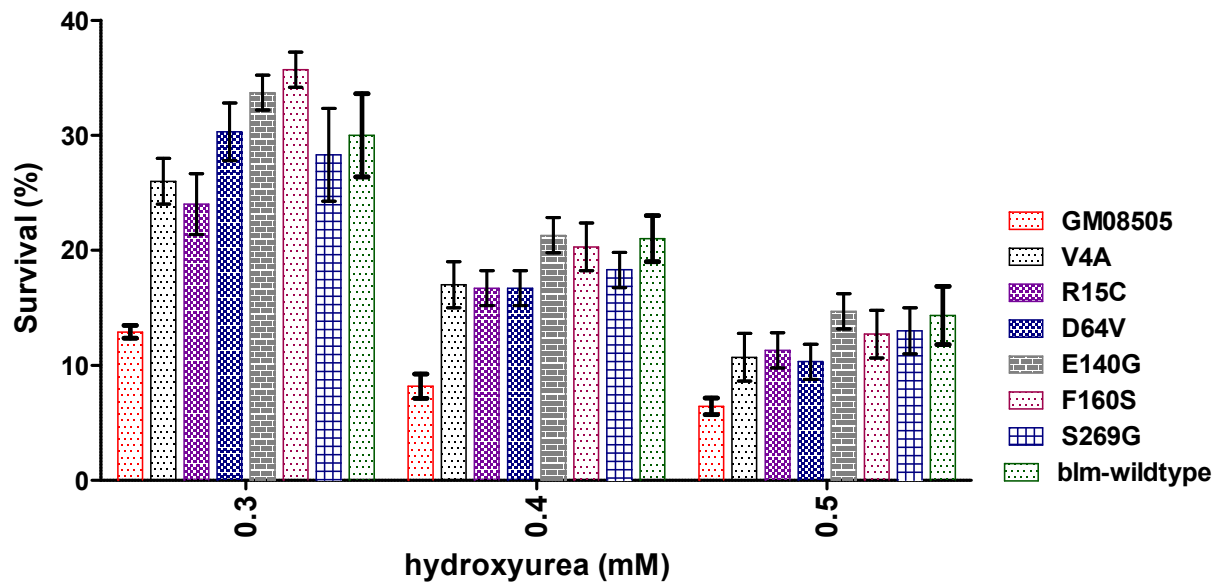
Figure S2.4. Ability of BLM N-terminal variants to suppress HU sensitivity of GM08505 cells

GM08505 cells expressing various BLM variants were exposed to increasing HU concentrations and surviving colonies were scored after four weeks. Three independently generated stable cell lines were analyzed for BLM and every BLM variant. Mean +/-SD is shown.
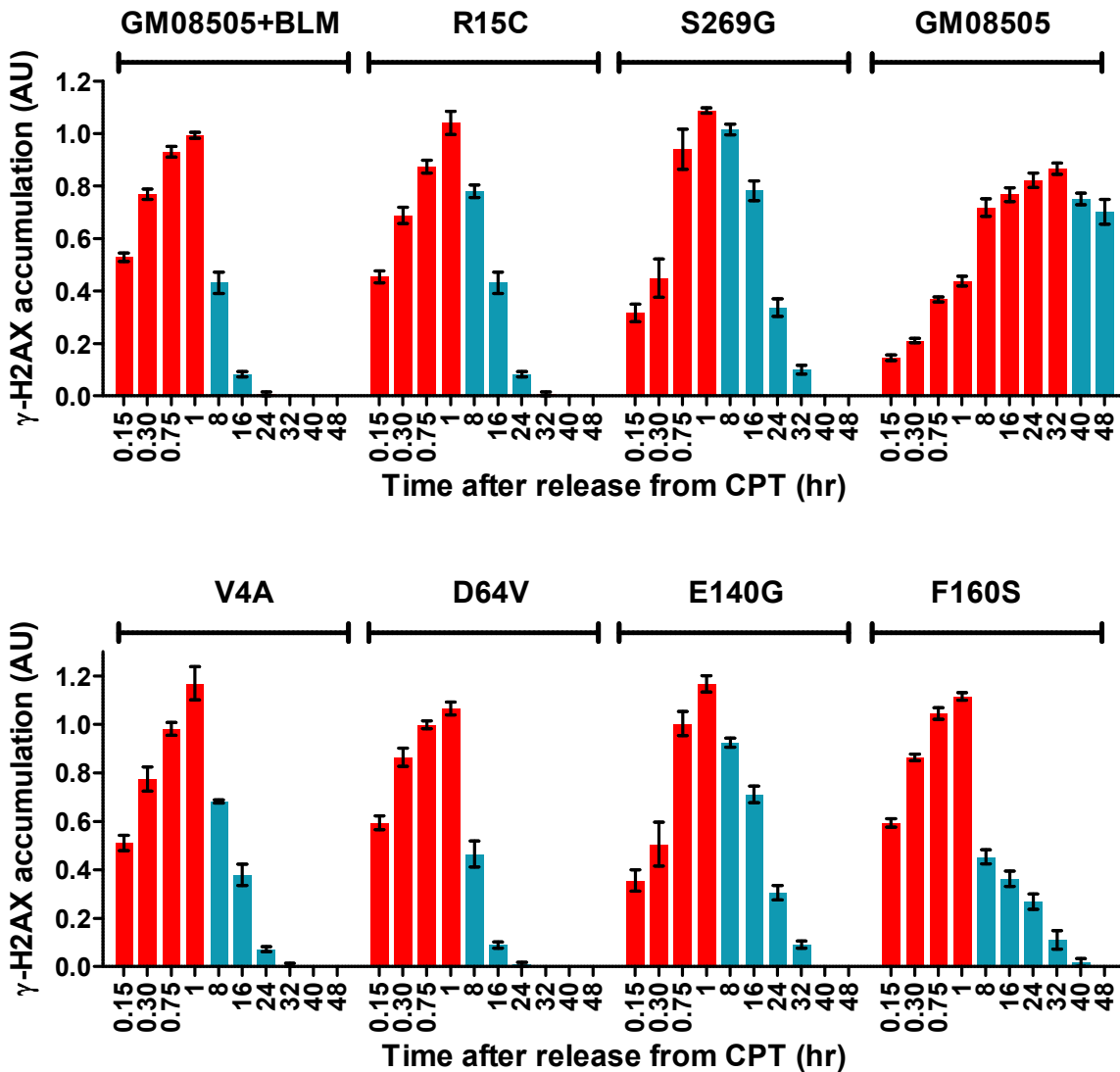
Figure S2.5. Response of cells expressing BLM N-terminal variants to CPT mediated DNA double strand break

Accumulation and elimination γH2AX was quantified with respect to histone H3 levels by Western blot. Increasing levels of γH2AX are indicated in red, and declining levels in blue. Three independent, stable cell lines were analyzed for GM08505 cells expressing wildtype BLM or BLM variants. Mean ± SD is shown.
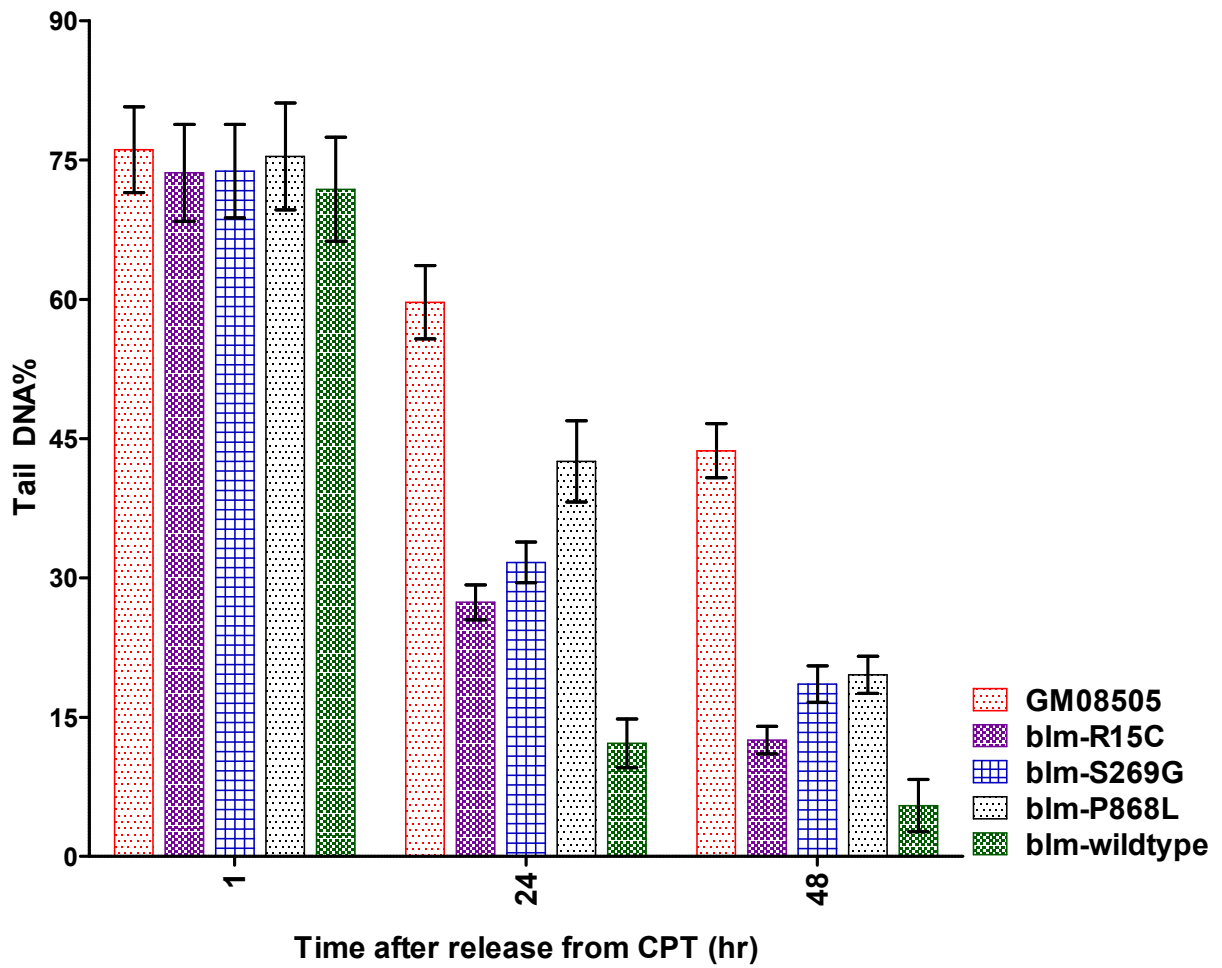
Figure S2.6. Replication dependent DNA double-strand break repair efficiency of cells expressing BLM N-terminal variants
Tail DNA% from 150 neutral comets from GM08505 cells and three independent stable cell lines expressing wildtype BLM or BLM variants was quantified using OpenComet. Mean ± SD is shown.

Table 2.1. Overview of BLM variants evaluated in this study

Nucleotide change[a]	Amino acid change[b]	dbSNP ID	Allele Frequency	Prediction Tools				Cell line ID
				PolyPhen[c]	PolyPhen2[d]	SIFT[e]	FIS[f]	
c.2069C>T[g]	p.Pro690Leu		n.a.	■ 2.724	■ 1	■ 0	■ 4.875	KSVS1405
c.2150G>C	p.Arg717Thr	rs28406486	n.a.	■ 2.008	■ 0.985	■ 0.15	■ 0.85	KSVS1406
c.2371C>T	p.Arg791Cys	rs55880859	0.0002[h]	■ 2.495	■ 0.981	■ 0.01	■ 2.81	KSVS1402
c.2407T>C	p.Trp803Arg	rs148394770	n.a.	■ 3.757	■ 1	■ 0	■ 4.965	KSVS1407
c.2432A>G	p.Tyr811Cys	rs145029382	n.a.	■ 2.616	■ 1	■ 0	■ 4.955	KSVS1408
c.2603C>T	p.Pro868Leu	rs2227935	0.0513[h]	■ 2.724	■ 0.729	■ 0.02	■ 2.395	KSVS1403
c.2915G>T	p.Gly972Val	rs367543034	n.a.	■ 2.397	■ 1	■ 0	■ 2.295	KSVS1409
c.3358G>A	p.Gly1120Arg	rs139773499	n.a.	■ 2.172	■ 0.999	■ 0	■ 3.285	KSVS1404
blm^Ash indel			0.01[i]					GM08505
	WT							KSVS1415

[a] GenBank RefSeq: *NM* _000057.3

[b] GenBank RefSeq: *NP*_000048.1

[c] Prediction using PolyPhen (http://genetics.bwh.harvard.edu/pph/index.html): red, probably damaging

[d] Prediction using PolyPhen-2 (http://genetics.bwh.harvard.edu/pph/): red, probably damaging; yellow, possibly damaging

[e] Prediction using SIFT (http://sift.jcvi.org/): red, damaging; green, tolerated

[f] Predicted Functional Impact Score via Mutation Assessor (http://mutationassessor.org/) ; red, high; yellow, medium; low: green

[g] From reference German et al. (2007)

[h] Minor allele frequency from dbSNP (http://www.ncbi.nlm.nih.gov/SNP/)

[i] Frequency in the Ashkenazi Jewish population from Li et al. (1998)

Table 2.2. Summary of functional assays

Amino acid change[a]	HU sensitivity[b]	Chromosome abnormalities[c]		γ-H2AX accumulation[d]	γ-H2AX elimination[d]	% DNA in Comet Tail[e]
		SCEs	Quadriradials			
p.Pro690Leu	+++	1.353±0.074	0.91±0.13	+++	+++	n.d.
p.Arg717Thr	+++	n.d.	n.d.	n.d.	n.d.	n.d.
p.Arg791Cys	+/-	0.774±0.044	0.190±0.09	+	++	n.d.
p.Trp803Arg	+++	1.506±0.238	0.696±012	n.d.	n.d.	n.d.
p.Tyr811Cys	+++	n.d.	n.d.	n.d.	n.d.	n.d.
p.Pro868Leu	+/-	0.809±0.116	0.130±0.07	+	++	63.16/19.14
p.Gly972Val	+++	n.d.	n.d.	n.d.	n.d.	n.d.
p.Gly1120Arg	+/-	0.941±0.102	0.182±0.08	+	++	n.d.
blm[Ash] indel	+++	1.44±0.05	1.330±0.16	+++	+++	70.40/32.40
WT	-	0.18±0.05	0.272±0.12	-	-	67.84/10.22

[a] GenBank RefSeq: NP_000048.1

[b] +++ significantly more sensitive to HU than wildtype cells at all tested HU concentrations (0.1-0.5 mM); +/- significantly more sensitive than wildtype cells at low HU concentrations (0.1-0.3 mM), but not significant difference at higher HU concentration (0.4-0.5 mM)

[c] SCEs are shown as SCEs per chromosome with standard deviation; quadriradials are shown as number of quadriradial chromosomes per metaphase with standard deviation; n.d. not determined

[d] DNA damage response was assessed by accumulation and decline of phosphorylated H2AX; + and +++ denote mild and severe delays in the accumulation and/or decline of phosphorylated H2AX after treatment with 1 μM CPT; n.d. not determined

[e] DNA double-strand breaks were visualized by means of neutral comet assay; % tail DNA 1 hr post-release/% DNA 48 post-release after treatment with 1 μM CPT; n.d. not determined

REFERENCES

Adzhubei, I. A., S. Schmidt, L. Peshkin, V. E. Ramensky, A. Gerasimova, P. Bork, et al. 2010. A method and server for predicting damaging missense mutations. *Nat. Methods* **7**:248–249.

Bachrati, C. Z., R. H. Borts, and I. D. Hickson. 2006. Mobile D-loops are a preferred substrate for the Bloom's syndrome helicase. *Nucleic Acids Res.* **34**:2269–2279.

Barakat, A., M. Ababou, R. Onclercq, S. Dutertre, E. Chadli, N. Hda, et al. 2000. Identification of a novel BLM missense mutation (2706T>C) in a Moroccan patient with Bloom's syndrome. *Hum. Mutat.* **15**:584–585.

Barretina, J., G. Caponigro, N. Stransky, K. Venkatesan, A. A. Margolin, S. Kim, et al. 2012. The cancer cell line encyclopedia enables predictive modelling of anticancer drug sensitivity. *Nature***483**:603–607.

Bayani, J., and J. A. Squire. 2001. *Sister chromatid exchange*. John Wiley & Sons Inc, Current Protocols in Cell Biology.

Bennett, R. J., and J. L. Keck. 2004. Structure and function of RecQ DNA helicases. *Crit. Rev. Biochem. Mol. Biol.* **39**:79–97.

Bergeron, K. L., Murphy, E. L., Brown, L. W., & Almeida, K. H. (2011). Critical interaction domains between bloom syndrome protein and RAD51. *The protein journal*, *30*(1), 1-8.

Bloom, D. 1954. Congenital telangiectatic erythema resembling lupus erythematosus in dwarfs; probably a syndrome entity. *AMA Am. J. Dis. Child* **88**:754–758.

Bodian, D. L., McCutcheon, J. N., Kothiyal, P., Huddleston, K. C., Iyer, R. K., Vockley, J. G., & Niederhuber, J. E. (2014). Germline variation in cancer-susceptibility genes in a healthy, ancestrally diverse cohort: implications for individual genome sequencing. *PloS one*, **9:**e94554. doi:10.1371/journal.pone.0094554

Campos, P. B., R. C. Sartore, S. N. Abdalla, and S. K. Rehen. 2009. Chromosomal spread preparation of human embryonic stem cells for karyotyping. *J. Vis. Exp* **31**:e1512.

Celeste, A., S. Petersen, P. J. Romanienko, O. Fernandez-Capetillo, H. T. Chen, O. A. Sedelnikova, et al. 2002. Genomic instability in mice lacking histone H2AX. *Science* **296**:922–927.

Chaganti, R. S., S. Schonberg, and J. German. 1974. A manyfold increase in sister chromatid exchanges in Bloom's syndrome lymphocytes. *Proc. Natl Acad. Sci. USA* **71**:4508–4512.

Chester, N., F. Kuo, C. Kozak, C. D. O'Hara, and P. Leder. 1998. Stage-specific apoptosis, developmental delay, and embryonic lethality in mice homozygous for a targeted disruption in the murine Bloom's syndrome gene. *Genes Dev.* **12**:3382–3393.

Chowdhury, D., M. C. Keogh, H. Ishii, C. L. Peterson, S. Buratowski, and J. Lieberman. 2005. gamma-H2AX dephosphorylation by protein phosphatase 2A facilitates DNA double-strand break repair. *Mol. Cell* **20**:801–809.

Croteau, D.L., Popuri , V., Opresko, P.L., and Bohr, V.A. 2014. Human RecQ helicases in DNA repair, recombination, and replication. *Ann. Rev. Biochem.* **83**:1519-1552.

Daley, J. M., T. Chiba, X. Xue, H. Niu, and P. Sung. 2014. Multifaceted role of the Topo IIIalpha-RMI1-RMI2 complex and DNA2 in the BLM-dependent pathway of DNA break end resection. *Nucleic Acids Res.* **42**:11083–11091.

Douglas, P., G. B. Moorhead, R. Ye, and S. P. Lees-Miller. 2001. Protein phosphatases regulate DNA-dependent protein kinase activity. *J. Biol. Chem.* **276**:18992–18998.

Dozier, C., M. Bonyadi, L. Baricault, L. Tonasso, and J. M. Darbon. 2004. Regulation of Chk2 phosphorylation by interaction with protein phosphatase 2A via its B' regulatory subunit. *Biol. Cell***96**:509–517.

Ellis, N. A., A. M. Roe, J. Kozloski, M. Proytcheva, C. Falk, and J. German. 1994. Linkage disequilibrium between the FES, D15S127, and BLM loci in Ashkenazi Jews with Bloom syndrome. *Am. J. Hum. Genet.* **55**:453–460.

Ellis, N. A., J. Groden, T. Z. Ye, J. Straughen, D. J. Lennon, S. Ciocci, et al. 1995. The Bloom's syndrome gene product is homologous to RecQ helicases. *Cell* **83**:655–666.

Ellis, N. A., S. Ciocci, M. Proytcheva, D. Lennon, J. Groden, and J. German. 1998. The Ashkenazic Jewish Bloom syndrome mutation blmAsh is present in non-Jewish Americans of Spanish ancestry. *Am. J. Hum. Genet.* **63**:1685–1693.

Ellis, N. A., M. Proytcheva, M. M. Sanz, T. Z. Ye, and J. German. 1999. Transfection of BLM into cultured bloom syndrome cells reduces the sister-chromatid exchange rate toward normal. *Am. J. Hum. Genet.* **65**:1368–1374.

Ellis, N. A., M. Sander, C. C. Harris, and V. A. Bohr. 2008. Bloom's syndrome workshop focuses on the functional specificities of RecQ helicases. *Mech. Ageing Dev.* **129**:681–691.

Exome Variant Server N. G. E. S. P. E. 2015. SEATTLE, WA. Available at http://Evs.Gs.Washington.Edu/Evs/.

Fernandez-Capetillo, O., H. T. Chen, A. Celeste, I. Ward, P. J. Romanienko, J. C. Morales, et al. 2002. DNA damage-induced G2-M checkpoint activation by histone H2AX and 53BP1. *Nat. Cell Biol.***4**:993–997.

Foucault, F., C. Vaury, A. Barakat, D. Thibout, P. Planchon, C. Jaulin, et al. 1997. Characterization of a new BLM mutation associated with a topoisomerase II alpha defect in a patient with Bloom's syndrome. *Hum. Mol. Genet.* **6**:1427–1434.

1000 Genomes Project Consortium 2012. An integrated map of genetic variation from 1092 human genomes. *Nature* **491**: 56–65.

90

German, J., and N. A. Ellis. 1998. Bloom syndrome. Pp. 267–288 *in* B. Vogelstein, K. W. Kinzler. *The genetic basis of human cancer*. McGraw-Hill, Health Professions Division, New York.

German, J., and E. Passarge. 1989. Bloom's syndrome. XII. Report from the Registry for 1987. *Clin. Genet.* **35**:57–69.

German, J., M. M. Sanz, S. Ciocci, T. Z. Ye, and N. A. Ellis. 2007. Syndrome-causing mutations of the BLM gene in persons in the Bloom's syndrome registry. *Hum. Mutat.* **28**:743–753.

Goodarzi, A. A., J. C. Jonnalagadda, P. Douglas, D. Young, R. Ye, G. B. Moorhead, et al. 2004. Autophosphorylation of ataxia-telangiectasia mutated is regulated by protein phosphatase 2A. *EMBO J.* **23**:4451–4461.

Goss, K. H., M. A. Risinger, J. J. Kordich, M. M. Sanz, J. E. Straughen, L. E. Slovek, et al. 2002. Enhanced tumor formation in mice heterozygous for Blm mutation. *Science* **297**:2051–2053.

Groden, J., and J. German. 1992. Bloom's syndrome. XVIII. Hypermutability at a tandem-repeat locus. *Hum. Genet.* **90**:360–367.

Groden, J., Y. Nakamura, and J. German. 1990. Molecular evidence that homologous recombination occurs in proliferating human somatic cells. *Proc. Natl Acad. Sci. USA* **87**:4315–4319.

Gruber, S. B., N. A. Ellis, K. K. Scott, R. Almog, P. Kolachana, J. D. Bonner, et al. 2002. BLM heterozygosity and the risk of colorectal cancer. *Science* **297**:2013.

Guo, R. B., P. Rigolet, H. Ren, B. Zhang, X. D. Zhang, S. X. Dou, et al. 2007. Structural and functional analyses of disease-causing missense mutations in Bloom syndrome protein. *Nucleic Acids Res.***35**:6297–6310.

Gyimesi, M., G. M. Harami, K. Sarlos, E. Hazai, Z. Bikadi, and M. Kovacs. 2012. Complex activities of the human Bloom's syndrome helicase are encoded in a core region comprising the RecA and Zn-binding domains. *Nucleic Acids Res.* **40**:3952–3963.

Gyori, B. M., G. Venkatachalam, P. S. Thiagarajan, D. Hsu, and M.-V. Clement. 2014. OpenComet: an automated tool for comet assay image analysis. *Redox. Biol.* **2**:457–465.

Hickson, I. D. 2003. RecQ helicases: caretakers of the genome. *Nat. Rev. Cancer* **3**:169–178.

Holm, C., J. M. Covey, D. Kerrigan, and Y. Pommier. 1989. Differential requirement of DNA replication for the cytotoxicity of DNA topoisomerase I and II inhibitors in Chinese hamster DC3F cells. *Cancer Res.* **49**:6365–6368.

Honkanen, R. E., and T. Golden. 2002. Regulators of serine/threonine protein phosphatases at the dawn of a clinical era? *Curr. Med. Chem.* **9**:2055–2075.

Huber, M. D., M. L. Duquette, J. C. Shiels, and N. Maizels. 2006. A conserved G4 DNA binding domain in RecQ family helicases. *J. Mol. Biol.* **358**:1071–1080.

International HapMap Consortium 2003. The international HapMap project. *Nature* **426**:789–796.

Johnson, R. D., and M. Jasin. 2000. Sister chromatid gene conversion is a prominent double-strand break repair pathway in mammalian cells. *EMBO J.* **19**:3398–3407.

Kadyk, L. C., and L. H. Hartwell. 1992. Sister chromatids are preferred over homologs as substrates for recombinational repair in *Saccharomyces cerevisiae*. *Genetics* **132**:387–402.

Kennedy, J. A., Daughdrill, G. W., and Schmidt, K. H. 2013. A transient α-helical molecular recognition element in the disordered N-terminus of the Sgs1 helicase is critical for chromosome stability and binding of Top3/Rmi1. *Nucleic acids research*, **41**, 10215-10227.

Keogh, M. C., J. A. Kim, M. Downey, J. Fillingham, D. Chowdhury, J. C. Harrison, et al. 2006. A phosphatase complex that dephosphorylates gammaH2AX regulates DNA damage checkpoint recovery. *Nature* **439**:497–501.

Kim, Y. M., and B. S. Choi. 2010. Structure and function of the regulatory HRDC domain from human Bloom syndrome protein. *Nucleic Acids Res.* **38**:7764–7777.

Kitano, K., S. Y. Kim, and T. Hakoshima. 2010. Structural basis for DNA strand separation by the unconventional winged-helix domain of RecQ helicase WRN. *Structure* **18**:177–187.

Kolas, N. K., J. R. Chapman, S. Nakada, J. Ylanko, R. Chahwan, F. D. Sweeney, et al. 2007. Orchestration of the DNA-damage response by the RNF8 ubiquitin ligase. *Science* **318**:1637–1640.

Kumar, P., S. Henikoff, and P. C. Ng. 2009. Predicting the effects of coding non-synonymous variants on protein function using the SIFT algorithm. *Nat. Protoc.* **4**:1073–1081.

Li, L., C. Eng, R. J. Desnick, J. German, and N. A. Ellis. 1998. Carrier frequency of the Bloom syndrome blmAsh mutation in the Ashkenazi Jewish population. *Mol. Genet. Metab.* **64**:286–290.

Lonn, U., S. Lonn, U. Nylen, G. Winblad, and J. German. 1990. An abnormal profile of DNA replication intermediates in Bloom's syndrome. *Cancer Res.* **50**:3141–3145.

Mirzaei, H., and K. Schmidt. 2012. Non-Bloom-syndrome-associated partial and total loss-of-function variants of BLM helicase. *Proc. Natl Acad. Sci. USA* **109**:19357–19362.

Newman, J. A., P. Savitsky, C. K. Allerston, A. C. W. Pike, E. Pardon, J. Steyaert, et al. 2013. Crystal structure of the Bloom's syndrome helicase BLM in complex with Nanobody. *Nucleic Acids Res.* **43**:5221–5235. *PDB ID: 4CDG*.

Nowsheen, S., F. Xia, and E. S. Yang. 2012. Assaying DNA damage in hippocampal neurons using the comet assay. *J. Vis. Exp.* **70**:e50049.

Olive, P. L., and J. P. Banath. 2006. The comet assay: a method to measure DNA damage in individual cells. *Nat. Protoc.* **1**:23–29.

Perry, P., and S. Wolff. 1974. New Giemsa method for the differential staining of sister chromatids. *Nature* **251**:156–158.

Pommier, Y. 2006. Topoisomerase I inhibitors: camptothecins and beyond. *Nat. Rev. Cancer* **6**:789–802.

Ramensky, V., P. Bork, and S. Sunyaev. 2002. Human non-synonymous SNPs: server and survey. *Nucleic Acids Res.* **30**:3894–3900.

Rao, V. A., A. M. Fan, L. Meng, C. F. Doe, P. S. North, I. D. Hickson, et al. 2005. Phosphorylation of BLM, dissociation from topoisomerase IIIalpha, and colocalization with gamma-H2AX after topoisomerase I-induced replication damage. *Mol. Cell. Biol.* **25**:8925–8937.

Rasband, W. S. 1997–2014. *ImageJ*. U. S. National Institutes of Health, Bethesda, Maryland, USA. Available at http://imagej.nih.gov/ij/.

Reva, B., Y. Antipin, and C. Sander. 2011. Predicting the functional impact of protein mutations: application to cancer genomics. *Nucleic Acids Res.* **39**:e118.

Richards, S., Aziz, N., Bale, S., Bick, D., Das, S., Gastier-Foster, J., Grody, W. W., Hegde, M., Lyon, E., Spector, E., Voelkerding, K., Rehm, H. L., ACMG Laboratory Quality Assurance Committee (2015). Standards and guidelines for the interpretation of sequence variants: a joint consensus recommendation of the American College of Medical Genetics and Genomics and the Association for Molecular Pathology. *Genetics in medicine : official journal of the American College of Medical Genetics*, **17**: 405-24.

Rios-Doria, J., A. Velkova, V. Dapic, J. M. Galan-Caridad, V. Dapic, M. A. Carvalho, et al. 2009. Ectopic expression of histone H2AX mutants reveals a role for its post-translational modifications. *Cancer Biol. Ther.* **8**:422–434.

Rogakou, E. P., D. R. Pilch, A. H. Orr, V. S. Ivanova, and W. M. Bonner. 1998. DNA double-stranded breaks induce histone H2AX phosphorylation on serine 139. *J. Biol. Chem.* **273**:5858–5868.

Schagger, H. 2006. Tricine-SDS-PAGE. *Nat. Protoc.* **1**:16–22.

Schneider, C. A., W. S. Rasband, and K. W. Eliceiri. 2012. NIH Image to ImageJ: 25 years of image analysis. *Nat. Methods* **9**:671–675.

Sherry, S. T., M. H. Ward, M. Kholodov, J. Baker, L. Phan, E. M. Smigielski, et al. 2001. dbSNP: the NCBI database of genetic variation. *Nucleic Acids Res.* **29**:308–311.

Straughen, J. E., J. Johnson, D. McLaren, M. Proytcheva, N. Ellis, J. German, et al. 1998. A rapid method for detecting the predominant Ashkenazi Jewish mutation in the Bloom's syndrome gene. *Hum. Mutat.* **11**:175–178.

Stucki, M., J. A. Clapperton, D. Mohammad, M. B. Yaffe, S. J. Smerdon, and S. P. Jackson. 2005. MDC1 directly binds phosphorylated histone H2AX to regulate cellular responses to DNA double-strand breaks. *Cell* **123**:1213–1226.

Sturzenegger, A., K. Burdova, R. Kanagaraj, M. Levikova, C. Pinto, P. Cejka, et al. 2014. DNA2 cooperates with the WRN and BLM RecQ helicases to mediate long-range DNA end resection in human cells. *J. Biol. Chem.* **289**:27314–27326.

Swan, M. K., V. Legris, A. Tanner, P. M. Reaper, S. Vial, R. Bordas, et al. 2014. Structure of human Bloom's syndrome helicase in complex with ADP and duplex DNA. *Acta Crystallogr. D Biol. Crystallogr.* **70**:1465–1475.

Thorisson, G. A., A. V. Smith, L. Krishnan, and L. D. Stein. 2005. The International HapMap Project Web site. *Genome Res.* **15**:1592–1593.

Traverso, G., C. Bettegowda, J. Kraus, M. R. Speicher, K. W. Kinzler, B. Vogelstein, et al. 2003. Hyper-recombination and genetic instability in BLM-deficient epithelial cells. *Cancer Res.* **63**:8578–8581.

Tsukuda, T., A. B. Fleming, J. A. Nickoloff, and M. A. Osley. 2005. Chromatin remodelling at a DNA double-strand break site in *Saccharomyces cerevisiae*. *Nature* **438**:379–383.

Xie, A., N. Puget, I. Shim, S. Odate, I. Jarzyna, C. H. Bassing, et al. 2004. Control of sister chromatid recombination by histone H2AX. *Mol. Cell* **16**:1017–1025.

CHAPTER THREE:

GENERATION AND CHARACTERIZATION OF A DIPLOID *BLM* KNOCKOUT

CELL LINE

Note to reader: Unpublished data. Experiments were designed by Kristina H. Schmidt and Vivek M. Shastri. All experiments were performed by Vivek Shastri.

INTRODUCTION

Bloom syndrome (BS) is a chromosomal instability disorder typified by highly elevated SCE levels, increased chromosome breaks, and the presence of quadriradial chromosomes. Furthermore, BS shows a strong correlation between chromosomal instability and an increased predisposition to a wide range of cancers from a young age [1-3]. BLM directly functions in the response to DNA damage and stalled replication forks [4-6]. Abnormal replication timing of both early- and late-replicating loci in BS cells has been associated with constitutive DNA damage [7]. BS cells have an increased frequency of ultrafine anaphase bridges, suggesting a role for BLM in suppressing their formation and faithful chromosome segregation [8, 9]. Moreover, it has been reported that BS cells have increased numbers of micronuclei possibly resulting from persistent anaphase bridges breaking in late mitosis [10]. Studies have also implicated a role for BLM in telomere maintenance, with BS cells exhibiting slower telomeric replication [11-14]. Loss of BLM therefore leads to the failure of cellular mechanisms which maintain chromosomal stability. The immortalized BS patient derived cell line GM08505 is aneuploid. The potential

conundrum is whether the chromosomal instability phenotype is partly due to its ploidy or if it is aneuploid because of chromosomal instability.

Chromosomal instability and aneuploidy have been considered hallmarks of cancer cells and tumorigenesis [15, 16]. Chromosomal instability is a form of genomic instability and pertains to gain or loss of either whole chromosomes or chromosomal segments. Compared to normal cells, such events occur at a higher frequency in cancer cells [17]. Defects in DNA replication, telomere maintenance, chromosomal segregation, cell cycle checkpoint activation, and DNA damage response are some of the most critical cellular causes of chromosomal instability. Aneuploidy is an uneven chromosome number, and co-exists with and is considered to be an outcome of chromosomal instability [16-19]. Paradoxically, another school of thought considers aneuploidy as the driver of chromosomal instability [16, 20, 21]. It has been suggested that variable expression of genes on aneuploid chromosomes can potentially disrupt the function of their protein product, leading to chromosomal instability phenotypes [22]. Further adding to the complex relationship, it has been shown that aneuploidy is a deterrent to tumorigenesis [23]. To reconcile their co-existence in cancer cells, it has been proposed that chromosomal instability and aneuploidy are part of a vicious cycle, where one fuels the other and the end result is an increasingly diverse karyotype. This variation resulting from aneuploidy can directly impact gene expression [24].

In this study, we generate a diploid *BLM* knockout cell line to determine the impact of aneuploidy on cellular defects associated with loss of BLM function.

MATERIALS AND METHODS

Cell lines, plasmid constructs and transfections

GM08505 is an SV40-transformed skin fibroblast cell line (FCL) established from a patient with Bloom syndrome (Coriell Cell Repository). GM00637 is an SV40-transformed FCL from a non-Bloom syndrome individual (Coriell Cell Repository). Cells were grown in minimal essential medium (Corning) supplemented with 10% FBS and 2 mM glutamine at 37°C in the presence of 5% CO2. GM08505 cells were plated 24 hr before transfections at approximately 2×10^4 per cm^2. BLM cDNA cloned into pcDNA3 vector and mutated at stated sites was transfected by using Polyfect (Qiagen) according to the manufacturer's instructions. Stable clones were selected in the presence of 750 μg of G418 per ml. Clones were maintained in the presence of 350 μg of G418 per ml. BLM cDNA contained in pcDNA3 vector was a kind gift from Dr Ian Hickson, University of Copenhagen.

CRISPR/Cas9-mediated BLM knockout

A diploid BLM knockout cell line was derived from the GM00637 cell line using a CRISPR/Cas9 mediated genome engineering protocol [25]. Briefly, guide or gRNA sequences targeting exon 8 within BLM were designed using the CRISPR guide design tool, which identifies and ranks suitable target sites and predicts off-target sites for each intended target (http://tools.genome-engineering.org). gRNA sequences with the highest score and least off-target impacts were cloned into the pSpCas9(BB)-2A-Puro vector and transfected into GM00637 using Lipofectamine 2000 (Invitrogen). Selection and clonal isolation was performed in the presence of 0.125 μg/mL puromycin. Amplicons were generated to sub-clone *BLM* exon 8 genomic loci into pCR-TOPO II vector for verification by sequencing. The protein consequences

97

of frameshift mutations within clones KSVS1452 and KSVS1453 are described in Table 3.1. Further verification was carried out by immunoblotting.

Antibodies

Mouse monoclonal antibody BLM-(F5) (Santa Cruz Biotech) was used to detect BLM. Rabbit polyclonal antibody against γ-H2AX (PhosphoDetect Anti-H2AX [pSer139]; Upstate Cell Signaling Solutions) was used for the γ-H2AX accumulation assays. Rabbit polyclonal anti-histone H3 and mouse monoclonal anti-tubulin antibodies (Abcam) were used to validate loading and quantify fold changes.

Subcellular fractionation and immunoblotting

Nuclear extract were prepared from exponentially growing cells to detect BLM expression in vivo. Briefly, cells were lysed (20 mM Tris pH 7.4, 10 mM KCl, 1 μM EDTA, 0.2% NP40, 50% glycerol, 0.6 mM βME, 1 mM PMSF and protease inhibitor cocktail) for 2 min on ice, which was followed by nuclear extraction (20 mM Tris pH 7.4, 10 mM KCl, 0.4 M NaCl, 1 μM EDTA, 50% glycerol, 0.6 mM BME, 1 mM PMSF and protease inhibitor cocktail) for 30 min on ice. For the γ-H2AX accumulation assays, chromatin fractions were extracted from the nuclear extract pellet by using an acid extraction buffer (0.5 M HCl, 50% Glycerol, 100 mM βME) and subsequently neutralized using 40 mM Tris pH 7.4 with protease inhibitors and NaOH [26].

SCE analysis

SCEs were analyzed by using protocols described previously [27-29]. Briefly, cells were cultured for two cell cycles in growth medium supplemented with BrdU Labeling Reagent (Life

98

Technologies) at a dilution of 1:100. Metaphase arrest was induced by the addition of 0.1 μg/ml Colcemid for 1 hr before harvesting. Chromosome spreads were prepared after hypotonic treatment with 75 mM KCL and fixation with 3:1 (vol/vol) methanol-acetic acid. The metaphase spreads were then differentially stained using Hoechst 33258 (75μg/ml; Life Technologies) and Giemsa (3.5%; Life Technologies). Intact metaphases were imaged using the Plan-Apochromat 100x/1.40 Oil DIC M27 objective of a Zeiss Axiovert 100 deconvolution microscope. For each cell line, SCEs in >1500 chromosomes were scored.

Clonogenic cell survival assay

Cells were seeded at a density of 500 cells/well for colony formation. The next day, either fresh medium containing HU (0.1, 0.2, 0.3, 0.4 and 0.5 mM HU) or drug-free medium was added. The medium was removed after 48 hr and cells were washed with PBS before colonies were allowed to grow in fresh complete growth medium for up to 4 weeks. Colonies were fixed in 3:1 (vol/vol) methanol-acetic acid and stained with 0.01% crystal violet. Colonies with more than 50 cells were scored as survivors. The number of colonies at each dosage point was expressed as a percentage.

γ-H2AX accumulation assay

Exponentially growing cells were treated with 1μM CPT and harvested post release from treatment at various time points (10 min, 20 min, 30 min, 45 min, 1 hr, 8 hr, 24 hr and 48 hr). Chromatin fractions were run on a 16% Tricine-SDS polyacrylamide gel [30] and Western blots were probed with anti- γ-H2AX antibody (PhosphoDetect Anti-H2AX [pSer139]). Fold changes in γ-H2AX levels with respect to histone H3 levels were obtained using ImageJ [31].

Neutral comet assay

Neutral Comet assays were performed according to protocols described earlier [32, 33]. Briefly, damage was induced by the addition of 1 μM CPT to culture for 1 hr. Subsequently, the cells were grown in drug-free media for 1, 24 and 48 hr before being harvested. Single cell suspensions in 1% low melt agarose were plated on slides, lysed using neutral lysis buffer and electrophoresed at 25 V for 30 mins. The slides were immersed in 70% ethanol for fixation and subsequently stained using SYBR Gold (1:10,000 in PBS; Life Technologies). At least 50 comets were imaged for each clone at each time point and the mean of the tail DNA percentage was calculated using OpenComet, an open source software for automated analysis of comet assay images [34].

RESULTS

Indels in *BLM* exon 8 result in premature termination of BLM before motif IV of its helicase domain

We used diploid GM00637 cells, which have no known BLM deficiency or dysfunction, as the target of CRISPR/Cas9 mediated genome engineering to generate a diploid, functional *BLM* knockout cell lines. Indel events and single amino acid residue changes within the conserved helicase domain of BLM interfere with its helicase function, resulting in a complete loss of function [35-37]. Therefore, we chose to engineer indels within *BLM* exons 6-8 in order to induce frameshift mutations potentially resulting in premature termination of BLM either just before or at the beginning of its helicase core region. Based on an experimental design previously shown to be efficient [25], we designed multiple short guide or sgRNA sequences to enable CRISPR/Cas9 mediated indel events to occur within exons 6-8 and proceeded to

100

functionally screen clonal isolates (Figure 3.1.A and Table 3.1). Two of the exon 8 targeted clones did not show any signal upon immunoblotting to test for BLM expression (Figure 3.1.B). Sequencing the targeted exon 8 loci further revealed biallelic modifications within these two clones. The first clone, now designated KSVS1452 contained a 7 bp deletion in one allele and a 6 bp deletion/2 bp insertion in the other allele. The other clone, now designated KSVS1453, contained a 4 bp deletion/2 bp insertion in one allele and a 5 bp deletion/3 bp insertion in the other allele. Both allelic modifications in KSVS1452 resulted in BLM terminating at residue 686, whereas the allelic modifications in KSVS1453 resulted in BLM terminating at residues 676 and 682 (Figure 3.1.C and Table 3.2).

KSVS1452 and KSVS1453 are diploid and exhibit elevated SCE levels

We performed a karyotype using KSVS1452 and KSVS1453 cells to ascertain their ploidy. 35 metaphase spreads from each cell line were stained with Giemsa and ~1500 chromosomes were counted. Both the cell lines were found to be diploid (Figure 3.2.A). Since highly elevated levels of SCE are a hallmark of BLM$^{-/-}$ cells, we measured the SCE rates in KSVS1452 and KSVS1453 cells as our primary functional test. The cells were labeled with BrdU for two cell cycles and used to prepare metaphase spreads. These were differentially stained with Hoechst/Giemsa and SCEs from ~1500 chromosomes were scored. We found a 15-fold and 10-fold increase in the SCE frequencies in KSVS1452 and KSVS1453 cells compared to GM00637 cells (Figure 3.2.B and C). This is consistent with SCE frequencies observed in BS patient derived cells as well as BLM$^{-/-}$ cells expressing variants which have a null phenotype [36, 38].

101

KSVS1452 and KSVS1453 cells are hypersensitive to replication stress induction and exhibit reduced DSBR efficiency

BLM$^{-/-}$ cells and cells expressing BLM null variants are hypersensitive to the replication stress inducing drug hydroxyurea (HU) and the Top I poison camptothecin (CPT) [36]. To test their response to genotoxicity, cells were exposed to various concentrations of HU for 48 hrs before being released into drug free media and stained to score surviving colonies after 4 weeks. Both the cell lines exhibited increased sensitivity to HU compared to GM00637 cells (Figure 3.3).

Next, we induced replication-specific DSBs by growing the cells in the presence of 0.1µM CPT. Phosphorylation of histone H2A at Ser139 to form γ-H2AX is one of the earliest of markers of DSB formation [39]. Therefore, we measured accumulation of γ-H2AX in cells from various time-points post-CPT treatment release as an index of replication stress response initiation. Using a phospho-specific antibody recognizing γ-H2AX^{pSer139} for immunoblotting, we found that γ-H2AX accumulation in KSVS1452 and KSVS1453 cells peaked at 24 hr post-CPT release compared to 1 hr in GM00637 cells. Furthermore, γ-H2AX was eliminated rapidly in GM00637 cells after peaking as opposed to KSVS1452 and KSVS1453 cells (Figure 3.4).

Apart from being the one of the first DSB formation markers, γ-H2AX has also been implicated in recruiting DSB repair factors and maintaining replication stress response [40-42]. The remarkable disparity in γ-H2AX accumulation and elimination profiles between GM00637 and KSVS1452/KSVS1453 cells is similar to differences observed when comparing GM00637cells, BS patient derived cells and cells expressing BLM variants with a null phenotype [36]. As shown earlier, this impaired γ-H2AX accumulation/elimination corresponded

to inefficient DSBR. Therefore, we used a neutral comet assay to test the DSBR efficiency of KSVS1452/1453 cells. Cells were exposed to 0.1µM CPT and harvested at the same time-points used for testing γ-H2AX accumulation. Single cell suspensions were lysed and used for electrophoresis. At the end of 24 hrs, 14% of DSBs were unrepaired in GM00637 compared to 65% and 45% in KSVS1452 and KSVS1453 cells respectively (Figure 3.4).

DISCUSSION

In this study, two clonal isolates of a diploid fibroblast cell line with indels engineered within exon 8 of the *BLM* gene resulted in two functional BLM knockout cell lines. Remarkably, these cell lines exhibit cellular defects consistent with those observed in immortalized BS patient derived cells and cells expressing helicase dead or null mutants of BLM [36]. The BS patient derived cell line, GM08505, is aneuploid and some of the chromosomal instability phenotype could be attributed to its ploidy. We show that these cellular defects are directly associated with loss of BLM function. Despite being diploid, cells lacking functional BLM exhibited defects in cellular pathways associated with maintaining chromosomal stability. It remains to be seen whether this chromosomal instability would lead to aneuploidy in these two cell lines as they continue to be passaged and could shed more light on this relationship. SCE levels in BS patient derived cell lines have been shown to be restored to near normal levels by BLM complementation, presenting a system for structure-function analysis by complementing various BLM variants [36, 38]. It is interesting to note that the elevated SCE frequencies observed in these cell lines were comparable to that of BS patient derived cell line despite very little adaptation time. Based on our results, we propose that CRISPR/Cas9 mediated genome engineering can be used to generate compound heterozygous *BLM* mutant cell lines to understand the function of BLM in maintaining chromosomal stability.

103

Hypersensitivity to replication stress inducing agents and reduced DSBR efficiency in the two knockout cell lines provide additional evidence of BLM function in the response to replication induced DSBs. Specifically, delayed γ-H2AX accumulation and elimination suggest a direct role for BLM as an early DSB responder/recognizer during replication. This data also strengthens the association between BLM function and γ-H2AX dephosphorylation [36].

One approach to understand pathways compensating for/compounding defects associated with BLM deficiency is to perform a quantitative global proteome evaluation to identify dysregulated factors. However, the BS patient derived cell line GM08505 is aneuploid with a variable chromosome number. This can potentially lead to variable gene dosage and differential protein levels within the cell line. There is evidence of aneuploidy can directly affect gene expression and lead to a variable proteome levels [24]. Therefore, aneuploid cell lines are not conducive to be used for evaluating proteomes quantitatively. The two diploid *BLM* knockout cell lines generated in this study can now be used for a comparative quantitative proteomic approach to identify dysregulated factors. Additionally, these diploid cell lines provide a system to complement and study BLM function in the absence of potentially dysregulated factors in the aneuploid GM08505 cell line.

FIGURES AND TABLES

Table 3.1. Primers and gRNAs used in this study

Oligo ID	Sequence
3119BLM_E6sgRNA_F	CACCGGGAACGAACTGCTTCAGCAG
3120BLM_E6sgRNA_R	AAACCTGCTGAAGCAGTTCGTTCCC
3121BLM_E7sgRNA_F	CACCGTTCACTTGATGGCCCTATGG
3122BLM_E7sgRNA_R	AAACCCATAGGGCCATCAAGTGAAC
3124BLM_E8sgRNA_F	CACCGGCGATCAATGCTGCACTGCT
3125BLM_E8sgRNA_R	AAACAGCAGTGCAGCATTGATCGCC
3131pSpCas9_Chk-1	GGTATCCACGGAGTCCCAG
3132pSpCas9_Chk-2	GGACAGCACCGACAAGGC
3133pSpCas9_Chk-3	CAAGAACCTGTCCGACGC
3134pSpCas9_Chk-4	CCTTCCGCATCCCCTACTAC
3135pSpCas9_Chk-5	CCACGATCTGCTGAAAATTA
3136pSpCas9_Chk-6	GAGCTCGTGAAAGTGATGGG
3137pSpCas9_Chk-7	TTCGACAATCTGACCAAGGC
3138pSpCas9_Chk-8	CAAGACCGAGATTACCCTGG
3139pSpCas9_Chk-9	CCTGATCATCAAGCTGCCTA
3140pSpCas9_Chk-10	ACCCTGATCCACCAGAGCAT
3164BLMEx6-1_F	GCTAGACAGATAAGTTTACAGCAGC
3165BLMEx6-1_R	ATGATCATCCTTATGCCATTTCCAG
3166BLMEx7-1_F	ACCACTCTAAGTGAAAAATGGACAG
3167BLMEx7-1_R	TATCATAGGAAGGTTGGGTTTCTCT
3168BLMEx8-1_F	AAAGTAGTGGTAGGTGCTGTAGAAA
3169BLMEx8-1_R	GTTGCAAATAAACTGCCAGAAATGG
3170BLMEx7-2_F	ACTACAGATTTGCTTTTGTGGCCTA
3171BLMEx7-2_R	CCAGTTGCTACTTACAAAGGACTTCT
3172BLMEx8-2_F	GCTGTACTTTCACTGTATTCATGTACT
3173BLMEx8-2_R	CTTTCTCACTATGGTACAGGAGGTT
3174BLMEx6-2_F	TTACAGTCATGAGCCACCATGC
3175BLMEx6-2_R	ACGAATGTTAAAGGAGTGGTTTGAA

Table 3.2. Consequences of targeted frameshift mutations within *BLM* exon 8

Cell line	*BLM* genomic consequence	BLM amino acid sequence	BLM protein consequence
GM00637		DKSAQNLASRNLKH ERFQSLSFPHTKEM MKIFHKKFGLHNFR TNQLEAINAALLGE DCFILMPT	
KSVS1452	*BLM* exon 8 (c.del2040_2 046; g.del90,763,1 23_90,763,13 0)	DKSAQNLASRNLKH ERFQSLSFPHTKEM MKIFHKKFGLHNFR TNQLEAINAALKTV LS	BLM (p.Leu681Lys Ter686)
KSVS1452	*BLM* exon 8 (c.delins2036 _2041AG; g.delins90,76 3,119_90,763 ,124AG)	DKSAQNLASRNLKH ERFQSLSFPHTKEM MKIFHKKFGLHNFR TNQLEAINAELVKT VLS	BLM (p.Leu678Ala Ter686)
KSVS1453	*BLM* exon 8 (c.delins2039 _2042AC; g.delins90,76 3,122_90,763 ,125AC)	DKSAQNLASRNLKH ERFQSLSFPHTKEM MKIFHKKFGLHNFR TNQLEAINAALH	BLM (p.Leu678HisT er682)
KSVS1453	*BLM* exon 8 (c.delins2025 _2029GTA; g.delins90,76 3,108_90,763 ,112GTA)	DKSAQNLASRNLKH ERFQSLSFPHTKEM MKIFHKKFGLHNFR TNQLEA	BLM p.(676IleTer*)
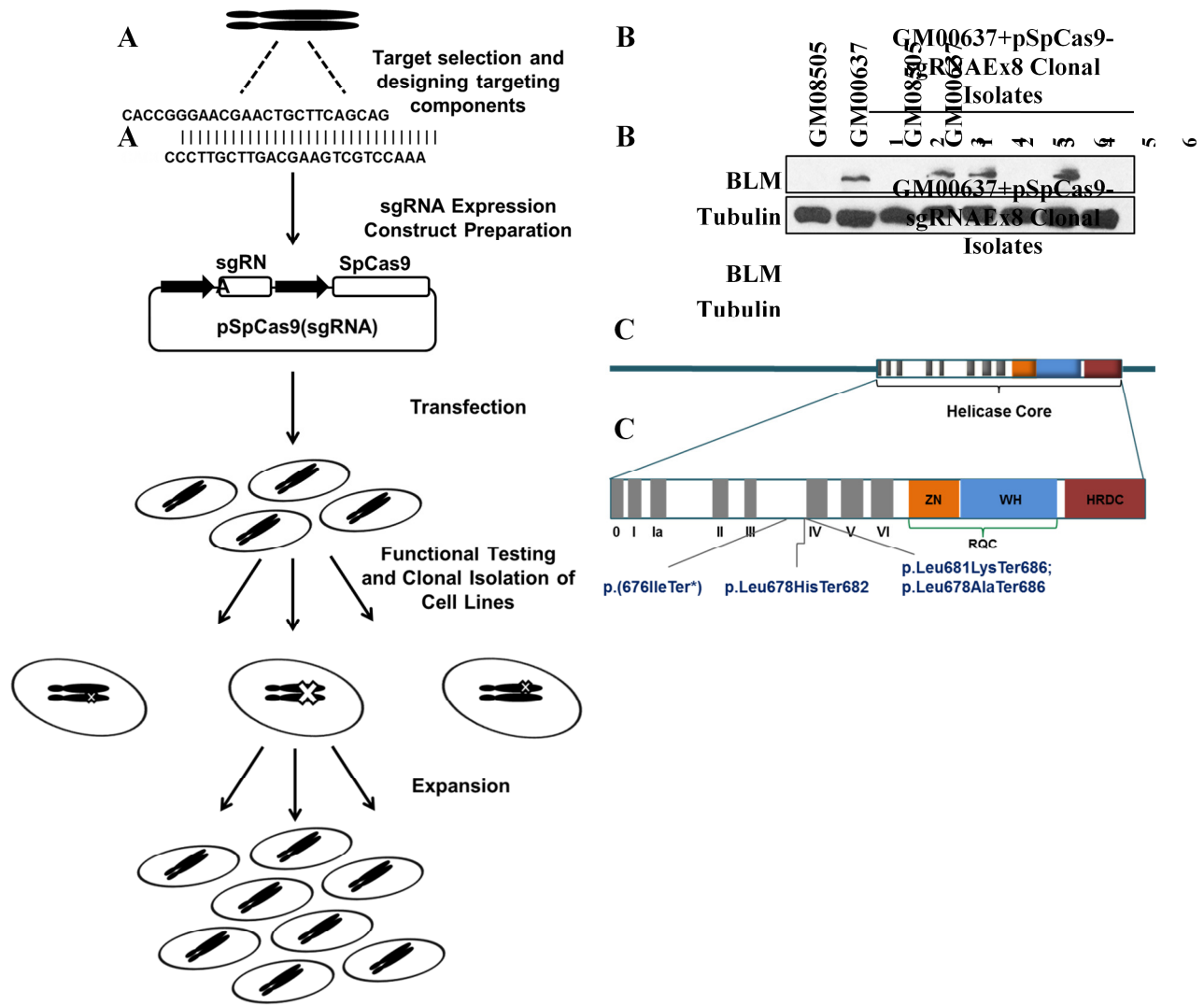
Figure 3.1. CRISPR/Cas9 mediated *BLM* knockout
Schematic representation of protocol used to generate CRISPR/Cas9 mediated *BLM* knockout
cell lines (A). Immunoblot showing absence of BLM signal; Clone 6 is KSVS1452 and clone 4
is KSVS1453 (B). 2-D map of BLM showing the protein consequences of BLM after indels were
engineered in exon 8 (C).

107
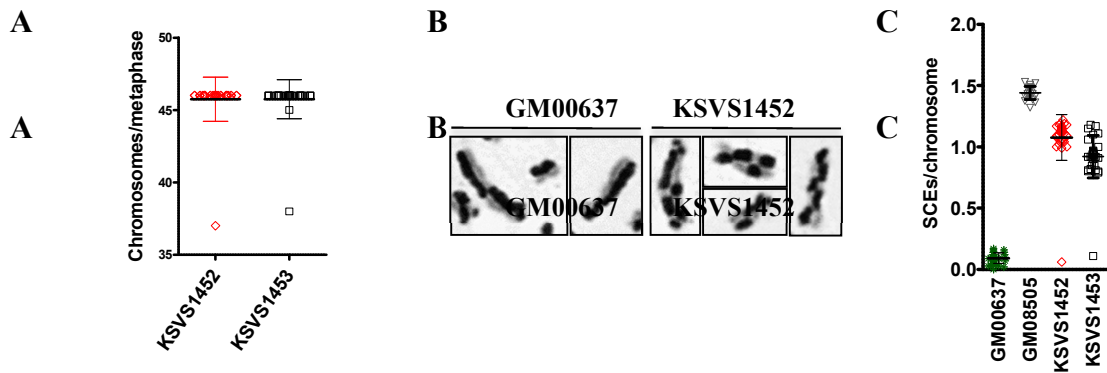
Figure 3.2. Chromosomal aberrations in *BLM* knockout cell lines
KSVS1452 and KSVS1453 cells are diploid (A). KSVS1452 cells showing SCEs characteristic
of BS cells (B). SCEs scored from ~1500 chromosomes show elevated SCE frequencies in
KSVS1452 and KSVS1453 compared to the parental GM00637 cell line.
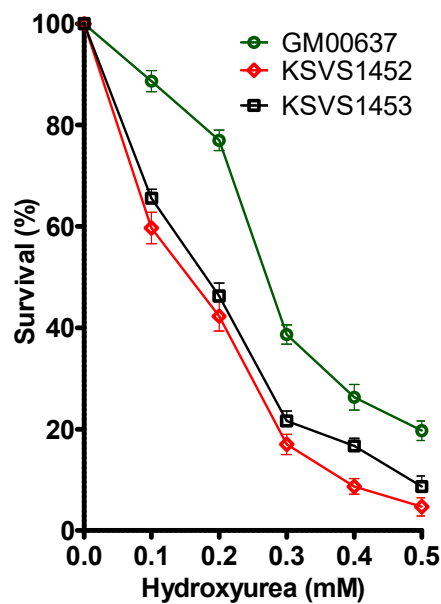
Figure 3.3. KSVS1452 and KSVS1453 exhibit hypersensitivity to hydroxyurea
Cells were exposed to hydroxyurea and surviving colonies were scored four weeks after relase
from treatment.

108
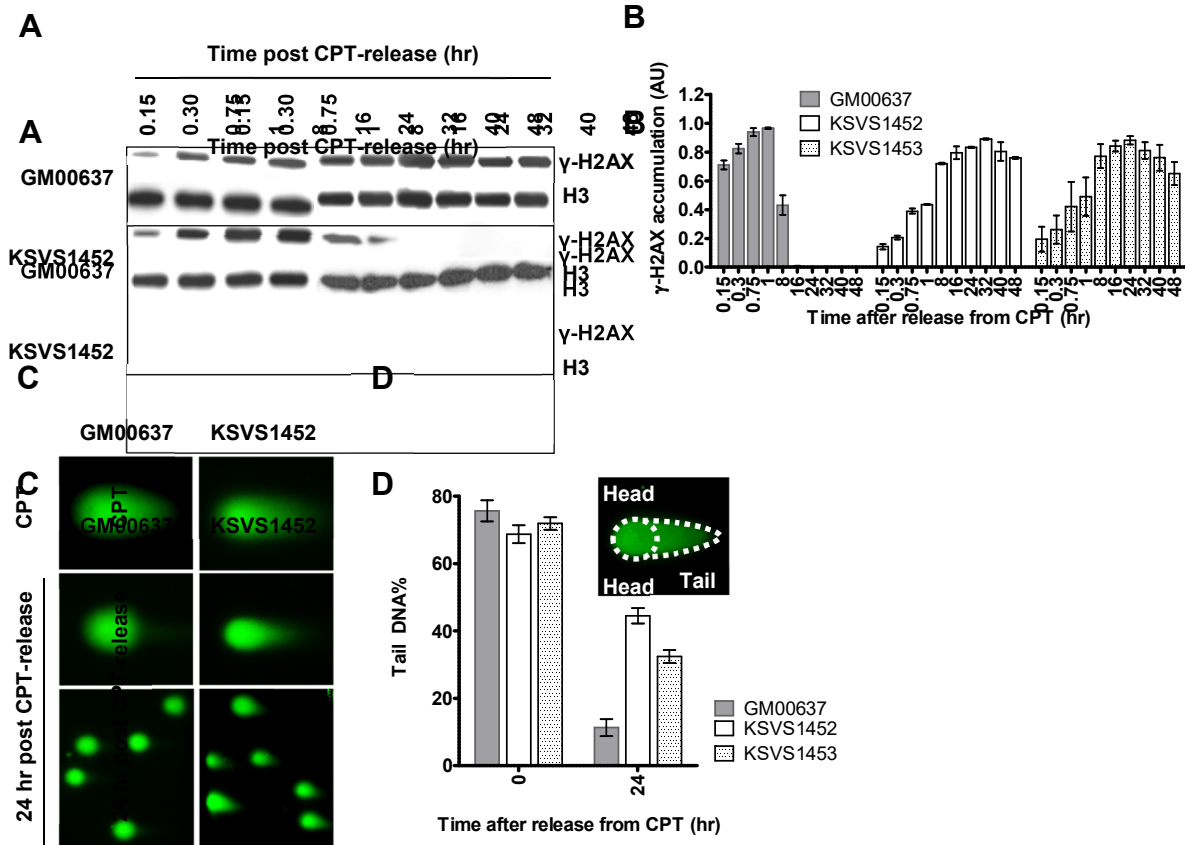
Figure 3.4. Response to replication stress induced double strand breaks
KSVS1452 and KSVS1453 cells exhibit delayed response to replication stress with a concomitant decrease in DSBR efficiency.

REFERENCES

1.   Chaganti, R.S.K., S. Schonberg, and J. German, *A Manyfold Increase in Sister Chromatid Exchanges in Bloom's Syndrome Lymphocytes.* Proceedings of the National Academy of Sciences, 1974. **71**(11): p. 4508-4512.

2.   German J., E.N.A., *Bloom Syndrome*. The Genetic Basis of Human Cancer ed. K.W.K.E. B. Vogelstein. 1998.

3.   Hickson, I.D., *RecQ helicases: caretakers of the genome.* Nat Rev Cancer, 2003. **3**(3): p. 169-78.

4.   Davies, S.L., P.S. North, and I.D. Hickson, *Role for BLM in replication-fork restart and suppression of origin firing after replicative stress.* Nature Structural &Amp; Molecular Biology, 2007. **14**: p. 677.

5.   Franchitto, A. and P. Pichierri, *Protecting genomic integrity during DNA replication: correlation between Werner's and Bloom's syndrome gene products and the MRE11 complex.* Hum Mol Genet, 2002. **11**(20): p. 2447-53.

6.   Frei, C. and S.M. Gasser, *RecQ-like helicases: the DNA replication checkpoint connection.* J Cell Sci, 2000. **113 (Pt 15)**: p. 2641-6.

7.   Rassool, F.V., et al., *Constitutive DNA damage is linked to DNA replication abnormalities in Bloom's syndrome cells.* Oncogene, 2003. **22**: p. 8749.

8.   Chan, K.L., P.S. North, and I.D. Hickson, *BLM is required for faithful chromosome segregation and its localization defines a class of ultrafine anaphase bridges.* Embo j, 2007. **26**(14): p. 3397-409.

9.   Rouzeau, S., et al., *Bloom's syndrome and PICH helicases cooperate with topoisomerase IIalpha in centromere disjunction before anaphase.* PLoS One, 2012. **7**(4): p. e33905.

10. Rosin, M.P. and J. German, *Evidence for chromosome instability in vivo in bloom syndrome: Increased numbers of micronuclei in exfoliated cells.* Human Genetics, 1985. **71**(3): p. 187-191.

11. Drosopoulos, W.C., S.T. Kosiyatrakul, and C.L. Schildkraut, *BLM helicase facilitates telomere replication during leading strand synthesis of telomeres.* The Journal of Cell Biology, 2015. **210**(2): p. 191-208.

12. Lillard-Wetherell, K., et al., *Association and regulation of the BLM helicase by the telomere proteins TRF1 and TRF2.* Hum Mol Genet, 2004. **13**(17): p. 1919-32.

13. Pan, X., et al., *FANCM, BRCA1, and BLM cooperatively resolve the replication stress at the ALT telomeres.* Proc Natl Acad Sci U S A, 2017. **114**(29): p. E5940-9.

14. Sobinoff, A.P., et al., *BLM and SLX4 play opposing roles in recombination-dependent replication at human telomeres.* The EMBO Journal, 2017. **36**(19): p. 2907-2919.

15. Hanahan, D. and R.A. Weinberg, *Hallmarks of cancer: the next generation.* Cell, 2011. **144**(5): p. 646-74.

16. Potapova, T.A., J. Zhu, and R. Li, *Aneuploidy and chromosomal instability: a vicious cycle driving cellular evolution and cancer genome chaos.* Cancer metastasis reviews, 2013. **32**(3-4): p. 377-389.

17. Gollin, S.M., *Mechanisms leading to chromosomal instability.* Seminars in Cancer Biology, 2005. **15**(1): p. 33-42.

18. Giam, M. and G. Rancati, *Aneuploidy and chromosomal instability in cancer: a jackpot to chaos.* Cell division, 2015. **10**: p. 3-3.

19. Nicholson, J.M. and D. Cimini, *Cancer karyotypes: survival of the fittest.* Front Oncol, 2013. **3**: p. 148.

20. Weaver, B.A. and D.W. Cleveland, *The aneuploidy paradox in cell growth and tumorigenesis.* Cancer cell, 2008. **14**(6): p. 431-433.

21. Sheltzer, J.M., et al., *Aneuploidy drives genomic instability in yeast.* Science, 2011. **333**(6045): p. 1026-30.

22. Pfau, S.J. and A. Amon, *Chromosomal instability and aneuploidy in cancer: from yeast to man.* EMBO reports, 2012. **13**(6): p. 515-527.

23. Williams, B.R., et al., *Aneuploidy affects proliferation and spontaneous immortalization in mammalian cells.* Science (New York, N.Y.), 2008. **322**(5902): p. 703-709.

24. Pavelka, N., et al., *Aneuploidy confers quantitative proteome changes and phenotypic variation in budding yeast.* Nature, 2010. **468**: p. 321.

25. Ran, F.A., et al., *Genome engineering using the CRISPR-Cas9 system.* Nat Protoc, 2013. **8**(11): p. 2281-2308.

26. Rios-Doria, J., et al., *Ectopic expression of histone H2AX mutants reveals a role for its post-translational modifications.* Cancer Biol Ther, 2009. **8**(5): p. 422-34.

27. Bayani, J. and J.A. Squire, *Sister Chromatid Exchange*, in *Current Protocols in Cell Biology*. 2001, John Wiley & Sons, Inc.

28. Campos, P.B., et al., *Chromosomal Spread Preparation of Human Embryonic Stem Cells for Karyotyping.* 2009(31): p. e1512.

29. Perry, P. and S. Wolff, *New Giemsa method for the differential staining of sister chromatids.* Nature, 1974. **251**(5471): p. 156-158.

30. Schagger, H., *Tricine-SDS-PAGE.* Nat. Protocols, 2006. **1**(1): p. 16-22.

31. Rasband, W.S., *ImageJ.* U. S. National Institutes of Health, Bethesda, Maryland, USA, http://imagej.nih.gov/ij/, 1997-2014.

32. Nowsheen, S., F. Xia, and E.S. Yang, *Assaying DNA Damage in Hippocampal Neurons Using the Comet Assay.* 2012(70): p. e50049.

33. Olive, P.L. and J.P. Banath, *The comet assay: a method to measure DNA damage in individual cells.* Nat. Protocols, 2006. **1**(1): p. 23-29.

34. Gyori, B.M., et al., *OpenComet: An automated tool for comet assay image analysis.* Redox Biology, 2014. **2**(0): p. 457-465.

111

35.   Ellis, N.A., et al., *The Ashkenazic Jewish Bloom syndrome mutation blmAsh is present in non-Jewish Americans of Spanish ancestry.* American journal of human genetics, 1998. **63**(6): p. 1685-1693.

36.   Shastri, V.M. and K.H. Schmidt, *Cellular defects caused by hypomorphic variants of the Bloom syndrome helicase gene BLM.* Molecular Genetics & Genomic Medicine, 2016. **4**(1): p. 106-119.

37.   Suhasini, A.N. and R.M. Brosh, Jr., *Disease-causing missense mutations in human DNA helicase disorders.* Mutation research, 2013. **752**(2): p. 138-152.

38.   Ellis, N.A., et al., *Transfection of BLM into cultured bloom syndrome cells reduces the sister-chromatid exchange rate toward normal.* Am J Hum Genet, 1999. **65**(5): p. 1368-74.

39.   Rogakou, E.P., et al., *DNA double-stranded breaks induce histone H2AX phosphorylation on serine 139.* J Biol Chem, 1998. **273**(10): p. 5858-68.

40.   Celeste, A., et al., *Genomic instability in mice lacking histone H2AX.* Science, 2002. **296**(5569): p. 922-7.

41.   Fernandez-Capetillo, O., et al., *DNA damage-induced G2-M checkpoint activation by histone H2AX and 53BP1.* Nat Cell Biol, 2002. **4**(12): p. 993-7.

42.   Kolas, N.K., et al., *Orchestration of the DNA-damage response by the RNF8 ubiquitin ligase.* Science, 2007. **318**(5856): p. 1637-40.

CHAPTER FOUR:

CELL CYCLE SPECIFIC INTERACTIONS WITH MCM6 UNCOVER A NOVEL ROLE

FOR BLM IN GENOME STABILITY

Note to reader: Unpublished data. Experiments were designed by Kristina H. Schmidt and Vivek M. Shastri. All experiments were performed by Vivek M. Shastri.

SUMMARY

The Bloom syndrome DNA helicase BLM contributes to chromosome stability through its roles in double-strand break repair by homologous recombination (HR), suppression of recombination at Gquadruplexes, and DNA replication fork restart during the DNA-damage response. Here, we report that BLM physically interacts with the Mcm6 subunit of the replicative MCM helicase and that this interaction is mediated by two distinct bindings sites in BLM and Mcm6 that differentially regulate BLM/MCM interaction in G1 and in normal or perturbed S-phase. Unlike other replisome components, BLM binds to the Cdt1-binding domain of Mcm6 and can compete with Cdt1 for Mcm6 binding in G1. We demonstrate the significance of BLM and the novel BLM/Mcm6 interaction for unfolding G-quadruplex structures in G1 phase, suggesting that the BLM/Mcm6 interaction contributes to genome stability by assisting replisome assembly and initiation at G-quadruplex-rich origins.

INTRODUCTION

Genomic instability is a hallmark of disorders in which DNA repair genes are dysfunctional (Zeman and Cimprich, 2014). The prevention of genomic instability also depends on multiple pathways ensuring timely progression of replication and appropriate response to DNA damage. The tumor suppressor gene BLM encodes a 3'-5' DNA helicase of the conserved RecQ DNA helicase family, which has been implicated in key roles during DNA recombination and repair to maintain genome stability (Bachrati and Hickson, 2003, Hickson, 2003, Karow et al., 1997, Ouyang KJ et al., 2008). Null mutations in BLM cause Bloom syndrome (BS), an autosomal recessive disorder characterized by short stature, an extreme predisposition to a wide range of cancers from an early age and, at the cellular level, elevated levels of sister chromatid exchanges (SCEs), chromosome aberrations and hypersensitivity to DNA-damaging agents (Chaganti et al., 1974, German, 1998, German et al., 2007). The best understood function of BLM is the dissolution of double Holliday junctions during HR-mediated DNA double strand break (DSB) repair where BLM acts in a complex with TopoIIIα, Rmi1 and Rmi2 to yield noncrossover products (Karow et al., 2000, Wu and Hickson, 2003). BLM also controls early steps of HR by contributing to the processing of DSB ends into single stranded 3' overhangs for strand invasion and through its ability to reverse the strand invasion step (Daley et al., 2014).

BLM helicase function is also required for efficient restart of stalled replication forks in the presence of replication stress. In the absence of BLM, cells exposed to replication-stress-inducing agents like hydroxyurea (HU) display compromised fork reactivation and delayed cell division (Sidorova et al., 2013). Of all stalled replication forks, fewer than 40% restart in BS cells (Davies et al., 2007). Studies have shown BLM localization to stalled replication forks that develop into DSBs (Davalos and Campisi, 2003). Chromatin recruitment of DNA-damage-

114

response factors like BRCA1, 53BP1 and the MRN complex to stalled replication forks is delayed in BS cells, leading to BLM being associated with a role in their recruitment and facilitating fork protection (Davalos and Campisi, 2003, Franchitto and Pichierri, 2002). These observations establish BLM as an important factor in the replication stress response.

BLM's function in recombinational repair has been proposed as a plausible mechanism by which it promotes fork restart upon replication stress induction. Notably, in vitro analyses have shown that BLM can promote regression of model replication forks (Machwe et al., 2006, Ralf et al., 2006). Moreover, the high level of SCEs in BS cells has been viewed as possible evidence of illegitimate mitotic recombination products when collapsed replication forks undergo DSB repair (Wu et al., 2001).

In vitro, BLM has been shown to bind and unwind G-quadruplex (G4) structures (Popuri et al., 2008, Sun et al., 1998, Wu et al., 2015). *In vivo*, G4s are stable secondary DNA structures that impede replication fork progression, especially at telomeres (Bochman et al., 2012, Lam et al., 2013, Lopes et al., 2011). However, reports of a direct role of BLM in G4 unwinding *in vivo* have remained sparse (van Wietmarschen et al., 2018). There is evidence of slow moving replication forks originating within the G4- rich telomeric sequences in BS cells (Drosopoulos et al., 2015). However, instead of BLM, other RecQ helicases, most notably WRN, appear to have specialized in G4 unwinding during telomere replication, and defects in WRN lead to telomere dysfunction and an adult premature aging syndrome (Werner syndrome) whereas BLM defects do not (Kudlow et al, 2007). Further underscoring BLM's specificity to a variety of non-canonical DNA substrates, BLM can also unwind model DNA:RNA hybrids and R-loops *in vitro*, which can cause replication fork stalling (Grierson et al., 2012). Observations of R-loop accumulation causing DNA damage in BS cells and BLM/R-loop proximity *in vivo* seem to

115

imply BLM involvement in maintaining replisome stability at sites of collision with R-loops (Chang et al., 2017).

The six-subunit minichromosome maintenance (MCM) complex is an essential component of the eukaryotic replisome and functions in DNA replication initiation and elongation. It is the catalytic subunit of the major replicative helicase complex and is loaded onto DNA replication origins in a stepwise manner by the licensing factor Cdt1 (Evrin et al., 2009, Liu et al., 2012, Remus et al., 2009). An excessive amount of the MCM complex is loaded onto replication origins, but not all fire in the following S-phase. These so called dormant origins fire under low levels of endogenous replication stress and may prevent DSBs forming from stalled DNA replication forks (Ibarra et al., 2008). The MCM complex also serves as an important component of the replication checkpoint and is an effector of the ATR– FANCD2–FANCI pathway activated in response to replication stress (Chen et al., 2015, Cortez et al., 2004, Lossaint et al., 2013, Yu et al., 2016). It is evident that the MCM complex has functions beyond its role in duplex unwinding to safeguard genomic integrity. However, it requires assistance from specialized DNA helicases to move through challenging loci containing non-canonical DNA structures (Leman and Noguchi, 2013).

Here, we performed a proteomic analysis of the BLM complex in mid-S-phase to identify the mechanism by which BLM contributes to stable genome duplication in unperturbed cells. We identified the MCM subunit Mcm6 as a novel BLM interactor and show that BLM uses multiple, distinct binding sites to differentially associate with Mcm6 during pre-initiation complex formation in G1, at active replisomes in S-phase, and during the DNA-damage response. Unique among replisome components, BLM binds to the Cdt1-binding domain of Mcm6 in S-phase and competes with Cdt1 for Mcm6 binding *in vitro* and in G1 phase. Our findings reveal BLM as a

constitutive component of active replisomes in unperturbed S-phase and uncover the importance of BLM and the BLM/Mcm6 interaction in the absence of DNA replication in G1 phase when G4s ubiquitously form at replication origins and may interfere with pre-replication complex formation and the G1/S transition.

RESULTS

BLM forms a complex with Mcm6 in G1 and S-phase

To identify the composition of the BLM complex during unperturbed DNA replication, we performed a proteomic screen in mid-S-phase when BLM expression peaks. We synchronized GM00637 cells (*BLM*$^{+/+}$, normal skin fibroblasts) in G1 phase, released them into S-phase for 3 hours, immunoprecipitated endogenous BLM from nuclear extracts and identified co-immunoprecipitates by mass spectrometry. Across three biological replicates, Mcm2, Mcm6, and Mcm7 subunits of the MCM helicase were the top identified hits in addition to known BLM interactors TopoIIIα (Wu et al., 2000), Rmi2 (Singh et al., 2008), and PML (Bischof et al., 2001) (Fig. 1A). Of these, only Mcm6 was not identified in the isogenic *BLM* knockout cell line (KSVS1452). We verified the BLM/Mcm6 interaction by reciprocal co-immunoprecipitation using recombinant BLM and Mcm6 (Fig. 1B) and detected the interaction between endogenous BLM and Mcm6 in GM00637 cells not only in S-phase, but also in G1 (Fig. 1C). As expected, the interaction was not detected in the isogenic KSVS1452 cell line with a CRISPR-mediated, biallelic disruption of exon 8 of *BLM* (Fig. 1C, Fig. S1A-G).

Using antibodies directed against endogenous BLM and Mcm6, we observed that BLM forms foci in G1 and in S-phase and that all BLM foci colocalize with Mcm6 (Fig. 1D, 1F and 1G). The vast majority (95%) of Mcm6/BLM foci in unperturbed S-phase were at sites of active

117

DNA replication as indicated by EdU incorporation (Fig. 1E and 1H). These findings suggest that BLM is a component of pre-initiation complexes in G1 and a constitutive component of active replisomes in unperturbed S-phase. Starting at mid-S-phase, occasional BLM foci appeared that were not in the same complex as Mcm6 (Fig. 1G). These foci make up ~4-8% of all BLM foci in the second half of S-phase and predominantly colocalize with PML (Fig. S1H), suggesting that BLM may be sequestered to PML bodies as genome duplication nears completion or where it may be modified and degraded (Ouyang et al., 2009, Singh et al., 2008). Lack of colocalization with 53BP1 in unperturbed S-phase (Fig. S1I) suggests that most of these BLM foci are not indicative of spontaneous DSBs in late S-phase.

BLM binds to the N-terminal domain of Mcm6 via a pseudo-PIP-box

The Mcm2-7 proteins, which make up the hexameric MCM complex, can be divided into an Nterminal domain, which contains the oligonucleotide-binding (OB) domain, and a C-terminal domain, which contains the conserved ATPase core and an extension defined by a winged-helix (WH) domain (Riera et al., 2017). In human Mcm6, the N-terminal domain spans from residues 1-325 and the Cterminal domain spans residues 326-821. Using a mammalian two-hybrid assay, we determined that BLM interacts with both of these Mcm6 domains (Fig. 2A, 2B). Dividing BLM into its two major domains– the disordered N-terminal tail (residues 1-647) and the C-terminal helicase domain (residues 648-1417) (Fig. S2A) – we determined that the interaction with the N- and the C-terminal Mcm6 segments occurred via the first 647 residues of BLM. We narrowed down the binding site for the N-terminal segment of Mcm6 to residues 80-120 of BLM (Fig. 2A, see also Fig. S2B). This disordered region in BLM contains the conserved sequence ^{83}QQRVKDFF^{90} (Fig. 2C), reminiscent of a PCNA-interacting protein (PIP) box (Boehm and Washington, 2016). Mutating this sequence to AxxAxxAA (hereafter referred to as

118

blm-QVFF), significantly reduced the two-hybrid interaction between Mcm6 and BLM, which still contains the second Mcm6 binding site, was (Fig. 2E). Alanine substitution of other hydrophobic residues in the 80-120 region of BLM, such as L107/L108 or F111, did not have a significant effect on Mcm6 binding (Fig. S2D).

Prompted by the resemblance of the Mcm6-binding site to a PIP-box, we tested by coimmunoprecipitation if the 83QQRVKDFF90 sequence also mediates an interaction between BLM and PCNA. We did identify an interaction of PCNA with wild-type BLM, the blm-QVFF mutant, and an Nterminal truncation of BLM that is missing the first 160 amino acids, but not with a peptide of residues 1-120 of BLM (Fig. S2E). Thus, PCNA is indeed in a complex with BLM, but the PIP-box-like Mcm6- binding site is not involved in PCNA binding.

A second site in BLM binds to the Cdt1-binding domain of Mcm6

In addition to the interaction with the N-terminal domain of Mcm6, we identified a second interaction between the BLM N-terminal tail (residues 1-647) and the C-terminal domain of Mcm6 (residues 325-821). Further dividing the Mcm6-C-terminal domain revealed a two-hybrid interaction between BLM and residues 708-821 of Mcm6 (Fig. 2B, see also Fig. S2C), which make up the winged helix (WH) domain that binds to Cdt1 and is required for MCM loading at origins (Fernández-Cid et al., 2013, Zhang et al., 2010, Wei et al., 2010). BLM does not bind to the ATP-ase domain of Mcm6 (Fig. 2B, residues 325-707) where most replisome components bind Mcm6, including Cdc45, TIM, TIPIN, Claspin, RPA2, MCM-BP, Mcm10 and Mcm4 (Hosoi A, 2015). In the two-hybrid assay, residues 708-821 of Mcm6 bound to residues 220-285 of BLM (Fig. 2B, see also Fig. S2C). The most striking feature in this disordered region of BLM is a stretch of four hydrophobic residues embedded in an acidic patch, ^{235}VICI^{238} in

119

human BLM, that is conserved in mammals, birds and Xenopus (Fig. 2D). Two additional hydrophobic residues nearby, W230 and L231, are conserved in mammals. Mutating the VICI or WLVICI residues to alanine (blm-VICI, blm-WLVICI) significantly reduced the two-hybrid interaction with Mcm6 (Fig. 2F).

Based on where BLM binds Mcm6, we termed the BLM region that binds the N-terminal domain of Mcm6 and is disrupted by the QVFF mutation the Mcm6-N-terminal binding domain (MBD-N) and the BLM region that binds the C-terminal domain of Mcm6 and is disrupted by the WLVICI mutation the Mcm6-C-terminal binding domain (MBD-C).

MBD-N or MBD-C of BLM acts as G1- and S-phase-specific Mcm6 binding sites

Using co-immunoprecipitations from synchronized cells, we determined that wildtype BLM and Mcm6 interact in unperturbed G1 and S-phase and after induction of replication-dependent DSBs by camptothecin (CPT) (Fig. 3A). Since BLM binds to the Cdt1-binding domain of Mcm6, we also assessed the interaction between Mcm6 and Cdt1. As expected, Mcm6 and Cdt1 interacted in G1, but not in S-phase when Cdt1 levels decrease rapidly. Notably, we also observed a rapid increase in Cdt1 levels in S-phase cells exposed to CPT (Fig. 3B) and the re-establishment of the Mcm6/Cdt1 complex (Fig. 3A). Cdt1 levels decreased immediately upon removal of CPT (Fig. 3B). Cdt1 levels in both, wildtype cells and BLM-deficient cells, responded similarly to CPT (Fig. S3A).

The blm-QVFF mutant failed to bind Mcm6 in G1, but co-immunoprecipitated normally with Mcm6 in S-phase, including after CPT treatment (Fig. 3C). In support of this G1-specific defect of the QVFF mutation, we observed the same Mcm6-binding pattern for an N-terminal truncation of BLM that removes the QVFF residues (blm-Δ160) and for the milder blm-QVF

120

mutation, which retains minimal Mcm6 binding in G1 (Fig. S4A and S4B). Remarkably, the blm-WLVICI (MBD-C) mutant had the opposite phenotype of the blm-QVFF (MBD-N) mutant. It bound Mcm6 normally in G1, but poorly in S-phase, and not at all after exposure to CPT (Fig. 3D). The milder VICI mutation retained slightly more interaction with Mcm6 in S-phase and after CPT treatment (Fig. S4C). Thus, BLM uses to two distinct sites - residues 83-90 (MBD-N) and residues 231-238 (MBD-C) - to bind to Mcm6 in G1 and in Sphase, respectively.

We also noticed a conserved acidic patch with several hydrophobic residues

(^{291}FDDDDYDTDF^{300}) just downstream of MBD-C (Fig. 3E). Nearby serine 304 was previously shown to be phosphorylated in S-phase where it is involved in binding TopBP1 (Blackford et al, 2015; Sun et al, 2017). We found that mutating F291/Y296/F300 to alanine (blm-FYF) had no effect on TopBP1 binding to BLM in unperturbed S-phase, but reduced TopBP1 binding after CPT exposure (Fig. S4D). Similar to TopBP1, blm-FYF immunoprecipitated with Mcm6 in unperturbed S-phase, but lost most of its association after exposure to CPT (Fig. 3F). In contrast to the BLM/Mcm6 interaction, however, the first 240 residues of BLM, which contain both Mcm6 binding sites, were not sufficient for the BLM/TopBP1 interaction (Fig. S4E), thus separating the TopBP1 and Mcm6 binding sites in BLM. The FYF mutation significantly reduced the two-hybrid between BLM and Mcm6, and mutating both QVFF and FYF led to a further reduction (Fig. 3G). Remarkably, the blm-QVFF-FYF double mutant completely failed to immunoprecipitate Mcm6 in both G1 and S-phase (Fig. 3H). These observations suggest that in unperturbed S-phase residues 83-90 (QVFF) and 291-300 (FYF) of BLM contribute to Mcm6 binding, but that binding through one of these sites is sufficient for BLM association with Mcm6 as long as the major BLM/Mcm6 binding site in S-phase, WLVICI (MBD-C), is intact.

121

Importance of the BLM/Mcm6 interaction in replication stress response

G-quadruplexes (G4s) are secondary DNA structures which cannot be unwound by the replicative helicase and impede replication fork progression (Bochman et al., 2012, Lopes et al., 2011). There are currently three mammalian DNA helicases implicated in G4 unwinding *in vivo*: BLM, WRN, and FANCJ (London et al., 2008, Mohaghegh et al., 2001b, Budhathoki et al., 2014). The Werner syndrome helicase WRN is primarily associated with the replication of telomeric DNA, leading to telomere dysfunction and premature aging seen in Werner syndrome patients (Crabbe et al., 2004). BLM and FANCJ have been implicated in the replication stress response at forks stalled at internal genomic sites, including those that form G4s (Cantor and Nayak, 2016, London et al., 2008). Here, we found that BLM-deficient cells are hypersensitive to the G4-stabilizing agent pyridostatin (PDS) and that the association of BLM with Mcm6 is essential to resist PDS (Fig. 3I). Compared to KSVS1452 cells transiently expressing wildtype BLM, cells transiently expressing BLM mutants that fail to interact with Mcm6 in either G1 (blm-QVFF) or S-phase (blm-WLVICI) exhibited significantly decreased survival at all concentrations of PDS tested. Combining the blm-QVFF and blm-FYF mutations, which completely disrupts BLM/Mcm6 association in both G1 and in S-phase, caused PDS hypersensitivity greater than either single mutants and was comparable to cells not expressing BLM (Fig. 3I), indicating a further role for the QVFF and FYF sites in stabilizing BLM/Mcm6 interaction in response to replication stress.

BLM mutants that interrupted the interaction with Mcm6 in both G1 (blm-QVFF) and S-phase (blm-WLVICI, blm- FYF, blm-QVFF-FYF) caused hypersensitivity to hydroxyurea (HU), which causes replication stress (Fig. 3J). However, the blm-QVFF mutants exhibited a wildtype phenotype at all but one of the HU concentrations tested.

www.manaraa.com

These findings suggest that the BLM/Mcm6 interaction is functionally significant in the response to replication stress.

Requirement of BLM for timely resumption of replication after DSB induction

To evaluate the importance of the Mcm6/BLM complex for the response to replicationdependent DSBs we monitored formation of foci containing BLM, Mcm6 and Cdt1 and their colocalization with EdU in unperturbed S-phase as well as during and after treatment with CPT (Fig. 6 B and 6C, see also Fig. S3B). In unperturbed S-phase, the vast majority of Mcm6 foci colocalized with EdU in $BLM^{+/+}$ (94.7%) and BLM^{KO} cells (95.8%) and there was no significant difference in the number of replicating Mcm6 foci between $BLM^{+/+}$ and BLM^{KO} cells (p=0.41, Fig. 6). $BLM^{+/+}$ and BLM^{KO} cells responded similarly to CPT exposure, with a significant increase in the number of nonreplicating Mcm6 foci, as indicated by Mcm6 foci that do not colocalize with EdU, accompanied by a significant decrease in the number of active replisomes (Fig. 6A). However, 45 minutes after CPT exposure we observed significantly fewer replicating Mcm6 foci in BLM^{KO} cells (26% of all Mcm6 foci) than in wildtype cells (62% of all Mcm6 foci) (p<0.0001, Fig. 6C), suggesting that BLM is important for timely resumption of DNA replication after DSB induction.

G1-specific BLM/Mcm6 association via MBD-N suppresses Mcm6/Cdt1 complex formation

We showed above that BLM forms discrete foci in G1 and that all of these BLM foci colocalize with Mcm6. The QVFF mutation, both in the QVFF single mutant and in the QVFF-FYF double mutant, decreased BLM/Mcm6 colocalization and led to the appearance of BLM foci that did not colocalize with Mcm6 (Fig. 4A, see also Fig. S6B). Surprisingly, as the number

123

of Mcm6/BLM foci decreased, the number of Mcm6/Cdt1 foci increased in the QVFF mutants (Fig. 4A). We determined that of all Mcm6 foci in the QVFF and QVFF-FYF mutants, 72-75% colocalized with Cdt1 foci, which was similar to cells lacking BLM (82%) (Fig. 4B). In contrast, in wildtype cells and in the WLVICI and FYF mutant, where the BLM/Mcm6 association in G1 is intact, only 42-48% of Mcm6 foci colocalized with Cdt1 (Fig. 4B).

These observations suggest an inhibitory effect of BLM and the BLM/Mcm6 interaction on the association of Cdt1 with Mcm6 in G1. In support of this hypothesis, less Cdt1 co-immunoprecipitated with Mcm6 in cells expressing wildtype BLM than in cells expressing the blm-QVFF mutant or no BLM (Fig. 4C).

To further test if BLM and Cdt1 can compete for Mcm6 binding we used coimmunoprecipitations of the recombinant proteins (Fig. 4D, see also Fig. S5). Indeed, addition of increasing amounts of BLM (0.5 – 1.5 pmol) to a mixture of equimolar amounts of Mcm6 and Cdt1 (0.5 pmol) weakened the Mcm6/Cdt1 interaction in a dose-dependent manner, suggesting that BLM can weaken the Mcm6/Cdt1 complex (Fig. 4D). We found that the reverse was also true; adding increasing amounts of Cdt1 (0.5 – 1.5 pmol) disrupted the interaction between Mcm6 and BLM, indicating that Cdt1 interferes in BLM/Mcm6 complex formation (Fig. 4D).

S-phase specific BLM/Mcm6 interaction via MBD-C and FYF residues is required for the DNA damage response

Consistent with co-immunoprecipitations, disrupting MBD-C by the WLVICI mutation led to the accumulation of BLM and Mcm6 foci that do not colocalize in unperturbed S-phase cells (Fig. 4E). Remarkably, even though Mcm6 and Cdt1 do not interact in S-phase, we observed occasional Mcm6/Cdt1 foci in the blm-QVFF mutant, supporting the possibility that

the BLM/Mcm6 interaction via MBD-N inhibits the Mcm6/Cdt1 interaction. In contrast to the blm-WLVICI and blm-QVFF mutants, the blm-FYF mutant still exhibited a wildtype phenotype in unperturbed S-phase.

After exposure to CPT (Fig. 4F), we observed that wildtype cells responded with the formation of BLM/Mcm6/Cdt1 foci, which became the predominant foci type. Interestingly, the roles of the MBD-N and MBD-C binding sites in the DNA-damage response were reversed: the blm-QVFF mutant, which had significant defects in G1, showed a wildtype distribution of foci types and numbers with only a mild decrease in BLM/Mcm6/Cdt1 foci. In contrast, the blm-FYF mutations inhibited the formation of BLM/Mcm6/Cdt1 foci and the blm-WLVICI mutation completely abrogated it (Fig. 4F).

After exposing wildtype cells to CPT, we also noticed that ~25% of BLM foci no longer colocalized with Mcm6 (Fig. 4F); instead they associated with 53BP1, suggesting that some BLM relocalizes to DNA damage foci (Fig. S6A). This fraction of BLM foci that did not colocalize with Mcm6 increased after CPT exposure especially in the blm-FYF and blm-WLVICI mutants, making up 56% and 92% of all BLM foci, respectively (Fig. 4F, see also Fig. S6C and S6D).

Since co-immunoprecipitations suggested that the BLM/Mcm6 interaction affects the Mcm6- Cdt1 interaction, we also monitored foci formation in the blm-QVFF-FYF mutant, finding that it completely failed to form foci with Mcm6 in G1, unperturbed S-phase, and after CPT exposure, exhibiting a similar foci pattern as cells not expressing BLM (Fig. 4A, 4E and 4F). This observation is consistent with the failure of blm-QVFF-FYF to co-immunoprecipitate with Mcm6 in unperturbed S-phase and suggests cooperation between MBD-N and the FYF

residues in Mcm6 binding in unperturbed S-phase, with one site being sufficient for binding BLM to Mcm6 as longs MBD-C is intact. That the WLVICI residues in MBD-C are essential for association of BLM with Mcm6 in S-phase (Fig. 4C and Fig. 5B) further suggests that sites that are essential for the association of BLM with Mcm6 in G1 (QVFF) and after CPT (FYF), can contribute to BLM/Mcm6 binding in S-phase, but are secondary to the association of BLM with Mcm6 via the WLVICI residues.

DISCUSSION

In this study, we have identified a direct physical interaction of BLM with the MCM helicase subunit Mcm6 at active replisomes in S -phase and at inactive pre-initiation complexes in G1. We demonstrate that this BLM/Mcm6 interaction in the two cell-cycle phases is mediated by two distinct binding sites in the disordered N-terminal tail of BLM, one of which binds to the N-terminus of Mcm6 in G1-phase and one that binds to the Cdt1-binding domain of Mcm6 in S-phase. We also show that BLM can compete with Cdt1 for Mcm6 binding *in vitro* and that BLM and the BLM/Mcm6 interaction in G1 phase weaken Cdt1/Mcm6 complex formation *in vivo*.

Our finding that BLM uses distinct Mcm6 binding sites in G1 and in S-phase indicates that the BLM interactions with Mcm6 in G1 and in S-phase are functionally significant. BLM is not simply being loaded into the replisome in G1 as the blm-QVFF mutant, whose interaction with Mcm6 in G1 phase is severely impaired (50%), can still associate with BLM at near wildtype levels (90%) in S-phase, suggesting that BLM can associate with Mcm6 in S-phase independently of its prior association with Mcm6 in G1. This raises the question of what role the BLM/Mcm6 association plays during active replication in S-phase that extends to inactive replisomes in G1. Based on BLM's established functions in DNA repair by homologous

126

recombination, it could be suggested that BLM associates with active replisomes in S-phase to be instantly available for the repair of collapsed or stalled forks. Indeed, we observed that the strength of the BLM/Mcm6 association after CPT treatment depended on the ability of BLM to associate with Mcm6 in unperturbed S-phase (Fig. 5B and 5C, see also Fig. S6C and S6D). However, such a role of the BLM/Mcm6 interaction is unlikely to extend to G1 phase when replication is inactive.

One threat that active replisomes in S-phase and the formation of pre-initiation complexes in G1 have in common are G4 structures. Sequences capable of forming G4s are dispersed throughout the human genome and, importantly, have been identified at over 90% of origins of replication in the human genome (Rhodes and Lipps, 2015). In fact, the most efficient origins are CpG islands, which make up a third of all origins in the human genome (Cadoret et al., 2008, Sequeira-Mendes et al., 2009). Sequences with the potential to form G4 structures appear to play a ubiquitous and positive role in replication initiation (Prioleau and MacAlpine, 2016, Rhodes and Lipps, 2015, Valton and Prioleau, 2016). However, the current model of pre-RC formation in G1 and pre-IC formation at the G1/S transition does not include a DNA helicase capable of G4 unwinding. The evolutionarily conserved RecQ family of DNA helicases has several members with excellent G4-unwinding activity, most prominently BLM and WRN (Budhathoki et al., 2014, Mohaghegh et al., 2001a), but their functions have not been implicated in G1. Another RecQ-like helicase, RecQL4, is required for the initiation of DNA replication in human cells (Sangrithi et al., 2005) and appears to have an N-terminal domain that allows it to bind G4 structures (Keller et al., 2014). However, RecQL4 lacks the conserved RQC domain that enables BLM and WRN to unwind G4s, and RecQL4 is unable to unwind G4s *in vitro* (Singh et al., 2012).

The increased PDS sensitivity of BLM-deficient KSVS1452 cells expressing the blm-QVFF mutant, which interrupts BLM/Mcm6 interaction specifically in G1, indicates a possible role for the BLM/Mcm6 association in G1 that could be explored in the future. Based on BLM's exquisite ability to bind and unfold G4 structures, one role we could envisage is the unfolding of G4 structures that were recently proposed to form at origins of replication (Prioleau and MacAlpine, 2016, Rhodes and Lipps, 2015) or DNA-structure unwinding during the G1/S transition. However, PDS has also been shown to inhibit BLM's ability to unwind duplex DNA, suggesting that the cause for PDS hypersensitivity of the blm-QVFF mutant may not be limited to G4-unfolding (Li et al., 2001). Thus, further investigations are required to verify a potential role of BLM and the BLM/Mcm6 interaction in G1. For example, with a DNA combing assay using $BLM^{+/+}$ and $BLM^{-/-}$ cells, we will test if disruption of the BLM/Mcm6 association leads to less efficient origin firing (Marheineke and Hyrien, 2004, Patel et al., 2006). We will also quantify G4 structures in real-time during progression from G1 to S-phase in $BLM^{+/+}$ and $BLM^{-/-}$ cells as well as blm mutants using the new G4-specific fluorescent probe IMT (Zhang et al., 2018). Furthermore, we will perform immunofluorescence analyses to reveal the timing of the BLM/Mcm6 association in G1, specifically during pre-RC/pre-IC formation and the G1/S transition. As an alternative to an enzymatic role of BLM in G1, the association of BLM with Mcm6 in G1 could simply serve to load BLM into the replisome for a later function at the replisome in S-phase. There, BLM could assist the CMG helicase to unwind unusual DNA structures, such as G4s, during unperturbed growth, or be present to respond to replication stress.

Taken together, we propose the following model for BLM function and the BLM/Mcm6 interaction in G1 and unperturbed S-phase (Fig. 5): In G1, prior to the initiation of replication, BLM is recruited to origins by binding to Mcm6. At this stage, MBD-N of BLM binds the N-

terminal domain of Mcm6, but does not engage with the C-terminal Cdt1-binding domain of Mcm6. This arrangement may be necessary because Cdt1 is still bound to Mcm6 for the recruitment of MCM hexamers to the origin recognition complex ORC (Chen and Bell, 2011, Chen et al., 2007), thus making this site unavailable to the MBD-C site within BLM. Most replication factors that interact with Mcm6 and are thought to regulate the MCM helicase do so via the central ATPase domain, including Cdc45, RPA2, TIM, TIPIN, MCM10 and MCM-BP (Hosoi et al., 2015). That BLM binds to the two domains upstream and downstream of the Mcm6 ATPase domain suggests that the BLM/MCM interaction is unlikely to interfere in other MCM-protein interactions that are critical for the formation of the pre-initiation complex. Although dispensable for BLM/Mcm6 interaction in S-phase, we suggest that BLM association with MCM via MBD-N in G1 plays a functionally significant role which will be unraveled by further investigations.

In S-phase, Cdt1 is no longer bound to Mcm6 (Fig. 4E) and is degraded to prevent relicensing of origins (Arias and Walter, 2006, Jin et al., 2006, Nishitani et al., 2006) (see also Fig. S3A). Thus, in S-phase BLM can engage with the Cdt1-binding domain of Mcm6 using MBD-C, defined by the WLVICI residues. The interaction between the MBD-C of BLM and the C-terminal Cdt1-binding domain of Mcm6 is the most critical for the S-phase-specific interaction between BLM and Mcm6 at active replisomes (Fig. 3D, Fig. 4E). In addition to MBD-C, the interaction between the MBD-N of BLM and the N-terminus of Mcm6 also appears to remain intact in S-phase and, together with the FYF residues (BLM residues 291-300), continues to significantly contribute to the stability of the BLM/Mcm6 complex in unperturbed as indicated by the complete loss of Mcm6 binding by the double mutant blm-QVFF-FYF. The QVFFFYF mutation, which disrupts BLM/Mcm6 interaction in both G1 and S-phase, renders cells as

129

sensitive to PDS and nearly as sensitive to HU as cells not expressing any BLM, highlighting the significance of the BLM/Mcm6 interaction for normal cell function.

When S-phase cells are exposed to DNA damage, the S-phase specific interaction between MBC-C and the Cdt1-binding domain of Mcm6 remains essential for BLM/Mcm6 association. Interestingly, the FYF residues (BLM residues 291-300), which play no significant role in G1 and in unperturbed S-phase, become essential for the DNA-damage-specific BLM/Mcm6 interaction. These FYF residues are also critical for binding TopBP1 after DNA damage (Fig. S4D). TopBP1 had previously been shown to bind BLM in unperturbed S-phase in a manner that is dependent on phosphorylation of the nearby serine 304 (Blackford et al., 2015, Wang et al., 2013). The FYF residues, in contrast, are required for a TopBP1/BLM interaction after DNA-damage induction, and play no role in the TopBP1/BLM interaction in unperturbed S-phase (Fig. S4D).

Additionally, the VICI residues within MBD-C resemble an inverted SUMO-binding motif 2 (SBM2, [V/I] [V/I]X[V/I]), one of the three known SUMO-binding motifs (Minty et al., 2000, Song et al., 2004, Hannich et al., 2005, Hecker et al., 2006). Non-covalent binding of SUMO by residues V235/I236 in the VICI motif and nearby residues I218/L220 has been shown to be important for sumoylation of BLM at lysines 317,331, 344 and 347 (Eladad et al., 2005, Zhu et al., 2008). The possibility that MBD-C contains a SUMO-binding motif also raises the possibility that the MBD-C mediated BLM/Mcm6 interaction might be regulated by the SUMOylation status of Mcm6. In yeast, there is evidence of Mcm6 being SUMOylated in G1 and playing a regulatory role by counteracting MCM phosphorylation to impair replication initiation (Wei and Zhao, 2016). However, it is currently unknown if human Mcm6 is SUMOylated, and if so, whether SUMOylation plays a similar role in the G1/S transition. Our

130

observation that MBD-C mediates BLM/Mcm6 interaction in S-phase, *prima facie* suggests that this association is independent of SUMOylation status. Moreover, we show that as BLM localizes to PML in late S-phase its the overlap with Mcm6 foci decreases (Fig. 1G, Fig S1H), suggesting that BLM/Mcm6 and BLM/PML interactions occur at different time points within S-phase.

It is interesting to note that Cdt1 is degraded rapidly upon exposure of cells to ultraviolet light and ionizing radiation (Higa et al., 2003, Tanaka et al., 2017). In contrast, we observed that exposure of early-to-mid-S-phase cells to CPT induced a rapid increase in Cdt1 levels and colocalization of Cdt1 with Mcm6/BLM foci. These Cdt1/Mcm6/BLM foci accumulated just as Mcm6/BLM foci disappeared (Fig. 3B), suggesting that Cdt1 is recruited to replisomes rather than to new origins. What could the role of Cdt1 association with replisomes after DNA damage be? The low concentration of CPT (1 μM) used in this study induces single-strand nicks that lead to DSBs upon encounter with a replication fork (Helleday, 2003, Holm et al., 1989). Such damage-induced, one-ended DSBs in S-phase are processed and become substrates for homologous recombination. In budding yeast, they can be repaired by break-induced replication (BIR) that is initiated by Rad51-dependent strand invasion of a homologous duplex, such as the undamaged sister chromatid (Llorente et al., 2008). Single-strand invasion leads to formation of a displacement (D)-loop where the invading 3'end can initiate new DNA synthesis. Since a second DSB end is not available, this replicating D-loop can migrate until it encounters another replication fork or the end of the chromosome. Although this type of DNA replication appears to be different from that initiated at origins, it requires all of the essential replication factors (Lydeard et al., 2010). Interestingly, the list also includes Cdt1, but not other factors specific for pre-RC formation, such as ORC or Cdc6. This suggests that Cdt1 performs important replication

131

functions outside of pre-RC assembly in G1, possibly the establishment of recombination-dependent replication forks in S-phase (Lydeard et al., 2010).

How Cdt1 could perform this function at collapsed replication forks remains to be discovered, but there may be some clues. For example, Cdt1 has been shown to stabilize MCM in a conformation where the ring is open at the Mcm2/5 interface and this conformation inhibits MCM's ATPase activity, which is essential for CMG function (Frigola et al., 2017). Thus, one could envisage a scenario where, by favoring the open ring conformation, recruitment of Cdt1 to stalled replisomes (Cdt1/MCM/BLM foci) may contribute to the intra-S-phase DNA-damage response by halting replisomes and by allowing transfer of opened MCM rings to establish new forks at D-loops. Moreover, Cdt1 could regulate chromatin compaction surrounding stalled replisomes through its association with histone de/acetyltransferases (Miotto and Struhl, 2008, Wong et al., 2010). A later role in the re-establishment of active replisomes at DNA-damage sites is also plausible as Cdt1 has been shown to help recruit Cdc45 for formation of the active CMG helicase (Ballabeni et al., 2009).

Finally, we found that Mcm6 association with BLM in G1 phase diminished Mcm6 association with Cdt1 (Fig. 4B). In fact, twice as many Mcm6 foci colocalized with Cdt1 in the absence of BLM as in the presence of BLM, and disrupting the BLM/Mcm6 binding by introducing the QVFF mutation was nearly as effective in promoting the Mcm6/Cdt1 association as eliminating BLM. This ability of BLM to compete with Cdt1 for Mcm6 binding *in vivo* is also supported by reciprocal co-immunopreciptations of BLM, Mcm6 and Cdt1 from G1 cells and of equimolar amounts of the recombinant proteins *in vitro*. While the functional significance and the strength of the competition between BLM and Cdt1 is currently unclear, increasing BLM levels could play a role in displacing rapidly diminishing amounts of Cdt1 from Mcm6 or

132

preventing Cdt1 re-association with Mcm6 after MCM loading until Cdt1 is eliminated in S-phase.

METHODS

Experimental Model and Subject Details

GM00637 (BLM$^{+/+}$) and GM00637-derived KSVS1452 (BLM$^{-/-}$) fibroblast cells were maintained in Modified Eagle's Medium (MEM) supplemented with 10% fetal bovine serum (FBS), 1% penicillin-streptomycin-glutamine (PSG) and 2 mM L-glutamine.

CRISPR/Cas9-mediated BLM knockout

A diploid BLM knockout cell line was derived from the GM00637 cell line using a CRISPR/Cas9 mediated genome engineering protocol (Ran et al., 2013). Briefly, guide RNA (gRNA) sequences targeting exon 8 within BLM were designed using the CRISPR guide design tool, which identifies and ranks suitable target sites and predicts off-target sites for each intended target (http://tools.genome-engineering.org). gRNA sequences with the highest score and least off-target impacts were cloned into the pSpCas9(BB)-2A-Puro vector and transfected into GM00637 using Lipofectamine 2000 (Invitrogen). Selection and clonal isolation was performed in the presence of 0.125 µg/mL puromycin. BLM knockout clones were verified by sequencing and immunoblotting. Frameshift mutations within clone KSVS1452 resulted in the following protein consequence:

GM00637:

BLM exon 8:

GACAAGTCAGCACAAAATTTAGCATCCAGAAATCTGAAACATGAGCGTTTCCAAAG

TCTTAGTTTTCCTCATACAAAGGAAATGATGAAGATTTTTCATAAAAAATTTGGCCT

GCATAATTTTAGAACTAATCAGCTAGAGGCGATCAATGCTGACTGCTTGGTGAAGAC

TGTTTTATCCTGATGCCGACT

BLM:

DKSAQNLASRNLKHERFQSLSFPHTKEMMKIFHKKFGLHNFRTNQLEAINAALLGEDCF

ILMPT

KSVS1452:

BLM exon 8 (c.del2040_2046; g.del90,763,123_90,763,130):

GACAAGTCAGCACAAAATTTAGCATCCAGAAATCTGAAACATGAGCGTTTCCAAAG

TCTTAGTTTTCCTCATACAAAGGAAATGATGAAGATTTTTCATAAAAAATTTGGCCT

GCATAATTTTAGAACTAATCAGCTAGAGGCGATCAATGCTGACTGAAGACTGTTTTA

TCCTGATGCCGACT

BLM (p.Leu681LysTer686):

DKSAQNLASRNLKHERFQSLSFPHTKEMMKIFHKKFGLHNFRTNQLEAINAALKTVLS.

BLM exon 8 (c.delins2036_2041AG; g.delins90,763,119_90,763,124AG):

GACAAGTCAGCACAAAATTTAGCATCCAGAAATCTGAAACATGAGCGTTTCCAAAG

TCTTAGTTTTCCTCATACAAAGGAAATGATGAAGATTTTTCATAAAAAATTTGGCCT

GCATAATTTTAGAACTAATCAGCTAGAGGCGATCAATGCTGAGTTGGTGAAGACTGT

TTTATCCTGATGCCGACT

BLM (p.Leu678AlaTer686):

DKSAQNLASRNLKHERFQSLSFPHTKEMMKIFHKKFGLHNFRTNQLEAINAELVKTVLS.

134

Cell cycle synchronization and replication stress induction

For synchronization in G1 phase, cells were blocked in G2/M by serum starvation followed by nocodazole treatment (Xu et al., 2009). After being cultured in serum-free media for 22 hr, cells were released into media containing 10% FBS for 2 hr. Subsequently, they were treated with 50 ng/mL nocodazole for 16 hr before synchronized progression into G1 phase.

For synchronization in S-phase, cells were arrested at G1/S using a double-thymidine block (Jackman and O'Connor, 2001). Exponentially growing cells were cultured with 2 mM thymidine (Acros Organics) for 12 hr, released into fresh media for 16 hr and back into media supplemented with 2 mM thymidine for 14 hr. Three hours into S-phase, cells were treated with 1 µM camptothecin (CPT) for 1 hr and released into CPT-free media. Cells from time points before, during and post CPT-treatment were used for immunoprecipitations and co-localization analysis.

Immunoprecipitations

Nuclear lysates were prepared from exponentially growing cells for immunoprecipitations. Briefly, cells were lysed (20 mM Tris pH 7.4, 10 mM KCl, 1 µM EDTA, 0.2% NP40, 50% glycerol, 0.6 mM βME, 1 mM PMSF and protease inhibitor cocktail [Pierce]) for 2 min on ice to isolate nuclei. The nuclei were lysed with nuclear lysis buffer (20 mM Tris pH 7.4, 10 mM KCl, 0.4 M NaCl, 1 µM EDTA, 50% glycerol, 0.6 mM βME, 1 mM PMSF, and protease inhibitor cocktail) supplemented with 25 U/mL benzonase (Novagen) (Rios-Doria et al., 2009). Protein concentrations were determined using the Bradford assay and 1 mg nuclear lysates were precleared with 30 µl Protein G Agarose (Pierce) at 4°C for 1 hr. The precleared lysates were incubated overnight at 4°C with end-over-end mixing with either anti-BLM A300-

110A (4 μg; Bethyl), anti-MCM6 H8 (4 μg; Santa Cruz), anti-Cdt1 EPR17891 (2 μg; Abcam) or non-specific IgG crosslinked to Protein G Agarose (Pierce). The complexes were washed extensively with nuclear lysis buffer before elution. For LC-MS/MS, complexes were eluted in 50 μl 0.2 M glycine, pH 2.6 and immediately neutralized with 50 μl Tris, pH 8.0. For SDS-PAGE, complexes were eluted in 50 μl 2X Laemmli sample buffer by boiling at 95°C for 10 min.

Mass spectrometric analysis

Immunoprecipitation eluates were prepared for mass spectrometric analysis using the FASP Protein Digestion Kit (Expedeon) (Manza et al., 2005). Proteins were digested overnight by the addition of sequencing grade modified trypsin (Promega) in a 1:50 ratio to protein. Samples were desalted using C18 columns, concentrated in a vacuum concentrator and resuspended in 0.1% formic acid in H2O. Mass spectrometric analysis was performed on a Q Exactive Plus (Thermo). LC-MS/MS data was analyzed by using MaxQuant processing suite (Cox and Mann, 2008). The identified spectra were compared against the UniProt reference proteome data set for Homo sapiens (Proteome ID: UP000005640). The identified data set was sorted to only include entries with no identified peptides in eluates from non-specific IgG immunoprecipitations.

Immunofluorescent assays

Cells were cultured on glass coverslips (Corning) in a 6 well plate for at least 24 hr before cell cycle synchronization. For analyses in the presence of plasmid borne protein expression, cell cycle synchronization was initiated 24 hr post-transfection with Lipofectamine 2000. Cells at indicated time points within G1 and S-phase were washed with PBS and fixed

using 4% paraformaldehyde (PFA; Life Technologies) for 15 min at room temperature (RT). The cells were permeabilized by incubating with 0.25% Triton-X-100 in PBS for 15 min at RT. After blocking in 1% BSA in PBS-T (PBS+0.1% Tween-20) for 30 min, the cells were incubated overnight at 4°C with the following primary antibody dilutions prepared in the blocking buffer: anti-BLM (C-18) (1:50; Santa Cruz), anti-MCM6 (H-8) (1:50; Santa Cruz), anti-Cdt1 EPR17891 (1:100; Abcam), anti-BLM (1:200; Abcam), anti-MCM6 (1:500; Sigma-Aldrich), anti-53BP1 (E-10) (1:50; Santa Cruz) or anti-PML (PG-M3) (1:50; Santa Cruz). Cells were washed with PBS-T and incubated for 1 hr at RT with the following secondary antibody dilutions prepared in the blocking buffer: goat anti-Rabbit IgG (H+L) Cross-Adsorbed Secondary Antibody, Alexa Fluor 405 (2 ug/mL; ThermoFisher Scientific), goat anti-Mouse IgG (H+L) Cross-Adsorbed Secondary Antibody, Alexa Fluor Plus 488 (2 ug/mL; ThermoFisher Scientific), donkey anti-Rabbit IgG (H+L) Cross-Adsorbed Secondary Antibody, Alexa Fluor 555 (4 ug/mL; ThermoFisher Scientific) or donkey anti-Goat IgG (H+L) Secondary Antibody, Alexa Fluor 647 (6 ug/mL; Abcam). Cells were washed with PBS-T and the coverslips were mounted using VectaShield (Vector Labs) onto glass slides (Fisher). For EdU co-staining analyses, cells were first labeled with EdU for 15 mins using the Click-iT Plus EdU Alexa Fluor 594 Imaging Kit (ThermoFisher Scientific) as per the protocol provided. This was followed by primary and secondary antibody incubations as described previously. Images were acquired using an imaging system consisting of a PerkinElmer UltraVIEW imager and a Zeiss AxioVert 200 inverted microscope equipped with a 63x/1.4 Oil DIC Plan-Apochromat 0.19/0.17 objective. Foci from 30 merged images were counted for co-localization. Significance was assigned using a two-tailed Mann Whitney test and p-values < 0.05 were considered significant.

Mammalian hybrid assay

Using the Matchmaker Mammalian Assay Kit 2 (Clontech), BLM and MCM6 were cloned into the pVP16-AD and pM-DBD vectors respectively. Subsequently, pVP16-BLM and pM-MCM6 were used to generate fragments as well as mutants using primers described in Table S1. Interactions were assayed by co-transfecting them with the pG5SEAP reporter vector using Lipofectamine 2000. 72 hr post-transfection, activity of secreted human placental alkaline phosphatase (SEAP) expressed by the reporter vector was determined using the Great EscAPe SEAP Fluorescence Detection Kit (Clontech). According to the protocol provided, media from wells with the co-transfected cells was incubated with a fluorescent SEAP substrate in 96-well flat bottom non-binding microplates (Greiner). Fluorescence was detected at 440 nm after excitation at 340 nm in a Gen5 Microplate Reader (BioTek). All co-transfections were set up in triplicate and SEAP activity was expressed in terms of relative fluorescence units (RFU).

Competitive binding assay

Purified human BLM and purified human MCM6 (Abcam) were immunoprecipitated from two sets of mixtures also containing purified human Cdt1 (Origene) in IP buffer (25mM Tris, 150mM NaCl; pH 7.2) (Yanagi et al., 2002). In the first set, 0.5 pM each of BLM and MCM6 were mixed in the presence of increasing concentrations (0, 0.5, 0.75, 1, 1.25 and 1.5 pM) of Cdt1 and Protein-G agarose beads crosslinked with anti-BLM (Bethyl) or non-specific IgG. In the second set, 0.5 pM each of Cdt1 and MCM6 were mixed in the presence of increasing concentrations (0.5, 0.75, 1, 1.25 and 1.5 pM) of BLM and Protein-G agarose beads crosslinked with anti-MCM6 (Santa Cruz) or non-specific IgG. Both sets were incubated for 2 hr at 4°C with end over end mixing. The complexes were washed with IP buffer and

immunoprecipitates were dissolved in 20 µl 2X Laemmli sample buffer by boiling at 95°C for 10 min.

Nuclease-insoluble chromatin fraction isolation

Nuclease-insoluble chromatin fraction was isolated from cells before, during and after being released from 1 µM CPT-treatment in S-phase (Moiseeva et al., 2017, Aygun et al., 2008). Cells were lysed with cytoplasmic lysis buffer (10 mM Tris pH 7.9, 0.34 M sucrose, 3 mM calcium chloride, 2 mM magnesium acetate, 0.1 mM EDTA, 0.5% NP40, and protease inhibitor cocktail) for 2 min on ice to isolate nuclei. The nuclei were lysed with nuclear lysis buffer (20 mM HEPES pH 7.9, 3 mM EDTA, 10% glycerol, 150 mM potassium acetate, 1.5 mM magnesium chloride, and 0.1% NP40 and protease inhibitor cocktail) for 30 min on ice. The pelleted chromatin was incubated with nuclease incubation buffer (150 mM HEPES pH 7.9, 1.5 mM magnesium chloride, 10% glycerol, 150 mM potassium acetate, and protease inhibitor cocktail) supplemented with 0.15 U/µL benzonase (Novagen) for 10 min in a 37°C shaker. The nuclease-insoluble chromatin fraction was dissolved in 20 µl 2X Laemmli sample buffer by boiling at 95°C for 10 min.

Cell survival assay

Cells were seeded at a density of 1000 cells/well in a 6-well plate 24 hr post-transfection. They were released into media supplemented with pyridostatin (PDS; 0, 2, 4, 6, 8 and 10 µM) 24 hr after seeding and allowed to grow for 3 days. Alternately, 24 hr post-transfection, 1000 cells/well were seeded in a 6-well plate. They were released into media supplemented with hydroxyurea (HU; 0, 0.1, 0.2, 0.3, 0.4 and 0.5 mM) 24 hr after seeding. After 48 hr, the cells were released into drug-free media and allowed to grow for 7 days. Cells were washed with PBS

139

before being fixed in 3:1 (vol/vol) methanol-acetic acid and stained with 0.01% crystal violet.

Colonies containing more than 50 cells were scored as survivors.

FIGURES
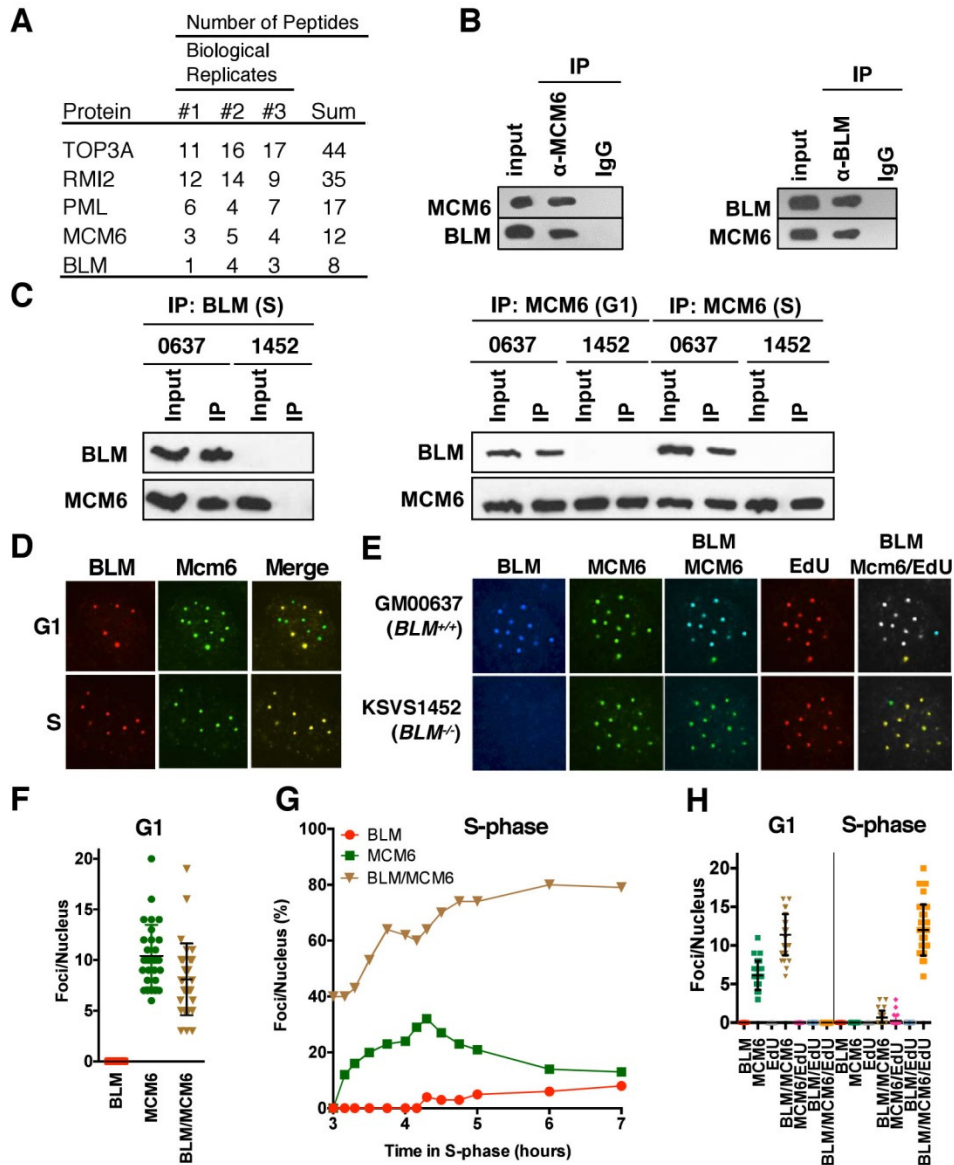
Figure 4.1. BLM is in a complex with Mcm6 in G1 and S-phase

(A) Co-immunoprecipitations of endogenous BLM were performed in triplicate on nuclear extracts from GM00637 cells in mid-S-phase and peptides identified by mass spectrometry. The same analysis in triplicate for the isogenic BLM knockout cell line (KSVS1452) yielded zero hits

for the listed proteins. Cell lines GM00637 and KSVS1452 are an isogenic pair of a $BLM^{+/+}$ and a CRISPR-mediated BLM^{KO} cell line, respectively. See Fig. S1A-G and Methods for details on construction and characterization of the KSVS1452 cell line. *(B)* Reciprocal co-immunoprecipitations of recombinant human BLM and Mcm6. *(C)* Reciprocal coimmunoprecipitations of endogenous BLM and Mcm6 from nuclear extracts of GM00637 cells were performed in G1 and S-phase. *(D)* BLM foci formation in G1 and S-phase and colocalization with Mcm6 *(E)* BLM colocalization with Mcm6 at active replisomes in S-phase as indicated by EdU incorporation. As expected, BLM foci are not detected in the KSVS1452 cell line. *(F)* Colocalization of all BLM foci with Mcm6 in G1. Blm, Mcm6 and Mcm6/BLM foci were counted in nuclei from 30 cells. Mean+/-SD is shown. *(G)* Colocalization of BLM and Mcm6 foci during the first half of S-phase. Appearance of occasional BLM foci that do not colocalize with Mcm6 in the second half of S-phase. See Figure S1I-J for colocalization of these BLM foci with PML and 53BP1. *(H)* Vast majority of BLM/Mcm6 foci in Sphase (>95%) are at active replisomes, indicated by incorporation of EdU. As expected, EdU incorporation is not observed in cells in G1. Foci in nuclei of 30 cells were counted. Data are presented as Mean+/-SD.

141
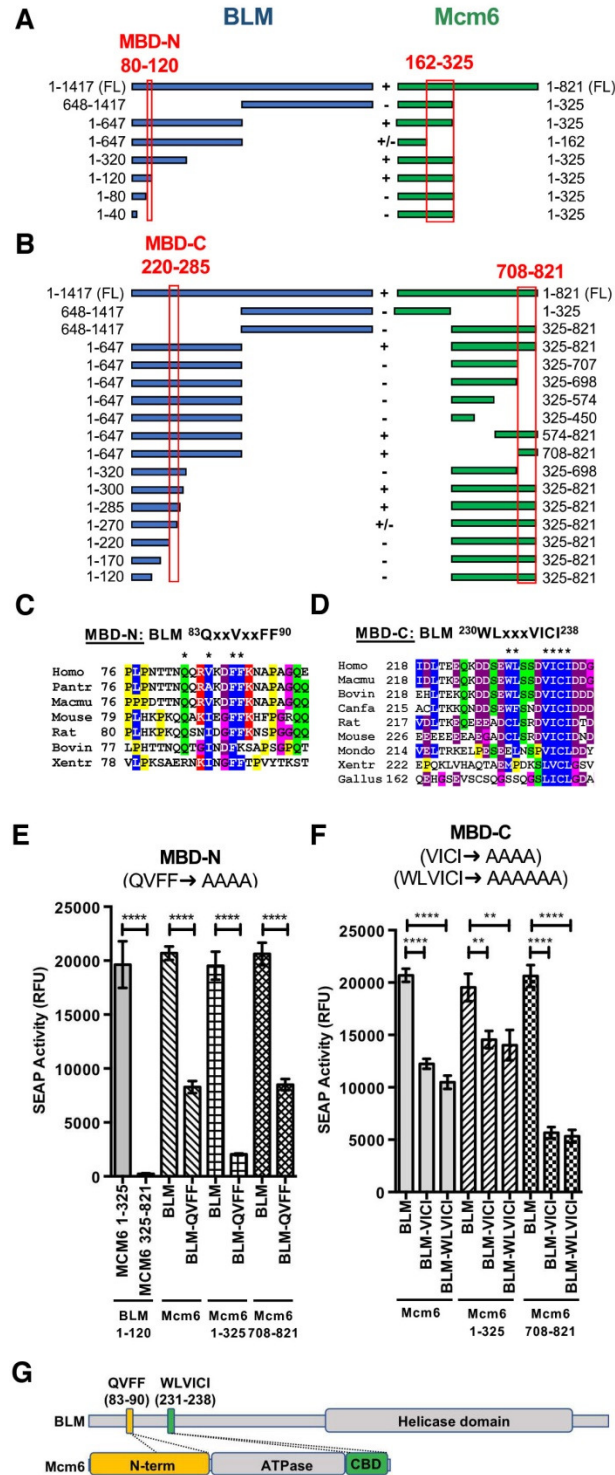
Figure 4.2. Two distinct sites in the disordered N-terminal tail of BLM interact with Mcm6
A) In a mammalian two-hybrid assay, residues 80-120 of BLM bind to the N-terminal domain of Mcm6. See also Fig. S2B. *(B)* Residues 220-285 of BLM bind to the C-terminal extension of Mcm6, which contains a winged-helix domain that also binds Cdt1 during pre-RC formation. See also Fig. S2C. *(C)* MBD-N contains a conserved PIP-box-like motif. *(D)* MBD-C contains

142

four conserved hydrophobic residues embedded in an acidic patch. Two additional hydrophobic residues nearby are conserved in mammals. *(E)* Mutation of QVFF residues in MBD-N to alanine disrupts BLM interaction with the N-terminus of Mcm6 in a two-hybrid assay. Despite the PIP-box-like motif, this segment of BLM is not involved in a novel interaction between BLM and PCNA (See Fig. S2D). *(F)* Mutation of VICI and WLVICI residues in MBD-C to alanine disrupt the BLM interaction with the C-terminus of Mcm6 in a two-hybrid assay. MBD-N, Mcm6 N-terminus binding domain; MBD-C, Mcm6 C-terminus binding domain. *(G)* Locations of the Mcm6 binding sites MBD-N and MBD-C in BLM and their interaction sites in Mcm6. Differences between means were analyzed by a *t*-test and presented as ** ($p<0.01$) and ****($p<0.0001$).
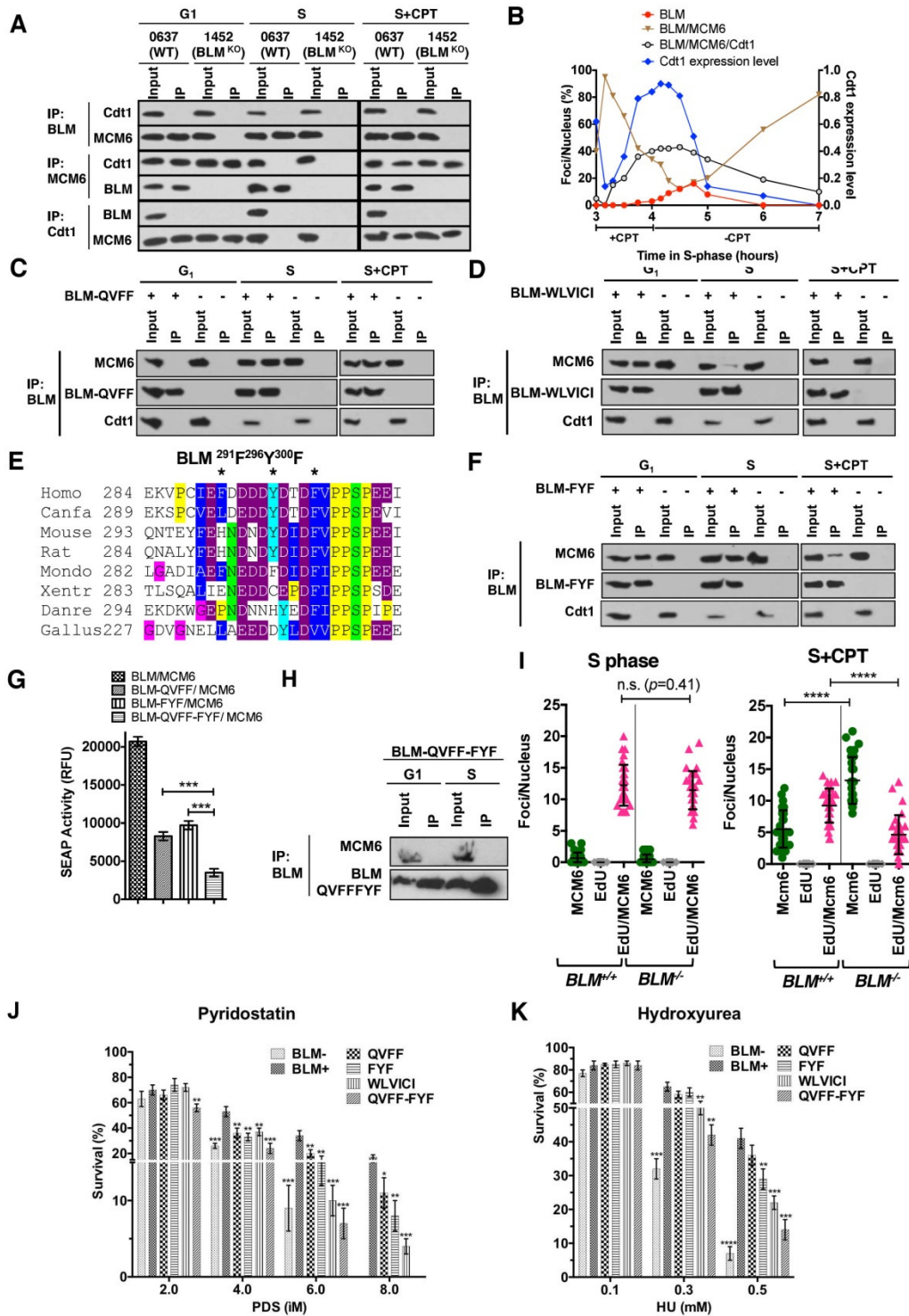
Figure 4.3. MBD-N and MBD-C regulate differential association of BLM with Mcm6 in G1 and S-phase

(A) GM00637 and KSVS1452 cells were synchronized in G1, released into S-phase for 3 hours, exposed to 1μM CPT for 1 hour and released into fresh media for 45 minutes. Reciprocal coimmunoprecipitation of BLM, Cdt1 and Mcm6 were performed in G1, S-phase and during

recovery from CPT exposure. *(B)* Exposure of $BLM^{+/+}$ cells to CPT in mid-S-phase causes a rapid increase in Cdt1 expression levels, which is accompanied by the appearance of BLM/Mcm6/Cdt1 and Mcm6/Cdt1 foci, respectively. Removal of CPT leads to rapid degradation of Cdt1 levels and a decrease of BLM/Mcm6/Cdt1 foci. See also Fig. S6A and S6B Cdt1 degradation in unperturbed S-phase and for the effect of CPT on BLM^{KO} cells. *(C)* KSVS1452 cells expressing the blm-QVFF mutant were analyzed as in *(A)*. See also Fig. S4A for co-immunoprecipitation of Mcm6 with BLM carrying the milder QVF mutation and Fig. S4B for co-immunoprecipitation Mcm6 with BLM carrying a deletion of residues 1- 160, which encompass MBD-N. *(D)* KSVS1452 cells expressing the blm-WLVICI mutant were analyzed as in *(A)*. See also Fig. S4C for co-immunoprecipitation of Mcm6 with BLM carrying the milder VICI mutation *(E)* Sequence alignment of residues 284-308 of human BLM with BLM homologs from other vertebrates. Residues mutated in the blm-FYF mutant are labeled with an asterisk. Phosphorylation of serine 304 was previously reported to play a role in BLM/TopBP1 binding in unperturbed S-phase (Blackford et al., 2015) *(F)* KSVS1452 cells expressing the blm-FYF mutant were analyzed as in *(A)*. See also Fig. S4D for the requirement of the FYF residues, but not MBD-C, for BLM/TopBP1 binding and Fig. S4E for the importance of the FYF residues for BLM/TopBP1 binding after CPT treatment, but not in unperturbed S-phase or G1 *(G)* Effect of the blm-FYF and blm-QVFF-FYF mutations on the BLM/Mcm6 interaction in a two-hybrid assay. Mean } SD is shown. Differences between means were analyzed by a *t*-test and presented as *** ($p<0.001$). *(H)* QVFF residues in MBD-N and FYF residues cooperate to bind Mcm6 in S-phase. KSVS1452 cells expressing the blm-QVFF-FYF mutant were analyzed in G1 and S-phase as in *(A)*. *(I)* BLM is required for timely resumption of DNA replication after exposure to CPT. Based on colocalization with EdU foci, the vast majority of BLM/Mcm6 foci in $BLM^{+/+}$ cells (94%) and in BLM^{KO} (KSVS1452) cells (95%) are replicating during unperturbed S-phase ($p=0.41$). After a 45-minute release from 1-hour CPT exposure, significantly fewer Mcm6 foci are replicating in BLM^{KO} cells (26%) than in $BLM^{+/+}$ cells (64%). See also Fig. S6D. Differences between foci numbers were analyzed by a Mann-Whitney test and are shown as ****($p<0.0001$); n.s., not significant. *(J)* Clonogenic assays were performed to measure survival of KSVS1452 cells expressing BLM mutants to increasing concentrations of the G4-stabilizer pyridostatin (PDS) and *(K)* hydroxyurea (HU). Mean +/-SD is reported. Significance of differences between means was analyzed by a *t*-test and is indicated by * ($p<0.05$), ** ($p<0.01$), *** ($p<0.001$) and ****($p<0.0001$).
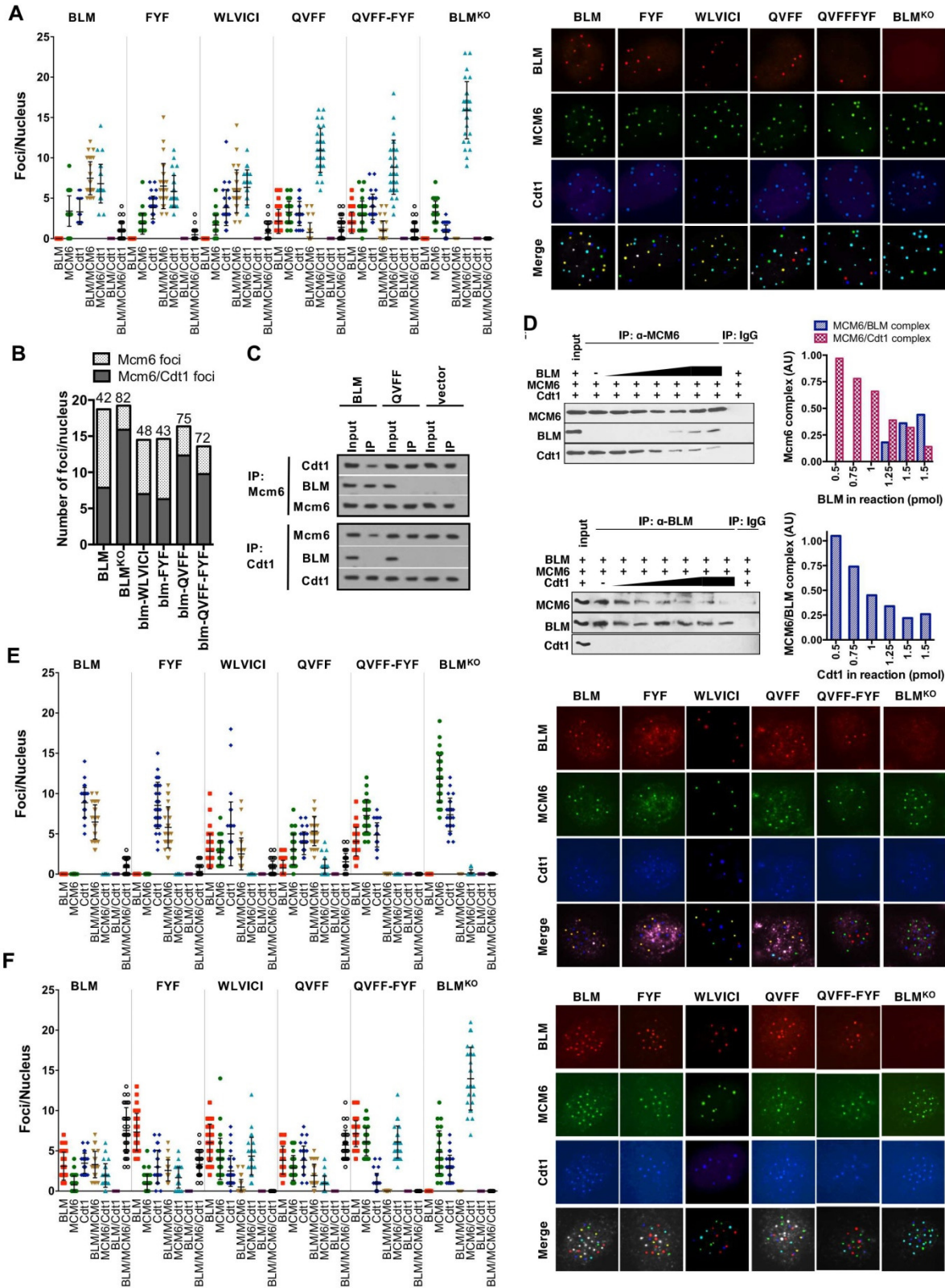
Figure 4.4. Effects of MBD-N, MBD-C, and FYF mutations on association between BLM, Mcm6 and Cdt1 *in vivo*

(A) BLM, Mcm6 and Cdt1 foci were counted in 30 nuclei from KSVS1452 (*BLM^KO^*) cells in

G1 phase transfected with plasmids expressing BLM mutants that disrupt the interaction with Mcm6. *(B)* Quantification of Mcm6 foci and Mcm6/Cdt1 foci in KSVS1452 (BLM^{KO}) cells transfected with BLM mutants. Numbers above the columns indicate the percentage of Mcm6 foci that colocalize with Cdt1 *(C)* The blm-QVFF mutation, which disrupts BLM/Mcm6 binding in G1, or absence of BLM (vector) increases Cdt1/Mcm6 interaction in G1. Reciprocal co-immunoprecipitations of Cdt1 and Mcm6 were performed on KSVS1452 (BLM^{KO}) cells in G1 phase transfected with empty vector or with plasmids expressing BLM or the blm-QVFF mutant. *(D)* BLM and Cdt1 compete for binding to Mcm6 *in vitro*. Coimmunoprecipitation of equimolar amounts of recombinant Mcm6 (0.5 μM) and recombinant BLM (0.5 μM) is disrupted by addition of increasing amounts of Cdt1 (0.5 – 1.5 μM). Co-immunoprecipitation of equimolar amounts of recombinant Mcm6 (0.5 μM) and recombinant Cdt1 (0.5 μM) is disrupted by increasing amounts of BLM (0.5 – 1.5 μM). See also Fig. S5 for reciprocal co-immunoprecipitations of the recombinant proteins. *(E)* BLM, Mcm6 and Cdt1 foci were counted in 30 nuclei from KSVS1452 (BLM^{KO}) cells in unperturbed S-phase transfected with plasmids expressing BLM mutants *(F)* BLM, Mcm6 and Cdt1 foci were counted in 30 nuclei from KSVS1452 (BLM^{KO}) cells in S-phase 45 minutes after release from a 1-hour exposure to 1 μM CPT transfected with plasmids expressing BLM mutants.
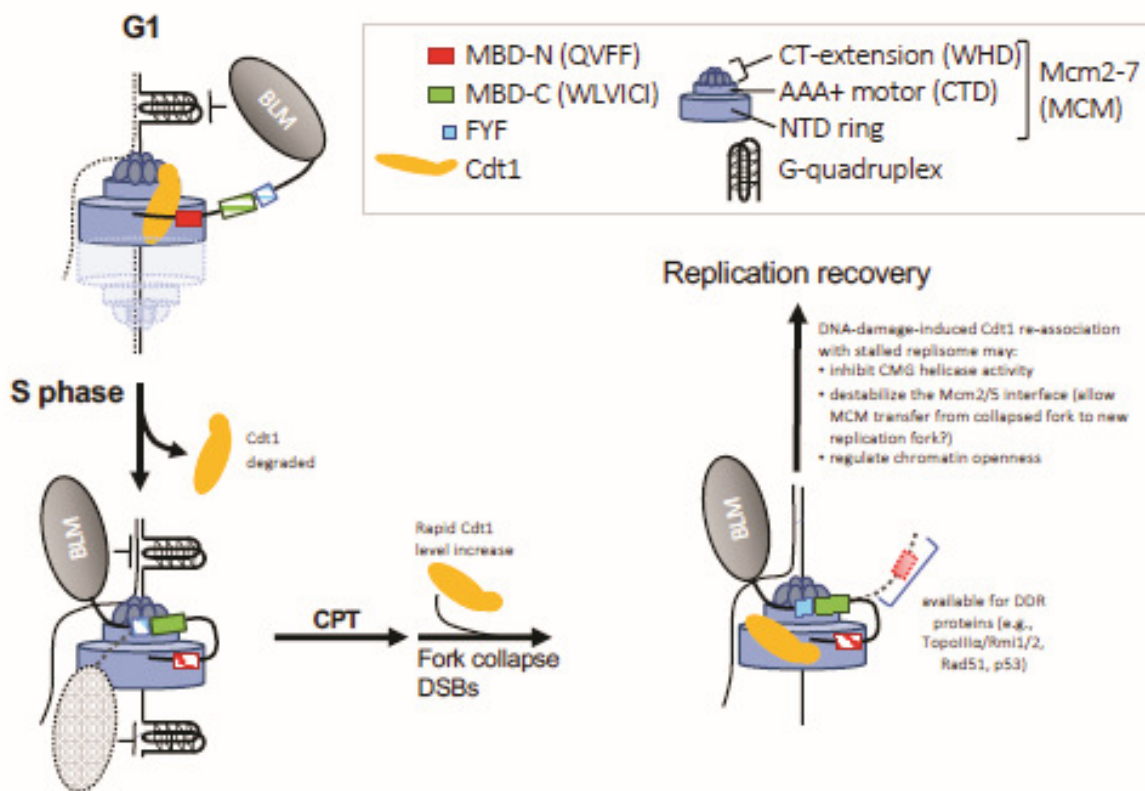
Figure 4.5. Model for the function of the BLM/Mcm6 interaction

In G1, BLM binds the N-terminal domain of Mcm6 via MBD-N, leaving the C-terminal extension of Mcm6 free to bind Cdt1 for origin loading. Cdt1 binding overcomes the autoinhibitory function of the C-terminal extension of Mcm6 and leads to ATP hydrolysis, Cdt1 release, and recruitment of the second MCM hexamer to origins. Upon S-phase entry, Cdt1 is rapidly degraded through multiple pathways. BLM/Mcm6 interaction is now stabilized by

147

binding the N- and C terminal extensions of Mcm6 through MBD-N, MBD-C and the FYF residues in its disordered tail. In contrast to G1, the association between MBD-C of BLM and the Cdt1-bindingdomain of Mcm6 is the dominant interaction in S-phase (filled rectangle) and cooperation between MBD-N and the FYF residues contributes to this interaction (patterned rectangles). BLM associates with Mcm6 in S-phase to support duplex unwinding by CMG when it encounters G4s. BLM would also be able to unfold G4 structures that may form in single-stranded DNA behind the fork (dotted line). In addition to G4 unfolding, BLM also associates with replisomes during replication stress. During exposure of cells to CPT, Cdt1 levels increase rapidly and Cdt1 associates with Mcm6/BLM at replisomes (Fig. 3B). In addition to the Cdt1-binding domain of Mcm6, Cdt1 also binds to other sites of Mcm6 and to other MCM subunits, most prominently Mcm2 and Mcm4 (Frigola et al., 2017). BLM/Mcm6 interaction in cells exposed to CPT is mediated by MBD-C binding to the C-terminal extension of Mcm6 and by the FYF residues (filled rectangles). In contrast, BLM association with the N-terminal domain of Mcm6 via the MBD-N site plays the smallest role in the DNA-damage response. The first 230 residues of the Nterminal tail of BLM encompassing MBD-N may bind DNA repair factors instead of Mcm6. During CPT exposure, Cdt1 may be recruited to replisomes to inhibit MCM ATPase activity to halt replication, to destabilize the Mcm2/5 interface to allow transfer of MCM, or regulate chromatin openness near collapsed forks (see text for details).
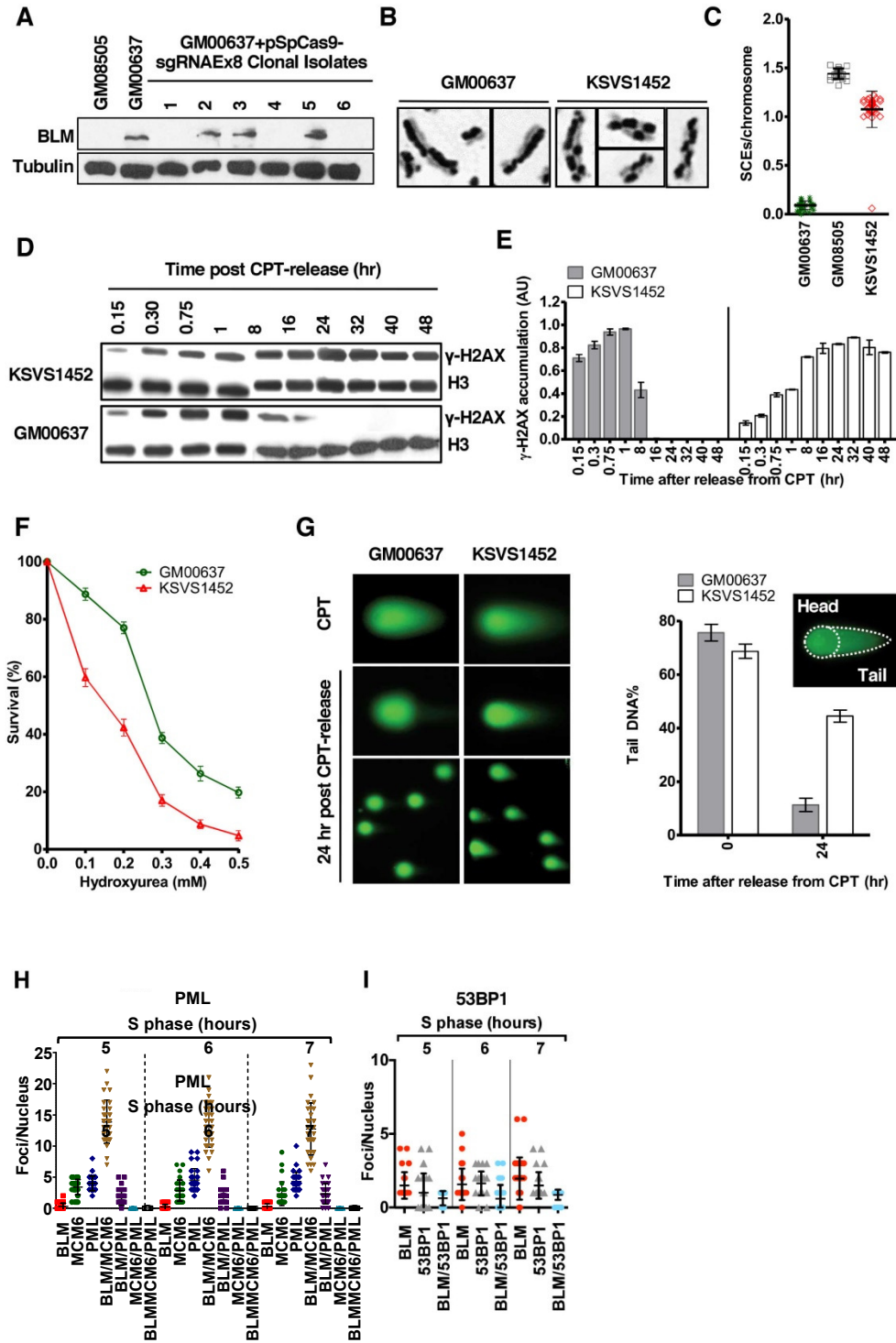
**Figure S4.1. Characterization of the BLMKO cell line KSVS1452 generated by CRISPR/Cas9-mediated biallelic disruption of BLM exon 8 in GM00637**

(A) Single cell clones were screened by Western blotting for absence of BLM expression. GM08505 is a skin fibroblast cell line from a Bloom's syndrome patient, showing absence of BLM expression. Fragment encompassing exon 8 was amplified by PCR, cloned and sequenced

to identify the disruptions in both alleles of *BLM* exon 8. For exact changes DNA and amino acid sequence changes identified in clone 6 (KSVS1452) see *Methods*. *(B)* Increased levels of sister-chromatid exchanges (SCEs) in KSVS1452. *(C)* SCEs in 1500 chromosomes for each cell line were counted. Mean } SD is shown. *(D)* Delayed elimination of H2AX phosphorylation in KSVS1452 after 1-hour exposure to camptothecin (CPT). *(E)* Quantification of γ-H2AX levels in KSVS1452 and GM00637 cells after CPT exposure. Mean+/-SD is shown from three experiments. *(F)* KSVS1452 cells are hypersensitive to hydroxyurea. Mean+/-SD is shown from three experiments. *(G)* Neutral comet assay shows delayed repair of DNA double-strand breaks after CPT exposure in KSVS1452 cells. 150 comets from three experiments per time point and cell line were analyzed. Mean+/-SD is shown. Experiments in panels *(B)* – *(G)* were performed exactly as previously described (Shastri & Schmidt, 2016). *(H)* Colocalization of BLM foci with PML and Mcm6 in the second half of S-phase. 30 nuclei from GM00637 were analyzed for each of the indicated time points. Mean+/-SD is shown. *(I)* Lack of colocalization of 53BP1 with BLM foci in the second half of S-phase. 30 nuclei from GM00637 were analyzed for each of the indicated time points. Mean+/-SD is shown.
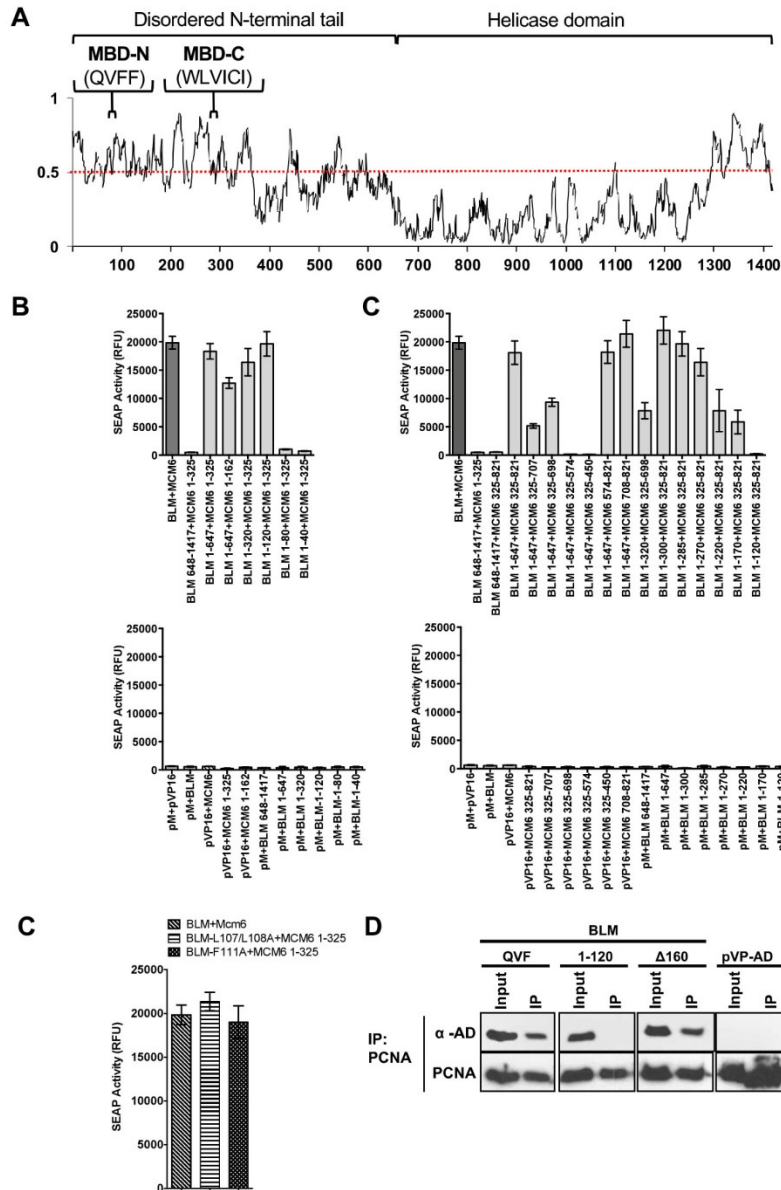
Figure S4.2. Identification of Mcm6 binding sites in the N-terminal tail of BLM
(A) BLM consists of a 647-residue long, intrinsically disordered N-terminal tail and a 770-residue Cterminal helicase domain. Disorder scores for every residue were calculated in IUPred (Dosztanyi et al, 2005). A disorder score of >0.5 indicates a discorded residue. *(B)* Two-hybrid analysis of the interaction between the N-terminal domain of Mcm6 (residues 1-325) and fragments of BLM. Mean } SD from three transfections is shown. Bottom panel shows the Mcm6 and BLM fragments in combination with empty bait and prey vectors. *(C)* Two-hybrid analysis of the interaction between fragments of the Cterminal domain of Mcm6 (residues 325-821) and fragments of BLM. Mean } SD from three transfections is shown. Bottom panel shows the Mcm6 and BLM fragments in combination with empty bait and prey vectors. *(D)* Mutation of residues L107 and L108 or F111 in MBD-N to alanine does not affect Mcm6 binding in the two-hybrid assay. Mean } SD from three transfections is shown. *(E)* The first 160 residues of BLM, which include the PIP-box-like sequence in MBD-N that binds Mcm6, is

151

not required PCNA binding. A BLM fragment encompassing the first 120 residues of BLM does not bind PCNA. KSVS1452 cells were transfected with plasmids (p-AD) expressing BLM mutants or fragments, and Mcm6 interaction was evaluated by co-immunoprecipitation.
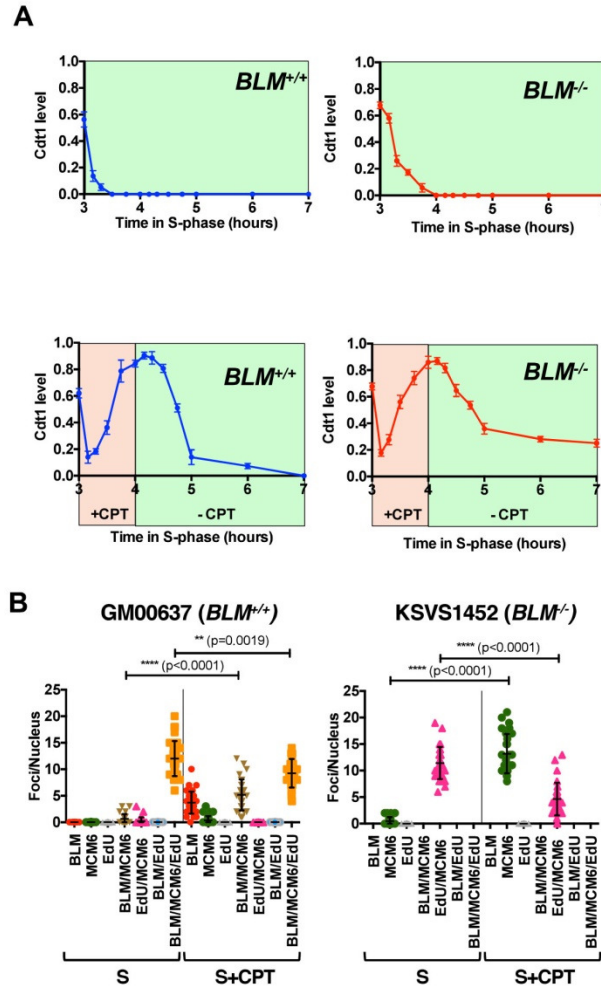
Figure S4.3. Effect of DNA-damage induction and recovery on Cdt1 levels and replisome activity

(A) Cdt1 levels were assessed by Western blotting in untreated *BLM+/+* (GM00637) and *BLMKO* (KSVS1452) cells and during a 1-hour exposure to 1 μM CPT followed by a 3-hour release into fresh media. Cdt1 levels from three independent experiments were quantified against GAPDH levels using ImageJ. Mean } SD is shown. *(B)* Foci formation between BLM, Mcm6 and Cdt1 was analyzed in 30 nuclei from GM00637 cells in unperturbed S-phase starting at 3 hours after release from G1. Average Cdt1 expression level from Figure S3A is overlayed on the right Y-axis. For simplicity, only BLM, BLM/Mcm6, and BLM/Mcm6/Cdt1 foci are shown. *(C)* Foci formation between BLM, Mcm6 and Cdt1 was analyzed in 30 nuclei from GM00637 cells during 1-hour exposure to CPT and after release into fresh media. *(D)* Comparison of colocalization of BLM, Mcm6 and BLM/Mcm6 foci with EdU foci in GM00637 and KSVS1452 cells in unperturbed S-phase and 45 minutes after release from CPT. Foci in 30 nuclei were

152

analyzed for each condition. Mean } SD is shown. Significance of differences between foci numbers was determined by a Mann-Whitney test.
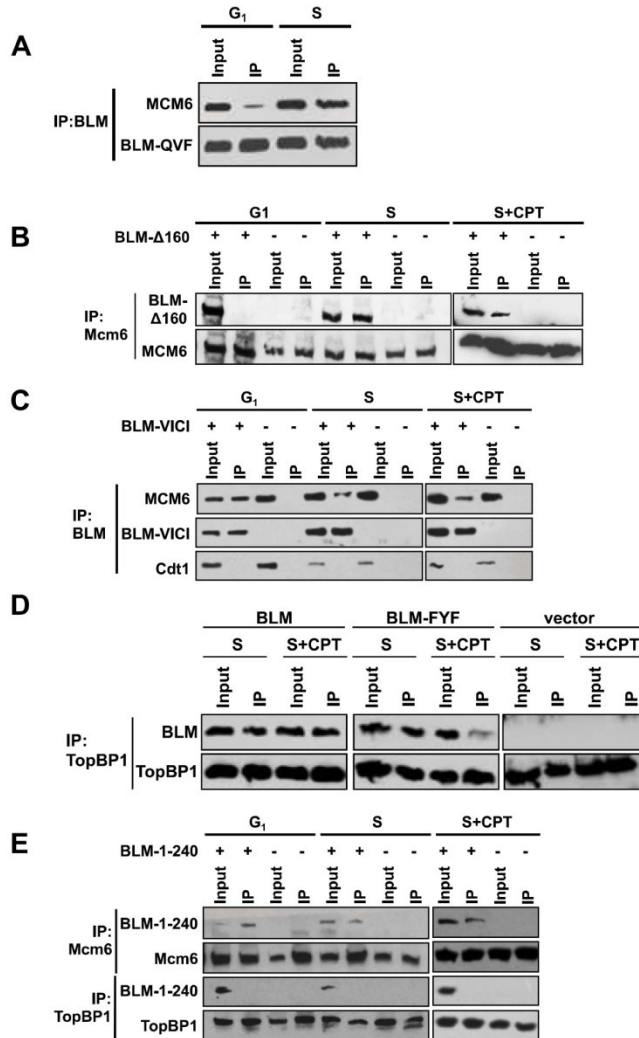
Figure S4.4. Interactions between the N-terminal tail of BLM and Mcm6 and TopBP1
(A) BLM-QVF poorly interacts with Mcm6 in G1, but normally in S-phase. *(B)* An N-terminal truncation of the first 160 residues of BLM fails to interact with Mcm6 in G1, but not in S-phase or after CPT exposure. *(C)* BLM-VICI co-immunoprecipitates with Mcm6 in G1, but does so poorly in S-phase, in the presence or absence of CPT. *(D)* The first 240 residues of BLM are sufficient for Mcm6 binding, but not for TopBP1 binding. Cells were transfected with a plasmid expressing BLM residues 1-240 and co-immunoprecipitation with Mcm6 and TopBP1 was evaluated by Western blot. *(E)* TopBP1 coimmunoprecipitates with BLM in perturbed and unperturbed S-phase. The blm-FYF mutation specifically disrupts the interaction between BLM and TopBP1 after exposure to CPT. Cells were transfected with plasmid expressing BLM or blm-FYF or with empty vector and co-immunoprecipitation with TopBP1 was evaluated by Western blot.
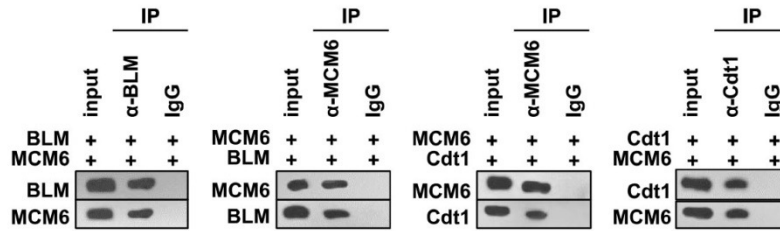
Figure S4.5. Interaction of recombinant Mcm6 with BLM and Cdt1
Reciprocal co-immunoprecipitations were performed using equimolar amounts of purified human BLM and Mcm6 or purified human Cdt1 and Mcm6.
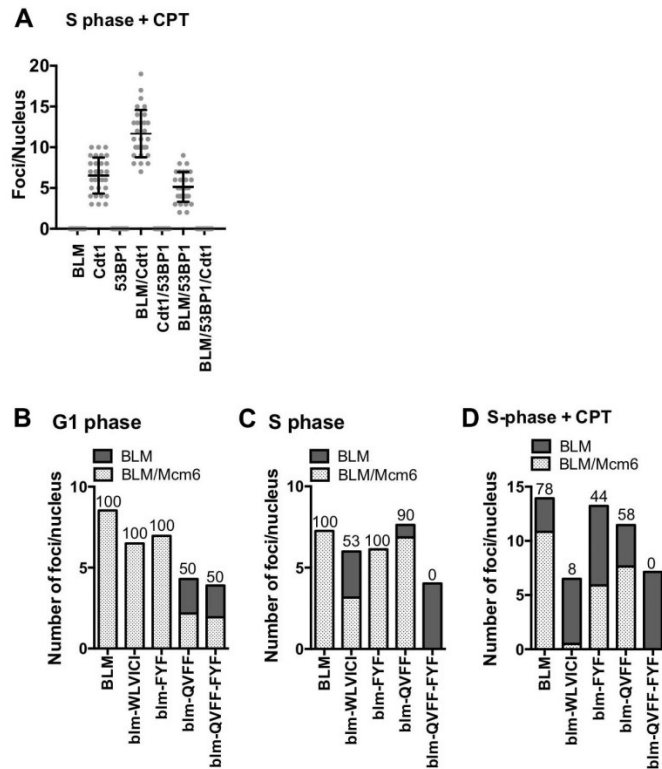
Figure S4.6. Colocalization of BLM with Mcm6 and 53BP1 in the absence and presence of DNA damage

(A) BLM foci colocalize with 53BP1 after exposure to CPT. Foci were counted in 30 nuclei of wildtype cells (GM00637) 45 minutes after removal of CPT. Cells not exposed to CPT did not form 53BP1 foci. *(B)* Quantification of Mcm6 foci and Mcm6/BLM foci in KSVS1452 (*BLMKO*) cells transfected with BLM mutants in G1 phase, in S-phase *(C)* and 45 minutes after

CPT exposure *(D)*. Numbers above the columns indicate the percentage of BLM foci that colocalize with Mcm6.

REFERENCES

ARIAS, E. E. & WALTER, J. C. 2006. PCNA functions as a molecular platform to trigger Cdt1 destruction and prevent re-replication. *Nat Cell Biol,* 8**,** 84-90.

AYGUN, O., SVEJSTRUP, J. & LIU, Y. 2008. A RECQ5-RNA polymerase II association identified by targeted proteomic analysis of human chromatin. *Proc Natl Acad Sci U S A,* 105**,** 8580-4.

BACHRATI, C. Z. & HICKSON, I. D. 2003. RecQ helicases: suppressors of tumorigenesis and premature aging. *Biochem J,* 374**,** 577-606.

BALLABENI, A., ZAMPONI, R., CAPRARA, G., MELIXETIAN, M., BOSSI, S., MASIERO, L. & HELIN, K. 2009. Human CDT1 associates with CDC7 and recruits CDC45 to chromatin during S phase. *J Biol Chem,* 284**,** 3028-36.

BISCHOF, O., KIM, S. H., IRVING, J., BERESTEN, S., ELLIS, N. A. & CAMPISI, J. 2001. Regulation and localization of the Bloom syndrome protein in response to DNA damage. *J Cell Biol,* 153**,** 367-80.

BLACKFORD, A. N., NIEMINUSZCZY, J., SCHWAB, R. A., GALANTY, Y., JACKSON, S. P. & NIEDZWIEDZ, W. 2015. TopBP1 interacts with BLM to maintain genome stability but is dispensable for preventing BLM degradation. *Mol Cell,* 57**,** 1133-1141.

BOCHMAN, M. L., PAESCHKE, K. & ZAKIAN, V. A. 2012. DNA secondary structures: stability and function of G-quadruplex structures. *Nat Rev Genet,* 13**,** 770-80.

BOEHM, E. M. & WASHINGTON, M. T. 2016. R.I.P. to the PIP: PCNA-binding motif no longer considered specific: PIP motifs and other related sequences are not distinct entities and can bind multiple proteins involved in genome maintenance. *Bioessays,* 38**,** 1117-1122.

BUDHATHOKI, J. B., RAY, S., URBAN, V., JANSCAK, P., YODH, J. G. & BALCI, H. 2014. RecQ-core of BLM unfolds telomeric G-quadruplex in the absence of ATP. *Nucleic Acids Res,* 42**,** 11528-45.

CADORET, J. C., MEISCH, F., HASSAN-ZADEH, V., LUYTEN, I., GUILLET, C., DURET, L., QUESNEVILLE, H. & PRIOLEAU, M. N. 2008. Genome-wide studies highlight indirect links between human replication origins and gene regulation. *Proc Natl Acad Sci U S A,* 105**,** 15837-42.

CANTOR, S. B. & NAYAK, S. 2016. FANCJ at the FORK. *Mutat Res,* 788**,** 7-11.

CHAGANTI, R. S. K., SCHONBERG, S. & GERMAN, J. 1974. A Manyfold Increase in Sister Chromatid Exchanges in Bloom's Syndrome Lymphocytes. *Proceedings of the National Academy of Sciences,* 71**,** 4508-4512.

CHANG, E. Y.-C., NOVOA, C. A., ARISTIZABAL, M. J., COULOMBE, Y., SEGOVIA, R., CHATURVEDI, R., SHEN, Y., KEONG, C., TAM, A. S., JONES, S. J. M., MASSON, J.-Y., KOBOR, M. S. & STIRLING, P. C. 2017. RECQ-like helicases Sgs1 and BLM regulate R-loop-associated genome instability. *The Journal of cell biology,* 216**,** 3991-4005.

CHEN, S. & BELL, S. P. 2011. CDK prevents Mcm2-7 helicase loading by inhibiting Cdt1 interaction with Orc6. *Genes Dev,* 25**,** 363-72.

CHEN, S., DE VRIES, M. A. & BELL, S. P. 2007. Orc6 is required for dynamic recruitment of Cdt1 during repeated Mcm2-7 loading. *Genes Dev,* 21**,** 2897-907.

CHEN, Y. H., JONES, M. J., YIN, Y., CRIST, S. B., COLNAGHI, L., SIMS, R. J., 3RD, ROTHENBERG, E., JALLEPALLI, P. V. & HUANG, T. T. 2015. ATR-mediated phosphorylation of FANCI regulates dormant origin firing in response to replication stress. *Mol Cell,* 58**,** 323-38.

CORTEZ, D., GLICK, G. & ELLEDGE, S. J. 2004. Minichromosome maintenance proteins are direct targets of the ATM and ATR checkpoint kinases. *Proceedings of the National Academy of Sciences of the United States of America,* 101**,** 10078-10083.

COX, J. & MANN, M. 2008. MaxQuant enables high peptide identification rates, individualized p.p.b.-range mass accuracies and proteome-wide protein quantification. *Nat Biotechnol,* 26**,** 1367-72.

CRABBE, L., VERDUN, R. E., HAGGBLOM, C. I. & KARLSEDER, J. 2004. Defective telomere lagging strand synthesis in cells lacking WRN helicase activity. *Science,* 306**,** 1951-3.

DALEY, J. M., CHIBA, T., XUE, X., NIU, H. & SUNG, P. 2014. Multifaceted role of the Topo IIIα-RMI1-RMI2 complex and DNA2 in the BLM-dependent pathway of DNA break end resection. *Nucleic acids research,* 42**,** 11083-11091.

DAVALOS, A. R. & CAMPISI, J. 2003. Bloom syndrome cells undergo p53-dependent apoptosis and delayed assembly of BRCA1 and NBS1 repair complexes at stalled replication forks. *J Cell Biol,* 162**,** 1197-209.

DAVIES, S. L., NORTH, P. S. & HICKSON, I. D. 2007. Role for BLM in replication-fork restart and suppression of origin firing after replicative stress. *Nature Structural &Amp; Molecular Biology,* 14**,** 677.

DROSOPOULOS, W. C., KOSIYATRAKUL, S. T. & SCHILDKRAUT, C. L. 2015. BLM helicase facilitates telomere replication during leading strand synthesis of telomeres. *The Journal of Cell Biology,* 210**,** 191-208.

ELADAD, S., YE, T. Z., HU, P., LEVERSHA, M., BERESTEN, S., MATUNIS, M. J. & ELLIS, N. A. 2005. Intra-nuclear trafficking of the BLM helicase to DNA damage-induced foci is regulated by SUMO modification. *Hum Mol Genet,* 14**,** 1351-65.

EVRIN, C., CLARKE, P., ZECH, J., LURZ, R., SUN, J., UHLE, S., LI, H., STILLMAN, B. & SPECK, C. 2009. A double-hexameric MCM2-7 complex is loaded onto origin DNA during licensing of eukaryotic DNA replication. *Proc Natl Acad Sci U S A,* 106**,** 20240-5.

FERNÁNDEZ-CID, A., RIERA, A., TOGNETTI, S., HERRERA, M. C., SAMEL, S., EVRIN, C., WINKLER, C., GARDENAL, E., UHLE, S. & SPECK, C. 2013. An ORC/Cdc6/MCM2-7 Complex Is Formed in a Multistep Reaction to Serve as a Platform for MCM Double-Hexamer Assembly. *Molecular Cell,* 50**,** 577-588.

FRANCHITTO, A. & PICHIERRI, P. 2002. Bloom's syndrome protein is required for correct relocalization of RAD50/MRE11/NBS1 complex after replication fork arrest. *J Cell Biol,* 157**,** 19-30.

FRIGOLA, J., HE, J., KINKELIN, K., PYE, V. E., RENAULT, L., DOUGLAS, M. E., REMUS, D., CHEREPANOV, P., COSTA, A. & DIFFLEY, J. F. X. 2017. Cdt1 stabilizes an open MCM ring for helicase loading. *Nat Commun,* 8**,** 15720.

GERMAN, J., AND ELLIS, N. A. 1998. *Bloom syndrome,* New York, McGraw-Hill, Health Professions Division.

GERMAN, J., SANZ, M. M., CIOCCI, S., YE, T. Z. & ELLIS, N. A. 2007. Syndrome-causing mutations of the BLM gene in persons in the Bloom's Syndrome Registry. *Hum Mutat,* 28**,** 743-53.

GRIERSON, P. M., LILLARD, K., BEHBEHANI, G. K., COMBS, K. A., BHATTACHARYYA, S., ACHARYA, S. & GRODEN, J. 2012. BLM helicase facilitates RNA polymerase I-mediated ribosomal RNA transcription. *Human molecular genetics,* 21**,** 1172-1183.

HANNICH, J. T., LEWIS, A., KROETZ, M. B., LI, S. J., HEIDE, H., EMILI, A. & HOCHSTRASSER, M. 2005. Defining the SUMO-modified proteome by multiple approaches in Saccharomyces cerevisiae. *J Biol Chem,* 280**,** 4102-10.

HECKER, C. M., RABILLER, M., HAGLUND, K., BAYER, P. & DIKIC, I. 2006. Specification of SUMO1- and SUMO2-interacting motifs. *J Biol Chem,* 281**,** 16117-27.

HELLEDAY, T. 2003. Pathways for mitotic homologous recombination in mammalian cells. *Mutat Res,* 532**,** 103-15.

HICKSON, I. D. 2003. RecQ helicases: caretakers of the genome. *Nat Rev Cancer,* 3**,** 169-78.

HIGA, L. A., MIHAYLOV, I. S., BANKS, D. P., ZHENG, J. & ZHANG, H. 2003. Radiation-mediated proteolysis of CDT1 by CUL4-ROC1 and CSN complexes constitutes a new checkpoint. *Nat Cell Biol,* 5**,** 1008-15.

HOLM, C., COVEY, J. M., KERRIGAN, D. & POMMIER, Y. 1989. Differential requirement of DNA replication for the cytotoxicity of DNA topoisomerase I and II inhibitors in Chinese hamster DC3F cells. *Cancer Res,* 49**,** 6365-8.

HOSOI, A., SAKAIRI, T. & YUKIO, I. 2015. Binding of MCM-interacting proteins to ATP-binding site in MCM6. *Research and Reports in Biology,* 2016**,** 31-40.

HOSOI A, S. T., YUKIO I 2015. Binding of MCM-interacting proteins to ATP-binding site in MCM6. *Research and Reports in Biology,* 2016**,** 31-40.

IBARRA, A., SCHWOB, E. & MÉNDEZ, J. 2008. Excess MCM proteins protect human cells from replicative stress by licensing backup origins of replication. *Proceedings of the National Academy of Sciences,* 105**,** 8956-8961.

JACKMAN, J. & O'CONNOR, P. M. 2001. Methods for synchronizing cells at specific stages of the cell cycle. *Curr Protoc Cell Biol,* Chapter 8**,** 8.3.1-8.3.20.

JIN, J., ARIAS, E. E., CHEN, J., HARPER, J. W. & WALTER, J. C. 2006. A family of diverse Cul4-Ddb1-interacting proteins includes Cdt2, which is required for S phase destruction of the replication factor Cdt1. *Mol Cell,* 23**,** 709-21.

KAROW, J. K., CHAKRAVERTY, R. K. & HICKSON, I. D. 1997. The Bloom's syndrome gene product is a 3'-5' DNA helicase. *J Biol Chem,* 272**,** 30611-4.

KAROW, J. K., CONSTANTINOU, A., LI, J. L., WEST, S. C. & HICKSON, I. D. 2000. The Bloom's syndrome gene product promotes branch migration of holliday junctions. *Proc Natl Acad Sci U S A,* 97**,** 6504-8.

KELLER, H., KIOSZE, K., SACHSENWEGER, J., HAUMANN, S., OHLENSCHLAGER, O., NUUTINEN, T., SYVAOJA, J. E., GORLACH, M., GROSSE, F. & POSPIECH, H. 2014. The intrinsically disordered amino-terminal region of human RecQL4: multiple DNA-binding domains confer annealing, strand exchange and G4 DNA binding. *Nucleic Acids Res,* 42**,** 12614-27.

LAM, E. Y., BERALDI, D., TANNAHILL, D. & BALASUBRAMANIAN, S. 2013. G-quadruplex structures are stable and detectable in human genomic DNA. *Nat Commun,* 4**,** 1796.

LEMAN, A. R. & NOGUCHI, E. 2013. The replication fork: understanding the eukaryotic replication machinery and the challenges to genome duplication. *Genes,* 4**,** 1-32.

LI, J. L., HARRISON, R. J., RESZKA, A. P., BROSH, R. M., JR., BOHR, V. A., NEIDLE, S. & HICKSON, I. D. 2001. Inhibition of the Bloom's and Werner's syndrome helicases by G-quadruplex interacting ligands. *Biochemistry,* 40**,** 15194-202.

LIU, C., WU, R., ZHOU, B., WANG, J., WEI, Z., TYE, B. K., LIANG, C. & ZHU, G. 2012. Structural insights into the Cdt1-mediated MCM2–7 chromatin loading. *Nucleic Acids Res,* 40**,** 3208-17.

LLORENTE, B., SMITH, C. E. & SYMINGTON, L. S. 2008. Break-induced replication: what is it and what is it for? *Cell Cycle,* 7**,** 859-64.

LONDON, T. B., BARBER, L. J., MOSEDALE, G., KELLY, G. P., BALASUBRAMANIAN, S., HICKSON, I. D., BOULTON, S. J. & HIOM, K. 2008. FANCJ is a structure-specific DNA helicase associated with the maintenance of genomic G/C tracts. *J Biol Chem,* 283**,** 36132-9.

LOPES, J., PIAZZA, A., BERMEJO, R., KRIEGSMAN, B., COLOSIO, A., TEULADE-FICHOU, M. P., FOIANI, M. & NICOLAS, A. 2011. G-quadruplex-induced instability during leading-strand replication. *Embo j,* 30**,** 4033-46.

LOSSAINT, G., LARROQUE, M., RIBEYRE, C., BEC, N., LARROQUE, C., DECAILLET, C., GARI, K. & CONSTANTINOU, A. 2013. FANCD2 binds MCM proteins and controls replisome function upon activation of s phase checkpoint signaling. *Mol Cell,* 51**,** 678-90.

LYDEARD, J. R., LIPKIN-MOORE, Z., SHEU, Y. J., STILLMAN, B., BURGERS, P. M. & HABER, J. E. 2010. Break-induced replication requires all essential DNA replication factors except those specific for pre-RC assembly. *Genes Dev,* 24**,** 1133-44.

MACHWE, A., XIAO, L., GRODEN, J. & ORREN, D. K. 2006. The Werner and Bloom syndrome proteins catalyze regression of a model replication fork. *Biochemistry,* 45**,** 13939-46.

MANZA, L. L., STAMER, S. L., HAM, A. J., CODREANU, S. G. & LIEBLER, D. C. 2005. Sample preparation and digestion for proteomic analyses using spin filters. *Proteomics,* 5**,** 1742-5.

MARHEINEKE, K. & HYRIEN, O. 2004. Control of replication origin density and firing time in Xenopus egg extracts: role of a caffeine-sensitive, ATR-dependent checkpoint. *J Biol Chem,* 279**,** 28071-81.

MINTY, A., DUMONT, X., KAGHAD, M. & CAPUT, D. 2000. Covalent modification of p73alpha by SUMO-1. Two-hybrid screening with p73 identifies novel SUMO-1-interacting proteins and a SUMO-1 interaction motif. *J Biol Chem,* 275**,** 36316-23.

MIOTTO, B. & STRUHL, K. 2008. HBO1 histone acetylase is a coactivator of the replication licensing factor Cdt1. *Genes Dev,* 22**,** 2633-8.

MOHAGHEGH, P., KAROW, J. K., BROSH JR, R. M., JR., BOHR, V. A. & HICKSON, I. D. 2001a. The Bloom's and Werner's syndrome proteins are DNA structure-specific helicases. *Nucleic Acids Res,* 29**,** 2843-9.

MOHAGHEGH, P., KAROW, J. K., BROSH, R. M., JR., BOHR, V. A. & HICKSON, I. D. 2001b. The Bloom's and Werner's syndrome proteins are DNA structure-specific helicases. *Nucleic Acids Res,* 29**,** 2843-9.

MOISEEVA, T., HOOD, B., SCHAMUS, S., O'CONNOR, M. J., CONRADS, T. P. & BAKKENIST, C. J. 2017. ATR kinase inhibition induces unscheduled origin firing through a Cdc7-dependent association between GINS and And-1. *Nat Commun,* 8**,** 1392.

NISHITANI, H., SUGIMOTO, N., ROUKOS, V., NAKANISHI, Y., SAIJO, M., OBUSE, C., TSURIMOTO, T., NAKAYAMA, K. I., NAKAYAMA, K., FUJITA, M., LYGEROU, Z. & NISHIMOTO, T. 2006. Two E3 ubiquitin ligases, SCF-Skp2 and DDB1-Cul4, target human Cdt1 for proteolysis. *EMBO J,* 25**,** 1126-36.

OUYANG KJ, WOO LL & NA, E. 2008. Homologous recombination and maintenance of genome integrity: Cancer and aging through the prism of human RecQ helicases. *Mechanisms of Ageing and Development,* 129**,** 425-440.

OUYANG, K. J., WOO, L. L., ZHU, J., HUO, D., MATUNIS, M. J. & ELLIS, N. A. 2009. SUMO modification regulates BLM and RAD51 interaction at damaged replication forks. *PLoS Biol,* 7**,** e1000252.

PATEL, P. K., ARCANGIOLI, B., BAKER, S. P., BENSIMON, A. & RHIND, N. 2006. DNA replication origins fire stochastically in fission yeast. *Mol Biol Cell,* 17**,** 308-16.

POPURI, V., BACHRATI, C. Z., MUZZOLINI, L., MOSEDALE, G., COSTANTINI, S., GIACOMINI, E., HICKSON, I. D. & VINDIGNI, A. 2008. The human RecQ helicases, BLM and RECQ1, display distinct DNA substrate specificities. *Journal of Biological Chemistry,* 283**,** 17766-17776.

PRIOLEAU, M. N. & MACALPINE, D. M. 2016. DNA replication origins-where do we begin? *Genes Dev,* 30**,** 1683-97.

RALF, C., HICKSON, I. D. & WU, L. 2006. The Bloom's Syndrome Helicase Can Promote the Regression of a Model Replication Fork. *Journal of Biological Chemistry,* 281**,** 22839-22846.

RAN, F. A., HSU, P. D., WRIGHT, J., AGARWALA, V., SCOTT, D. A. & ZHANG, F. 2013. Genome engineering using the CRISPR-Cas9 system. *Nat Protoc,* 8**,** 2281-308.

REMUS, D., BEURON, F., TOLUN, G., GRIFFITH, J. D., MORRIS, E. P. & DIFFLEY, J. F. 2009. Concerted loading of Mcm2-7 double hexamers around DNA during DNA replication origin licensing. *Cell,* 139**,** 719-30.

RHODES, D. & LIPPS, H. J. 2015. G-quadruplexes and their regulatory roles in biology. *Nucleic Acids Res,* 43**,** 8627-37.

RIERA, A., BARBON, M., NOGUCHI, Y., REUTER, L. M., SCHNEIDER, S. & SPECK, C. 2017. From structure to mechanism-understanding initiation of DNA replication. *Genes Dev,* 31**,** 1073-1088.

RIOS-DORIA, J., VELKOVA, A., DAPIC, V., GALAN-CARIDAD, J. M., DAPIC, V., CARVALHO, M. A., MELENDEZ, J. & MONTEIRO, A. N. 2009. Ectopic expression

160

of histone H2AX mutants reveals a role for its post-translational modifications. *Cancer Biol Ther,* 8**,** 422-34.

SANGRITHI, M. N., BERNAL, J. A., MADINE, M., PHILPOTT, A., LEE, J., DUNPHY, W. G. & VENKITARAMAN, A. R. 2005. Initiation of DNA replication requires the RECQL4 protein mutated in Rothmund-Thomson syndrome. *Cell,* 121**,** 887-98.

SEQUEIRA-MENDES, J., DIAZ-URIARTE, R., APEDAILE, A., HUNTLEY, D., BROCKDORFF, N. & GOMEZ, M. 2009. Transcription initiation activity sets replication origin efficiency in mammalian cells. *PLoS Genet,* 5**,** e1000446.

SIDOROVA, J. M., KEHRLI, K., MAO, F. & MONNAT, R. 2013. Distinct functions of human RECQ helicases WRN and BLM in replication fork recovery and progression after hydroxyurea-induced stalling. *DNA repair,* 12**,** 128-139.

SINGH, D. K., POPURI, V., KULIKOWICZ, T., SHEVELEV, I., GHOSH, A. K., RAMAMOORTHY, M., ROSSI, M. L., JANSCAK, P., CROTEAU, D. L. & BOHR, V. A. 2012. The human RecQ helicases BLM and RECQL4 cooperate to preserve genome stability. *Nucleic Acids Res,* 40**,** 6632-48.

SINGH, T. R., ALI, A. M., BUSYGINA, V., RAYNARD, S., FAN, Q., DU, C.-H., ANDREASSEN, P. R., SUNG, P. & MEETEI, A. R. 2008. BLAP18/RMI2, a novel OB-fold-containing protein, is an essential component of the Bloom helicase–double Holliday junction dissolvasome. *Genes & Development,* 22**,** 2856-2868.

SONG, J., DURRIN, L. K., WILKINSON, T. A., KRONTIRIS, T. G. & CHEN, Y. 2004. Identification of a SUMO-binding motif that recognizes SUMO-modified proteins. *Proc Natl Acad Sci U S A,* 101**,** 14373-8.

SUN, H., KAROW, J. K., HICKSON, I. D. & MAIZELS, N. 1998. The Bloom's syndrome helicase unwinds G4 DNA. *J Biol Chem,* 273**,** 27587-92.

TANAKA, M., TAKAHARA, M., NUKINA, K., HAYASHI, A., SAKAI, W., SUGASAWA, K., SHIOMI, Y. & NISHITANI, H. 2017. Mismatch repair proteins recruited to ultraviolet light-damaged sites lead to degradation of licensing factor Cdt1 in the G1 phase. *Cell Cycle,* 16**,** 673-684.

VALTON, A. L. & PRIOLEAU, M. N. 2016. G-Quadruplexes in DNA Replication: A Problem or a Necessity? *Trends Genet,* 32**,** 697-706.

VAN WIETMARSCHEN, N., MERZOUK, S., HALSEMA, N., SPIERINGS, D. C. J., GURYEV, V. & LANSDORP, P. M. 2018. BLM helicase suppresses recombination at G-quadruplex motifs in transcribed genes. *Nature Communications,* 9**,** 271.

WANG, J., CHEN, J. & GONG, Z. 2013. TopBP1 controls BLM protein level to maintain genome stability. *Mol Cell,* 52**,** 667-78.

WEI, L. & ZHAO, X. 2016. A new MCM modification cycle regulates DNA replication initiation. *Nat Struct Mol Biol,* 23**,** 209-16.

WEI, Z., LIU, C., WU, X., XU, N., ZHOU, B., LIANG, C. & ZHU, G. 2010. Characterization and structure determination of the Cdt1 binding domain of human minichromosome maintenance (Mcm) 6. *J Biol Chem,* 285**,** 12469-73.

WONG, P. G., GLOZAK, M. A., CAO, T. V., VAZIRI, C., SETO, E. & ALEXANDROW, M. 2010. Chromatin unfolding by Cdt1 regulates MCM loading via opposing functions of HBO1 and HDAC11-geminin. *Cell Cycle,* 9**,** 4351-63.

WU, L., DAVIES, S. L., LEVITT, N. C. & HICKSON, I. D. 2001. Potential role for the BLM helicase in recombinational repair via a conserved interaction with RAD51. *J Biol Chem,* 276**,** 19375-81.

WU, L., DAVIES, S. L., NORTH, P. S., GOULAOUIC, H., RIOU, J. F., TURLEY, H., GATTER, K. C. & HICKSON, I. D. 2000. The Bloom's syndrome gene product interacts with topoisomerase III. *J Biol Chem,* 275**,** 9636-44.

WU, L. & HICKSON, I. D. 2003. The Bloom's syndrome helicase suppresses crossing over during homologous recombination. *Nature,* 426**,** 870-4.

WU, W.-Q., HOU, X.-M., LI, M., DOU, S.-X. & XI, X.-G. 2015. BLM unfolds G-quadruplexes in different structural environments through different mechanisms. *Nucleic Acids Research,* 43**,** 4614-4626.

XU, X., ROCHETTE, P. J., FEYISSA, E. A., SU, T. V. & LIU, Y. 2009. MCM10 mediates RECQ4 association with MCM2-7 helicase complex during DNA replication. *The EMBO journal,* 28**,** 3005-3014.

YANAGI, K.-I., MIZUNO, T., YOU, Z. & HANAOKA, F. 2002. Mouse Geminin Inhibits Not Only Cdt1-MCM6 Interactions but Also a Novel Intrinsic Cdt1 DNA Binding Activity. *Journal of Biological Chemistry,* 277**,** 40871-40880.

YU, J., WANG, R., WU, J., DANG, Z., ZHANG, Q. & LI, B. 2016. Knockdown of minichromosome maintenance proteins inhibits foci forming of mediator of DNA-damage checkpoint 1 in response to DNA damage in human esophageal squamous cell carcinoma TE-1 cells. *Biochemistry (Moscow),* 81**,** 1221-1228.

ZEMAN, M. K. & CIMPRICH, K. A. 2014. Causes and Consequences of Replication Stress. *Nature cell biology,* 16**,** 2-9.

ZHANG, J., YU, L., WU, X., ZOU, L., SOU, K. K., WEI, Z., CHENG, X., ZHU, G. & LIANG, C. 2010. The interacting domains of hCdt1 and hMcm6 involved in the chromatin loading of the MCM complex in human cells. *Cell Cycle,* 9**,** 4848-57.

ZHANG, S., SUN, H., WANG, L., LIU, Y., CHEN, H., LI, Q., GUAN, A., LIU, M. & TANG, Y. 2018. Real-time monitoring of DNA G-quadruplexes in living cells with a small-molecule fluorescent probe. *Nucleic Acids Res,* 46**,** 7522-7532.

ZHU, J., ZHU, S., GUZZO, C. M., ELLIS, N. A., SUNG, K. S., CHOI, C. Y. & MATUNIS, M. J. 2008. Small ubiquitin-related modifier (SUMO) binding determines substrate recognition and paralog-selective SUMO modification. *J Biol Chem,* 283**,** 29405-15.

CHAPTER FIVE:
PERSPECTIVES

Mutations and heterozygosity in *BLM* have been statistically associated with increased susceptibility to cancers [1-11]. Likewise, single nucleotide polymorphisms (SNPs) in the non-coding region of *BLM* have been linked with various malignancies [12, 13]. Epidemiological studies have provided evidence for a relationship between SNPs in genome stability maintenance genes and putative cancer risk [14]. It has been suggested that rare SNPs play a role in human diseases [15-17]. Of the 74 known coding SNPs in *BLM* resulting in missense variants, all but three are rare with allele frequencies <0.05. However, the significance and disease association of these missense variants were unknown. A study using humanized yeast model functionally characterized selected non-synonymous coding SNPs in *BLM* for the first time and identified BLM variants causing increased DNA-damage sensitivity [18]. Subsequently our study described in Chapter Two functionally characterized these BLM variants in human cells [19]. Within the broader context of determining their biological relevance, disease association and subsequent translation to clinical use, this can be perceived as the vital first step.

The next step would be to expand the functional annotation to all known BLM missense variants, including variants predicted to be benign, intermediate as well as damaging *in silico*, and provide functional evidence for their classification based on pathogenicity [20, 21]. The functional status of these variants can be ascertained in GM08505 or KSVS1452 cells by using the same functional complementation assays used in Chapters Two and Three. However, variants

mapping to known protein interaction sites in the disordered BLM N-terminal region might not be sensitive to the functional assays designed to test the impact of variants mapping to the conserved C-terminal domains involved in helicase activity. Variants which disrupt BLM interaction with some proteins but not others have not been identified yet and could play a role in delineating BLM function in various pathways. Those mapping to regions predicted to contain increased α-helical content and hypothesized to be involved in protein interactions in BLM can be analyzed for loss of protein interaction and subsequent impact on protein function [22-24]. This could lead to the identification of a new class of separation of function BLM variants with variable impact. The selection of functional assays to test the impact of such variants would be dependent on the specific interaction interrupted. Overall, these functional assays would provide evidence that certain phenotypes are the result of specific variants. This can be strengthened further by reproducing these results in assays using primary patient cells or animal models. Such comprehensive experimental evidence combined with allele frequencies in human population could provide critical insights into disease association of these rare variants. Clinically, this classification of variants can be useful in developing next-generation DNA screening (NGS) panels for diagnosis as well as developing personalized therapy [21, 25-27].

Consistent with replication defects observed in Bloom syndrome cells and the ascribed role of BLM in restarting replication forks, we have identified a novel interaction between BLM and Mcm6, a component of the replicative MCM complex in Chapter Four. We hypothesize that as a constitutive component of the replisome, BLM helps replication fork progression through regions containing secondary DNA structures such as G-quadruplexes. Using pyridostatin to stabilize G-quadruplex DNA, we have shown the necessity of BLM/Mcm6 interaction in surmounting secondary structures *in vivo*. Further assays monitoring the response of the

www.manaraa.com

replisome/replication forks to secondary DNA structure formation would be required. Although various specialized helicases have been shown to unwind G-quadruplex DNA, their selection and recruitment to unwind such structures *in vivo* might depend on the specific structural conformation and protein interactions [28]. Comparison studies have shown that unlike other specialized helicases, BLM is unique in binding to G-quadruplex conformations non-selectively [29, 30]. Coupled with our data identifying Mcm6 as a BLM interactor and the putative presence of BLM at active replisomes, this is a strong implication of BLM being the main specialized helicase assisting the replicative helicase in overcoming G-quadruplex formation during replication. A reporter based assay in the presence and absence of BLM/Mcm6 interaction could be used to monitor instability at loci predisposed to form G-quadruplex structures [31, 32].

Sequences with the potential to form G-quadruplexes are highly prevalent, including over 90% of DNA replication origins, and could form a frequent barrier to replication initiation [28, 33]. G-quadruplexes have been visualized in cells not undergoing replication, suggesting that these could be pre-formed structures encountered by the replisome before replication [34]. Taken together, our identification of BLM/Mcm6 interaction in G1 implies a novel role for BLM. However, this requires further *in vivo* verification. One approach would be to use DNA combing to investigate DNA replication origin firing in the presence and absence of BLM/Mcm6 interaction in G1 [35, 36]. Immunofluorescence analysis to test localization patterns of BLM and components of pre-RC as well as pre-ICs through G1 and G1/S would be another approach to dissect the function of BLM/Mcm6 interaction in G1. Furthermore, an IMT fluorescent probe can be used for real-time monitoring of G-quadruplex DNA in G1 cells with and without BLM/Mcm6 interaction. Our findings in Chapter Five open up the possibility of exploring G-

166

quadruplex stabilization as a therapeutic approach in Bloom syndrome patients, who otherwise face chemotherapy-induced toxicity [37-40].

Through our research, we have paved the way for disease-association studies with the first functional evaluation of BLM variants of uncertain significance in human cells. Eventually, we hope for the establishment of carrier screening panels for diagnosis and treatment options. We have established a system to evaluate the global proteome to investigate pathways dysregulated in the absence of functional BLM. Our discovery of cell cycle specific interaction between BLM and Mcm6 provides mechanistic insights into some of the phenotypes observed in Bloom syndrome cells. Furthermore, we indicate a novel role for BLM in G1. The functional relevance of this interaction could be potentially translated to therapeutic benefits. We believe that our contribution has led to a better understanding of BLM function and Bloom syndrome.

REFERENCES

1. Prokofyeva, D., et al., *Nonsense mutation p.Q548X in BLM, the gene mutated in Bloom's syndrome, is associated with breast cancer in Slavic populations.* Breast Cancer Res Treat, 2013. **137**(2): p. 533-9.

2. Sokolenko, A.P., et al., *High prevalence and breast cancer predisposing role of the BLM c.1642 C>T (Q548X) mutation in Russia.* Int J Cancer, 2012. **130**(12): p. 2867-73.

3. Goss, K.H., et al., *Enhanced tumor formation in mice heterozygous for Blm mutation.* Science, 2002. **297**(5589): p. 2051-3.

4. Baris, H.N., et al., *Prevalence of breast and colorectal cancer in Ashkenazi Jewish carriers of Fanconi anemia and Bloom syndrome.* Isr Med Assoc J, 2007. **9**(12): p. 847-50.

5. Laitman, Y., et al., *The risk for developing cancer in Israeli ATM, BLM, and FANCC heterozygous mutation carriers.* Cancer Genet, 2016. **209**(3): p. 70-4.

6. Antczak, A., et al., *A common nonsense mutation of the BLM gene and prostate cancer risk and survival.* Gene, 2013. **532**(2): p. 173-6.

7.   Bogdanova, N., et al., *Prevalence of the BLM nonsense mutation, p.Q548X, in ovarian cancer patients from Central and Eastern Europe.* Fam Cancer, 2015. **14**(1): p. 145-9.

8.   de Voer, R.M., et al., *Deleterious Germline BLM Mutations and the Risk for Early-onset Colorectal Cancer.* Sci Rep, 2015. **5**: p. 14060.

9.   Thompson, E.R., et al., *Exome sequencing identifies rare deleterious mutations in DNA repair genes FANCC and BLM as potential breast cancer susceptibility alleles.* PLoS Genet, 2012. **8**(9): p. e1002894.

10.   Abecasis, G.R., et al., *A map of human genome variation from population-scale sequencing.* Nature, 2010. **467**(7319): p. 1061-73.

11.   Frank, B., et al., *Colorectal cancer and polymorphisms in DNA repair genes WRN, RMI1 and BLM.* Carcinogenesis, 2010. **31**(3): p. 442-5.

12.   Ding, S.L., et al., *Genetic variants of BLM interact with RAD51 to increase breast cancer susceptibility.* Carcinogenesis, 2009. **30**(1): p. 43-9.

13.   Broberg, K., et al., *Association between polymorphisms in RMI1, TOP3A, and BLM and risk of cancer, a case-control study.* BMC Cancer, 2009. **9**(1): p. 140.

14.   Koberle, B., et al., *Single nucleotide polymorphisms in DNA repair genes and putative cancer risk.* Arch Toxicol, 2016. **90**(10): p. 2369-88.

15.   Jakkula, E., et al., *Genome-wide association study in a high-risk isolate for multiple sclerosis reveals associated variants in STAT3 gene.* Am J Hum Genet, 2010. **86**(2): p. 285-91.

16.   Nejentsev, S., et al., *Rare variants of IFIH1, a gene implicated in antiviral responses, protect against type 1 diabetes.* Science, 2009. **324**(5925): p. 387-9.

17.   Bomba, L., K. Walter, and N. Soranzo, *The impact of rare and low-frequency genetic variants in common disease.* Genome Biol, 2017. **18**(1): p. 77.

18.   Mirzaei, H. and K.H. Schmidt, *Non-Bloom syndrome-associated partial and total loss-of-function variants of BLM helicase.* Proceedings of the National Academy of Sciences, 2012. **109**(47): p. 19357.

19.   Shastri, V.M. and K.H. Schmidt, *Cellular defects caused by hypomorphic variants of the Bloom syndrome helicase gene BLM.* Molecular Genetics & Genomic Medicine, 2016. **4**(1): p. 106-119.

20.   Richards, S., et al., *Standards and guidelines for the interpretation of sequence variants: a joint consensus recommendation of the American College of Medical Genetics and Genomics and the Association for Molecular Pathology.* Genet Med, 2015. **17**(5): p. 405-24.

21.   Perreault-Micale, C., et al., *A rigorous approach for selection of optimal variant sets for carrier screening with demonstration of clinical utility.* Mol Genet Genomic Med, 2015. **3**(4): p. 363-73.

22.   Kennedy, J.A., S. Syed, and K.H. Schmidt, *Structural Motifs Critical for In Vivo Function and Stability of the RecQ-Mediated Genome Instability Protein Rmi1.* PLoS One, 2015. **10**(12): p. e0145466.

23.   Lacroix, E., A.R. Viguera, and L. Serrano, *Elucidating the folding problem of alpha-helices: local motifs, long-range electrostatics, ionic-strength dependence and prediction of NMR parameters.* J Mol Biol, 1998. **284**(1): p. 173-91.

24.   Munoz, V. and L. Serrano, *Elucidating the folding problem of helical peptides using empirical parameters. III. Temperature and pH dependence.* J Mol Biol, 1995. **245**(3): p. 297-308.

25.   Azimi, M., et al., *Carrier screening by next-generation sequencing: health benefits and cost effectiveness.* Mol Genet Genomic Med, 2016. **4**(3): p. 292-302.

26.   Umbarger, M.A., et al., *Next-generation carrier screening.* Genet Med, 2014. **16**(2): p. 132-40.

27.   Lauschke, V.M. and M. Ingelman-Sundberg, *How to Consider Rare Genetic Variants in Personalized Drug Therapy.* Clin Pharmacol Ther, 2018. **103**(5): p. 745-748.

28.   Lerner, L.K. and J.E. Sale, *Replication of G Quadruplex DNA.* Genes (Basel), 2019. **10**(2).

29.   Tippana, R., et al., *Single-molecule imaging reveals a common mechanism shared by G-quadruplex-resolving helicases.* Proc Natl Acad Sci U S A, 2016. **113**(30): p. 8448-53.

30.   Bharti, S.K., et al., *Specialization among iron-sulfur cluster helicases to resolve G-quadruplex DNA structures that threaten genomic stability.* J Biol Chem, 2013. **288**(39): p. 28217-29.

31.   Shishkin, A.A., et al., *Large-scale expansions of Friedreich's ataxia GAA repeats in yeast.* Mol Cell, 2009. **35**(1): p. 82-92.

32.   Kononenko, A.V., et al., *Mechanisms of genetic instability caused by (CGG)n repeats in an experimental mammalian system.* Nat Struct Mol Biol, 2018. **25**(8): p. 669-676.

33.   Rhodes, D. and H.J. Lipps, *G-quadruplexes and their regulatory roles in biology.* Nucleic Acids Res, 2015. **43**(18): p. 8627-37.

34.   Biffi, G., et al., *Quantitative visualization of DNA G-quadruplex structures in human cells.* Nat Chem, 2013. **5**(3): p. 182-6.

35.   Patel, P.K., et al., *DNA replication origins fire stochastically in fission yeast.* Mol Biol Cell, 2006. **17**(1): p. 308-16.

36.   Marheineke, K. and O. Hyrien, *Control of replication origin density and firing time in Xenopus egg extracts: role of a caffeine-sensitive, ATR-dependent checkpoint.* J Biol Chem, 2004. **279**(27): p. 28071-81.

37.   Ruggiero, E. and S.N. Richter, *G-quadruplexes and G-quadruplex ligands: targets and tools in antiviral therapy.* Nucleic Acids Res, 2018. **46**(7): p. 3270-3283.

38.   Biffi, G., et al., *Elevated levels of G-quadruplex formation in human stomach and liver cancer tissues.* PLoS One, 2014. **9**(7): p. e102711.

39.   Asamitsu, S., et al., *Recent Progress of Targeted G-Quadruplex-Preferred Ligands Toward Cancer Therapy.* Molecules, 2019. **24**(3).

40.   Ma, B., et al., *Combined modality treatment for locally advanced squamous-cell carcinoma of the oropharynx in a woman with Bloom's syndrome: a case report and review of the literature.* Ann Oncol, 2001. **12**(7): p. 1015-7.